Toward Catalytic Hydrogenolysis of Chlorofluorocarbons with Group 8 and 9 Complexes

Sophia Dang Tran Cherry

A dissertation

submitted in partial fulfillment of the

requirements for the degree of

Doctor of Philosophy

University of Washington

2016

Reading Committee:

D. Michael Heinekey, Chair

Brandi M. Cossairt

Gojko Lalic

Program Authorized to Offer Degree:

Chemistry

University of Washington

Abstract

Toward Catalytic Hydrogenolysis of Chlorofluorocarbons
with Group 8 and 9 Complexes

Sophia Dang Tran Cherry

Chair of the Supervisory Committee:
Professor and Chair D. Michael Heinekey
Department of Chemistry

Chlorofluorocarbons (CFCs) are man-made chemicals used for aerosols and refrigerants. CFCs are the sole cause of the hole in the ozone layer, and thus the use and production of these chemicals have been banned. There are, however, still CFCs waiting for disposal. Currently, CFCs are disposed of by burning in the presence of O_2 and CH_4 to form HF, HCl, and CO_2. This thesis discusses a targeted catalytic cycle for the transformation of CFCs to HCFCs (hydrochlorofluorocarbons). Chapter 2 discusses the development of multiple systems suitable for the hydrogenolysis of dichloromethane, and the acid-base limitations for CFC hydrogenolysis specifically. Chapter 3 discusses another targeted system for catalysis, (^{tBu}POCOP)Rh(CO) (^{tBu}POCOP = κ^3-C_6H_3-1,3-[OP(*t*Bu)$_2$]$_2$). Pincer ligand metallation is presumed to proceed *via* initial coordination to the phosphorous atoms followed by C—H oxidative addition. While investigating the use of this system, protonation of (^{tBu}POCOP)Rh(CO) resulted in formation of

[(^{tBu}POCOP)Rh(CO)H][B(C_6F_5)$_4$]. When examined in the solid state, the compound was revealed to have an agostic interaction between C_{ipso}—H and rhodium. This is one of few examples of an intermediate in the metallation of pincer ligands. The rhodium complex has been fully investigated in the solution state. Our studies have revealed exaggerated steric effects in (POCOP)Rh(CO) complexes in comparison to iridium analogues.

TABLE OF CONTENTS

LIST OF FIGURES

LIST OF SCHEMES

LIST OF TABLES

Acknowledgements

I have been in school for the last 23 years of my life, and it is finally coming to an end. It is surreal that such a major chapter in my life is closing. I would not be here if it were not for the many people who helped me.

First, I want to thank Mike Heinekey. Graduate school has been extremely difficult for me, both emotionally and intellectually. Mike has been more patient with me than I think he even knew he was capable of. He and I have had more progress talks in his office than any other student, I have made his head explode more times than either of us could count, and I have cried more tears in his office than any other student. I am eternally grateful that you never gave up on me. Thank you for everything.

I would like to also acknowledge my committee: Professor Brandi Cossairt, Professor Karen Goldberg, Professor David Kalman, and Professor Gojko Lalic. Your questions and discussions on my work have been invaluable. Thank you for the time you've taken to help me.

Next, I have to thank those who helped train me as an undergraduate. My undergraduate advisor, Jim Mayer, who gave me an opportunity to work in his lab. Thank you for always being on my side and encouraging me to continue on in chemistry. Tristan Tronic, my primary mentor in lab, a quiet man with a kind and patient heart. Thank you for your guidance and continued friendship, of which I deeply treasure. Jeffery Warren: thank you for taking me under your wing, and for all your encouragement through the years. Lisa Park has been a true sister to me. I miss our boisterous laugher in the office.

I have spent 10 years in the UW Chemistry program. During this time, I have met so many wonderful and smart people. You all have played a big role in my sanity on this wild ride. Thank you all for answering my endless questions, for taking the time to chat with me, and for making the UW inorganic division arguably the best division in all of the land. To my fellow past and present Heinekey group members: Andrew Chanez, Jonathan Goldberg, Louise Guard, Travis Hebden, David Lao, Travis "Spills" Lekich, Steve Matthews, Joe Meredith, Michael Rak, Samantha Robinson, Kate Schultz, Tony St. John, Gene Wong, and those I have missed—you all have made the Heinekey group a great place to be. Travis, as much as I hate your dad jokes, I'm sure I'll miss them once I'm out of here. Keep on spilling. Louise, I can't wait to share 'abeets' while discussing the next episode of DJM. Joe, you will always be my favorite TA, and genuinely one of my favorite people. Tony, thanks for teaching me how to gamble. Go Pens! To the inorganic division members past and present: Kate Allen, Charlie Barrows, Miriam Bowring, Miles Braten, Tim Brewster, Collin Carver, Michael Coggins, Carlos Rodriguez Del Rio, Jill Dempsey, Alex Fox, Rebecca Hayoun, Dustin Kramer, Ben Leipzig, Alex Miller, Mike Pegis, Jennifer Peper, Tom Porter, Jason Pratner, Julian Rees, Karena Smoll, Jenny Stein, Tyler Stevens, Jessica Wittman, Ash Wright, and everyone else I've exchanged words with. You all are amazing. Thank you from the bottom of my heart.

Dinner club, you have been the light of my time in graduate school. Ben, Carolyn, Cecily, Jon, Karena, Louise, Mike, Travis, Tyler, and Wilson, thank you for loving my food, for the cabin trips, the brunches, the Easter egg hunts, and all the memories. You are my people. Thank you for standing by me always. To all my other friends who have

joined in on the Secret Santas, the Easter brunches, the Thanksgivings, and all the other orphan holidays we've celebrated together—you have made my life rich with experiences. My "non-science" friends have kept me grounded, normal, and told me when I was being too nerdy. Melissa Siv, thank you for being my best friend forever. I love you. Nadine Coombs, thank you for always being there for me and chatting while I waited for the bus. Everyone else: Mikkel Jensen, Steven Siv, and my trolling for hotties crew (Kaitlin Gemar, Kirsten Varner, and Holly Watanabe). You are all superb human beings.

To my best friends whom I have met in grad school: you are amazing. You all have stood by me at my darkest times and lifted me up. Carolyn Valdez, you are an amazingly beautiful soul. Thank you from the bottom of my heart for always being one of my greatest cheerleaders. Our friendship is one that I cherish so deeply. I love you. David Lao, you are the most thoughtful person I've ever met. You have been the big brother I never had. Thank you for always making me laugh and keeping me calm. Love you. Wilson Bailey, my work mister, our chemistry (ha) is undeniable. Your tenacity for life, adventure, and knowledge is something I have always admired. Thank you for constantly encouraging me to believe in myself, to better myself, and not to sweat the small stuff. I have never met anyone like you before and I am eternally grateful to have you in my life. I love you. Reverend Jonathan Goldberg, I don't know how to put into words how much I appreciate you as a human being and as my work husband. Thank you for always being there for me. You are a wonderful old soul, and I genuinely treasure all the fantastic times we've had together. You have always been there to encourage me and believe in me when I never could. Thank you for being a mentor to me. I am going to miss our brunch dates, sitting next to you, and working with you so very much. I love you.

My siblings, Jennifer and Michael Tran, have supported me since childhood. No matter what happens, I know I can count on them. Michael, you are one of my best friends, no matter how long we go without talking, always remember that. Believe in yourself always, no matter what. I love you. My parents, Chanh and Linh Tran, are the most selfless and hard working people I know. I could never tell them enough how much I love them and appreciate what they have done for my siblings and myself. There are not enough words for me to express how I feel for them. I am thankful to get my work ethic and perseverance from my Dad, and my good looks, problem solving skills, and adorable laugh from my Mom. Both of my parents came to America in the 80s with a dream for a better life for their children. I hope that I have made that dream come true for them. I love you both so much.

Finally, to my wonderful husband, Mike Cherry: you are an amazing human being that I am so honored to call my husband. Thank you for your patience, for always making me smile, and always supporting my dreams no matter the cost or sacrifice. You have held me while I cried over failure, and you have cheered me on when I thought I had nothing left to give. I am so excited to walk along this life with you and to see where it will take us. I love you millions.

To all the future scientists and struggling graduate students who may be reading this, always remember to be kind to yourself. This is a hard road, but you have a mind and a certain set of skills that not many have. Keep working hard. Always keep a clear idea of what you want from grad school and life in front of you and never stop working towards that. Believe in yourself always.

Dedication

To my wonderful parents, Chanh and Linh Tran,
who have made so many sacrifices,
given so much,
always believed in me,
and worked so hard
to get me to where I am today.

Chapter 1

An Introduction to Chlorofluorocarbons and Catalysis

1.1 Introduction to Chlorofluorocarbons

Chlorofluorocarbons (CFCs) have been used as refrigerants, aerosols, and foam blowers since their initial industrial use in the 1930s.[1] Peak CFC production was reached in the mid 1980s at over 400 metric tons per year, CF_2Cl_2 specifically being the most commonly used CFC.[2] There has been extensive research towards understanding the environmental impact of CFCs.[3] The persistence of CFCs in the stratosphere (upper atmosphere) results in homolytic cleavage of C—Cl bonds by intense ultra-violet (UV) irradiation to generate chlorine radicals ($Cl^{\bullet}$, step A, Scheme 1-1). The $Cl^{\bullet}$ then initiates ozone (O_3) depletion *via* a radical chain mechanism (step B and C, Scheme 1-1), reacting with over 100,000 molecules of O_3 before termination (Step D, Scheme 1-1). Scheme 1-1 shows termination *via* a reaction of $Cl^{\bullet}$ with methane, which is the most common route to termination. The rate of $Cl^{\bullet}$-induced O_3 decomposition is faster than the natural rate of O_3 production, resulting in depletion of the ozone layer (Figure 1-1).

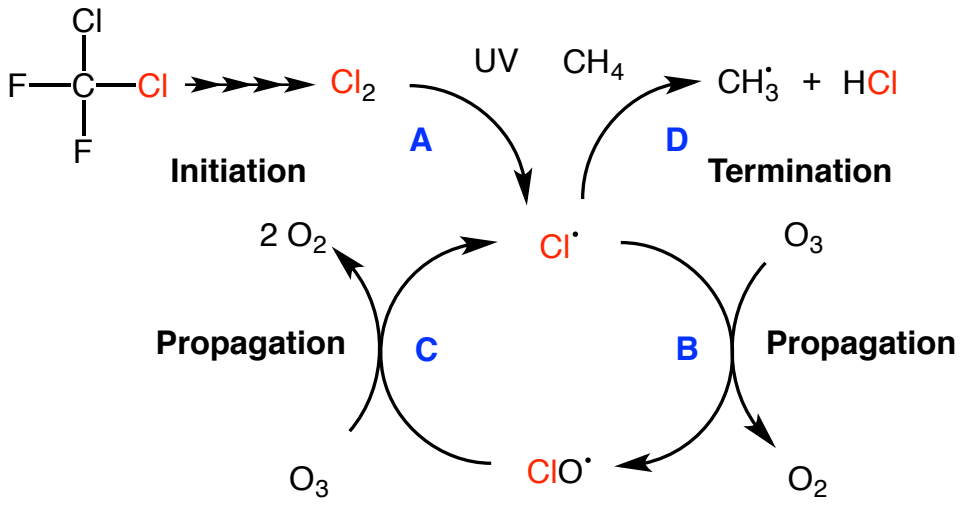

Scheme 1-1. The catalytic cycle of ozone depletion.

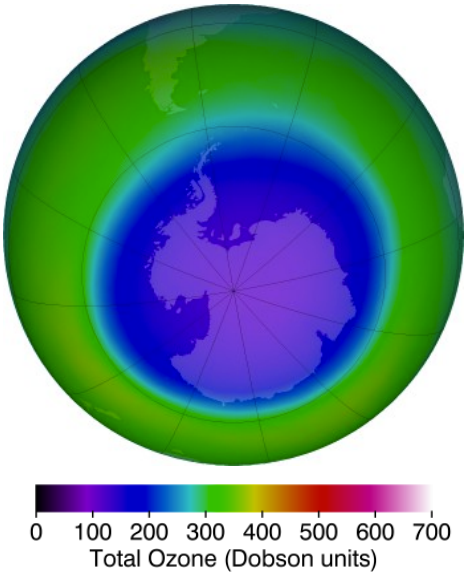

Figure 1-1. Satellite image of the ozone hole over the Antarctic obtained October 2015. A Dobson unit is used for ozone concentration measurement. It is based on the columnar density of ozone in the atmosphere (typically measured in atm-cm), 100 Dobson units is equal to 1 atm-cm.[4]

Due to the widespread use and environmental impacts of CFCs, the 1987 Montreal Protocol banned the production and use of all CFCs.[5] However, CFCs still remain in old appliances. According to a 2002 report from the United Nations there was 380,000 ODP (ozone depleting potential) tonnes of CFCs banked, and it was predicted that 140,000 ODP tonnes would still remain in 2010.[6] The current system for safe CFC disposal implemented by the Environmental Protection Agency involves the incineration of CFCs after safe collection from older appliances. Combustion of CFCs in the presence of CH_4 and O_2 yields CO_2, HCl, and HF, which are all low value chemicals.[7] It is of great interest to convert harmful CFCs to high-value hydrofluorocarbons (HFCs) or hydrochlorofluorocarbons (HCFCs). These are currently employed as replacements for CFCs in some applications. HFCs do not contain chlorine atoms and therefore have no risk of $Cl^{\bullet}$ generation. HCFCs have shorter half-lives than CF_2Cl_2 in the atmosphere because they react with hydroxyl radicals in the troposphere.[8] This thesis will discuss efforts towards developing a catalyst to effectively recycle CFCs to HCFCs or HFCs.

1.2 Metal Hydrides

1.2.1 *Synthesis and Characterization*

Metal-hydride compounds are of great importance to organometallic chemistry owing to the fact that insertion of unsaturated compounds into metal-hydride bonds is typically facile.[9] Consequently, metal-hydrides play an important role as intermediates in catalysis.[10] The first molecular metal-hydride species was synthesized in 1931 by Heiber, $H_2Fe(CO)_4$ (Figure 1-2).[11] Structural characterization of this complex and confirmation of the presence of an iron-hydride moiety had to await the development of modern spectroscopic techniques. In 1955, Wilkinson synthesized and thoroughly characterized Cp_2ReH (Cp = $(\eta^5\text{-}C_5H_5)^-$, cyclopentadienyl; Figure 1-2), catapulting the field of metal-hydrides forward.[12]

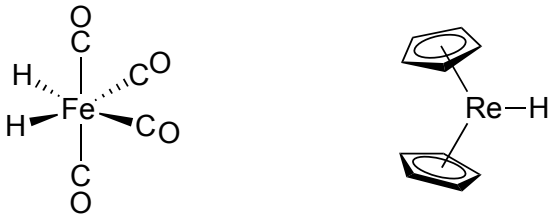

Figure 1-2. $H_2Fe(CO)_4$, synthesized by Heiber and coworkers (left).[11] Cp_2ReH, as characterized by Wilkinson and Birmingham (right).[12]

Metal-hydrides can be synthesized through a number of pathways: protonation of a metal center, use of hydride donors, oxidative addition of H_2, or β-hydride elimination from a ligand.[13] In the case where a metal center is basic, it can be protonated to form a metal-hydride (Scheme 1-2, A).[14] Main group hydride donors can also be used to form metal-hydride bonds where an electrophilic metal center reacts with H^- reagents. Common main group hydride donors include: sodium borohydride, lithium aluminum hydride, lithium triethylborohydride (super hydride), sodium hydride, etc. (Scheme 1-2, B).[15] In electron deficient species, the hydrogen bond can elongate to the point of oxidative addition (Scheme 1-2, C) after H_2 coordinates to an open site.[16] Finally, coordination of ligands with β-hydrogens can lead to β-hydrogen elimination to generate a metal hydride (Scheme 1-2, D).[13b]

H^+ reagents:

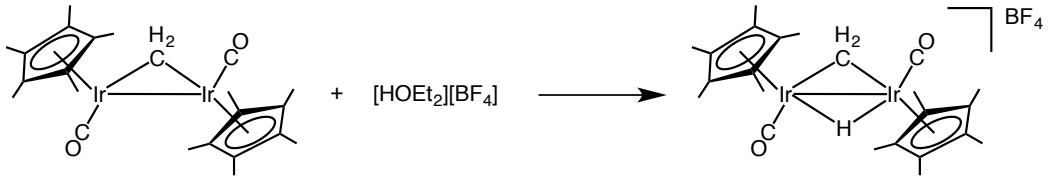

A

H^- reagents:

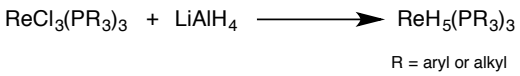

B

Oxidative Addition:

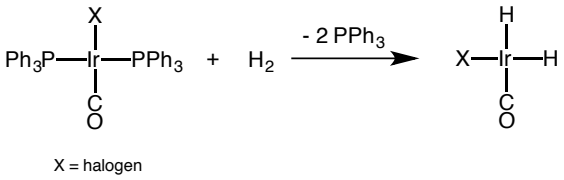

C

β–hydride elimination:

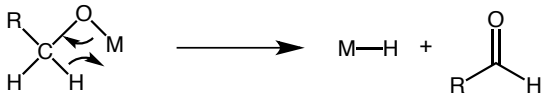

D

Scheme 1-2. Examples of reactions to form metal-hydrides.

The most commonly used method for characterization of hydrides is ^{1}H NMR spectroscopy. Hydride signals typically appear to high field of tetramethylsilane, as high as -60 ppm. Coupling to NMR active metal nuclei is also informative in stereochemical determination, as is coupling to phosphines which are ubiquitous in organometallic chemistry. Additionally, *cis*- and *trans*-coupling to other hydrides is informative (J = 1-10 Hz). Infrared (IR) spectroscopy can be used to identify metal-hydride stretches, showing up between 1500-2200 cm^{-1}. However, these bands are often weak in intensity, therefore hard to identify and unreliable. X-ray crystallography is also an inaccurate form of characterization as electron scattering by hydrogen atoms closely bound to electron rich metal centers are hard to identify in electron density maps.[17] Solid-state structures derived from neutron diffraction data are reliable, however these studies require much larger crystals and facilities equipped to collect this data are scarce.

1.2.2 *Reactivity with Carbon-Chlorine Bonds*

Metal-hydride bonds can be reactive towards C—Cl bonds. It has been found that a general trend of metal-hydride reactivity is 1st row > 2nd row > 3rd row transition metals.[18] The reaction is believed to proceed *via* a radical mechanism (Scheme 1-3).[19] First, a single electron transfer from M—H to R—Cl occurs. $R—Cl^{\bullet -}$ rapidly cleaves to form $R^{\bullet}$ and Cl^-; $M—H^{\bullet +}$ is deprotonated by Cl^- to form $M^{\bullet}$. The metal radical further reacts with chlorocarbons in solution to homolytically cleave R—Cl bonds to form M—Cl and $R^{\bullet}$. The radical chain reaction continues to propagate until termination. Based on this principle, we propose the use of first and second row late transition metal hydrides for the hydrogenolysis of CFCs.

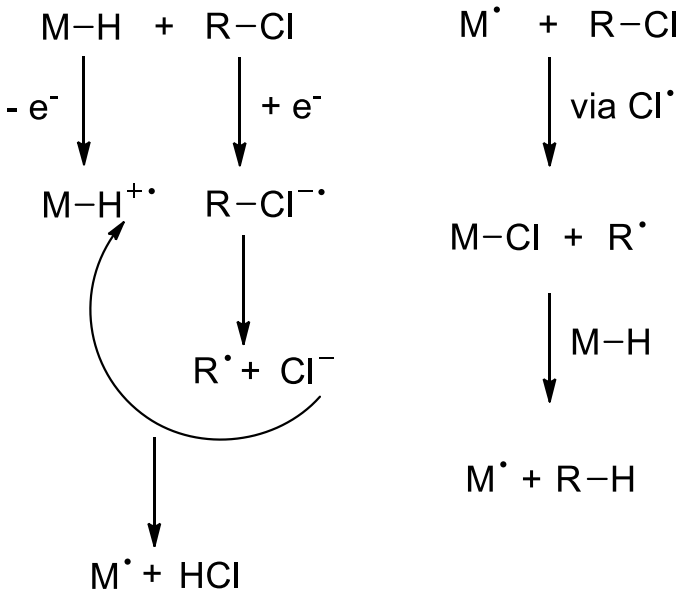

Scheme 1-3. Radical mechanism for chlorocarbons reacting with metal-hydrides.

1.3 Metal-Dihydrogen Complexes

In 1984, Kubas and coworkers reported the first example of a metal-dihydrogen complex.[20] *mer-trans*-$M(CO)_3(PCy_3)_2(H_2)$ (M = Mo, W; Figure 1-3) was isolable and fully characterized by IR spectroscopy, neutron diffraction, X-ray diffraction, and ^1H NMR spectroscopy to reveal a fully intact, albeit elongated, H_2 bond. Since the seminal work of Kubas, hundreds of H_2 complexes have been synthesized and fully

characterized.[21] This thesis discusses dihydrogen complexes as important species in proposed catalytic cycles.

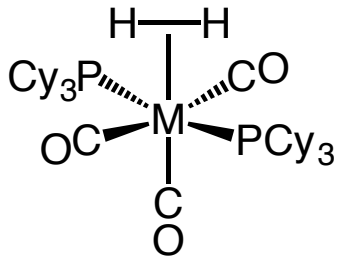

Figure 1-3. Original "Kubas Complex." M = Mo, W

Metal-dihydrogen species can be described as a three center, two electron interaction between a metal center and H_2 as a ligand. A variation of the Dewar-Chatt-Duncanson model for alkene coordination to a metal is commonly used to describe this coordination through a σ-bond.[22] The electron density from the H_2 σ-bond is donated to the metal center. Back donation from the metal *d*-orbitals into the σ* antibonding orbitals of H_2 can occur, which leads to elongation of the H_2 bond (Figure 1-4) and in some cases oxidative addition of H_2 to form a dihydride complex.

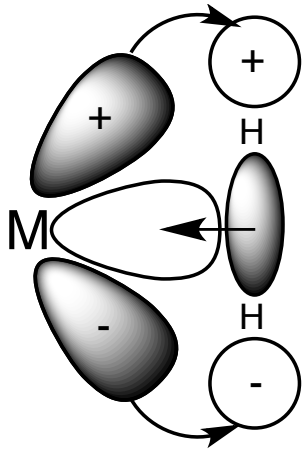

Figure 1-4. Orbital description of a three center, two electron interaction to form a metal-dihydrogen complex.

1.4 Acidity of Metal-Hydrides and Dihydrogen Complexes in Non-Aqueous Solutions

Metal-hydrides are thermodynamically competent acids, however kinetic effects play a large role. Due to the often large reorganization energy, metal-hydrides can have poor kinetic acidity.[23] Metal-*dihydrogen* species have a greater kinetic acidity due to little or no reorganization upon deprotonation. Typically, pK_a values are best measured and reported in H_2O. However, due to the relatively high autoionization of water ($K_w = 10^{-14}$), a wide range of pK_a values cannot be measured. Additionally, measuring the pK_a values for metal-dihydrogen species in water can be plagued by poor solubility and undesirable reactivity. Thus, pK_a values of metal-hydrides and -dihydrogen species have been recorded in organic solvents such as THF, DCM, and MeOH.[24] However, there are a number of underlying issues with measuring pK_a values in such solvents: (i) organic solvents have poor solvation of ions, therefore leading to ion pairing. This leads to more qualitative measurements opposed to *quantitative*. (ii) While a pK_a value could be internally consistent with a set of data, the lack of pK_a values of common organic and inorganic acids in non-aqueous solvents leads to data that is not very meaningful.[25] MeCN is a common organic solvent used for pK_a measurements due to the high autoionization ($K_{MeCN} = 10^{-44}$) and ability to solvate ions well, however when studying dihydrogen species, MeCN is often observed to displace the H_2 ligand.[25,26]

1.5 Introduction to Targeted Catalysis

1.5.1 *Previous Work with Hydrogenolysis of Chlorofluorocarbons*

Prior work on the hydrogenolysis of CFCs largely uses heterogeneous catalysts, such as Pd/Al_2O_3, Pd/C, RuO_2/C deposited on Nafion®, and Rh/C.[27] Three examples of homogeneous hydrogenolysis catalysts have been previously reported. Simon and Sisak used $RhCl_3(py)_3$ (py = pyridine) and pyridine for the hydrogenolysis of CHF_2Cl to form CHF_3 and CH_4.[28] Reactions were performed at 150 °C with 98.7 atm H_2 in steel autoclave reactors. While the reaction led to full conversion of CHF_2Cl, side reactions also occurred including the partial hydrogenation of pyridine. Mechanistic studies have been

performed, suggesting two potential pathways: (i) a base assisted route or (ii) HCl elimination to form difluorocarbene leading to CH_4 formation.

Kim and coworkers have developed a catalytic system towards conversion of CF_3CCl_3 to CF_3CHCl_2 avoiding over hydrogenolysis to CF_3CH_2Cl with the use of $RhCl(PPh_3)_3$ in THF.[29] Effects of hydrogen pressure and temperature were studied revealing no change in reactivity past 6.8 atm of H_2 and increased turnover frequency (TOF) with increased temperatures between 50-150 °C. Over 300 h^{-1} TOF was observed in reactions performed with 8 atm of H_2 at 150 °C. While the mechanism of catalysis has been studied, the exact mechanism is still unclear.

Roundhill and coworkers have developed a catalyst for hydrogenolysis using $RuCl_2(PPh_3)_3$ to transform CCl_4 and $CFCl_3$ to $CHCl_3$ and $CHFCl_2$, respectively (Scheme 1-4).[30] In the case of transforming CCl_4 to $CHCl_3$, the catalysis is performed at room temperature and with 1.1 atm of H_2 in a 1:1 solvent mixture of toluene and alcohol. Only 114 turnovers were observed over 13 days. Attempts to optimize the reaction were made, including addition of excess base (triethylamine, NEt_3) to aid formation of the active catalytic species, but increased reactivity was not observed. Similar conditions were used in screening the hydrogenolysis of $CFCl_3$ in a toluene/ethanol solvent mixture; only 17 turnovers were observed over 12 hours. Roundhill proposes a different catalytic mechanism than what has been previously reported. The presence of an alcohol serves as a hydride donor to $RuCl_2(PPh_3)_3$ *via* displacement of chloride from the alkoxide (formed *in situ*) followed by β-hydride elimination to form $RuHCl(PPh_3)_3$, the active catalytic species. $RuHCl(PPh_3)$ reacts with CCl_4 and $CFCl_3$ through a radical mechanism to regenerate $RhCl_2(PPh_3)$ and the hydrogenated product. The active catalytic species can also be formed in the presence of base and H_2, however this reaction is slow and catalytic reactions showed lower turnovers than in the absence of base (Scheme 1-4).

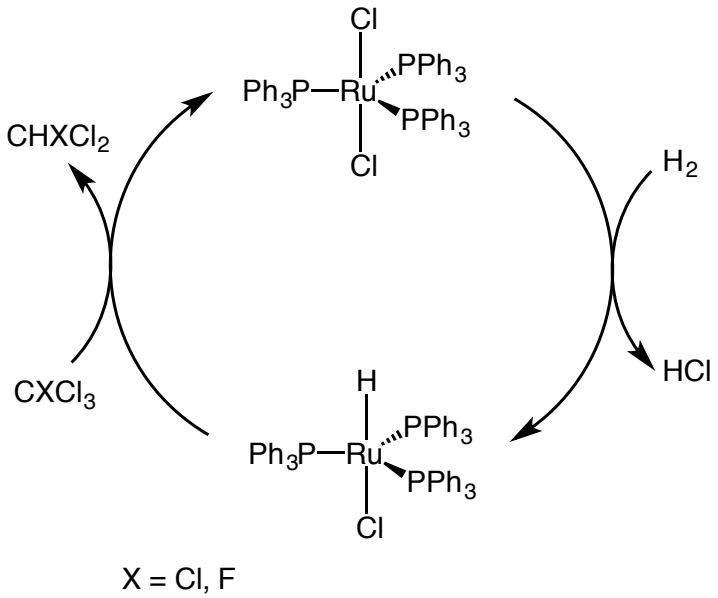

Scheme 1-4. Proposed catalytic cycle from Roundhill and coworkers. Formation of $Ru(PPh_3)HCl$ is proposed to form either by chloride displacement by H_2 followed by deprotonation, or by coordination of an alkoxide followed by β-hydride elimination (not pictured).

1.5.2 *Proposed Work in This Thesis*

HCFCs can be used as solvents for low temperature NMR spectroscopy experiments due to the low freezing points and unreactive behavior. A serendipitous finding by Mirjam van Roon (Heinekey Lab, 1997) demonstrated that despite the typical stability of HCFCs, $Fe(PP_3)H_2$ (PP_3 = tris-(2-(diphenylphosphino)ethyl)phosphine) reacted rapidly at room temperature with $CDFCl_2$ to quantitatively form $Fe(PP_3)HCl$ and CDHFCl. $Fe(PP_3)HCl$ also reacts with the solvent to quantitatively form $[Fe(PP_3)Cl]Cl$ and CDHFCl (Scheme 1-5).[31] The reaction could not be turned over and catalysis was never observed. van Roon reported that the bridgehead phosphine in PP_3 has a poor *trans*-effect, therefore the chloride is not very labile. This was reported to hinder the ability for catalysis due to the inability of $[Fe(PP_3)Cl]Cl$ to react with H_2.

Based on the previously reported systems, we aim to develop a catalyst for hydrogenolysis of CFCs based on a similar mechanism to the work of van Roon and the discussed mechanism by Roundhill and coworkers. Our aim is to develop a system which proceeds at mild temperatures and pressures of H_2.

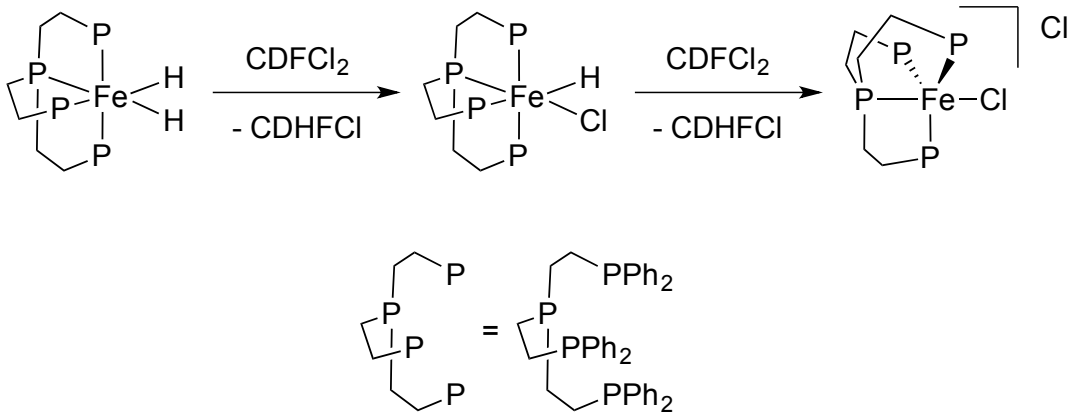

Scheme 1-5. An outline of the reactivity observed by van Roon with $Fe(PP_3)H_2$.

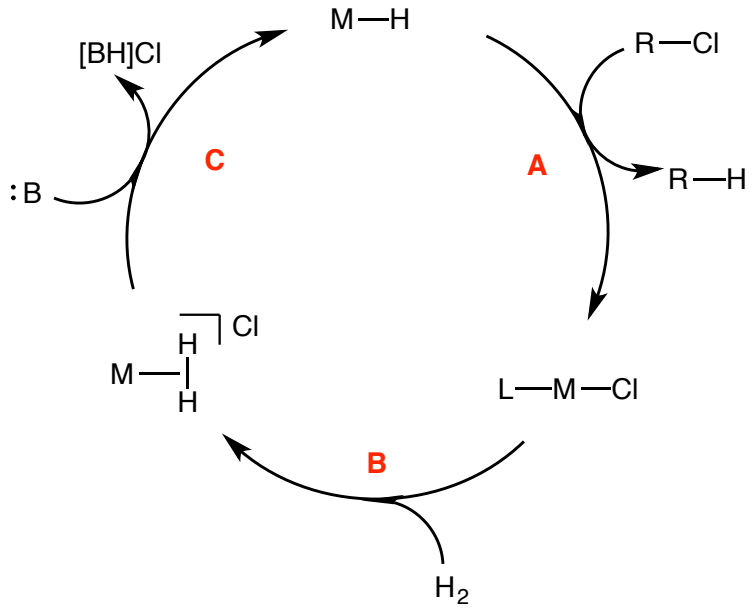

Scheme 1-6. A proposed generalized catalytic cycle for CFC hydrogenolysis.

Scheme 1-6 outlines a general targeted catalytic cycle for the desired catalytic hydrogenolysis of CFCs with a metal-hydride complex. We propose reacting a metal-hydride with a chlorocarbon to form a metal-chloride complex and the resulting hydrocarbon (step A, Scheme 1-6). Precedent for this step has been previously established.[31] Based on the issues with the system by van Roon, we propose a metal-chloride compound where the chloride is *trans* to L, where L is a strong *trans*-effect donor (step B, Scheme 1-6). Specifically, we have targeted a system where the chloride is *trans* to a hydride and has been reported to react with H_2 under mild conditions to form a

cationic metal-dihydrogen complex, *vide infra.*[32] Finally, the metal-dihydrogen complex can be deprotonated to regenerate the metal-hydride (step C, Scheme 1-6).

1.6 Notes for Chapter 1

1) *ESRL Global Monitoring Division.* http://www.esrl.noaa.gov/gmd/hats/publictn/elkins/cfcs.html (accessed January 2016).
2) *The Alternative Fluorocarbons Environmental Acceptability Study.* http://www.afeas.org/overview.php (accessed February 2015).
3) *Ozone Science: The Facts Behind the Phaseout | Ozone Layer Protection | US EPA.* http://www.epa.gov/ozone/science/sc_fact.html (Accessed January 2012).
4) *Ozone Hole Watch*. http://ozonewatch.gsfc.nasa.gov/monthly/monthly_2015-10_SH.html (Accessed December 2015).
5) *The Montreal Protocol on Substances that Deplete the Ozone Layer | Ozone Layer Protection | US EPA*. http://www.epa.gov/ozone/intpol/index.html (Accessed February 2015).
6) United Nations Environmental Program, Report of the Technology and Economic Assessment Panel (April 2002). NASA reported the rate of production of CF_2Cl_2 at 500,000 tons/year in the late 1980s, much of this has not been released into the atmosphere as of yet.
7) a) Tokuhashi, K.; Urano, Y.; Sadashige, H.; Kondo, S., *Combust. Sci. and Tech.* **1990**, *72*, 117-129. b) Prinn, R. G. and Golombek, A., *Nature*, **1990**, *344*, 47-49. c) Fisher, D. A.; Hales, C. H.; Wang, C.; Ko, M. K. W.; Sze, N. D., *Nature*, **1990**, *344*, 513-516. d) Wallington, T. J.; Hurley, M. D.; Ball, J. C.; Kalser, E. W., *Environ. Sci. Technol.*, **1992**, *26*, 1318-1324. e) *Chem. Eng. News,* **1996**, *74* (11), 4.
8) *ESLR Global Monitoring Division – Halocarbons and Other Atmospheric Trace Species.* http://www.esrl.noaa.gov/gmd/hats/flask/hcfc.html (Accessed October 2014).
9) a) Selmeczy, A. D. and Jones, W. D., *Inorg. Chim. Acta.*, **2000**, 138-150. b) Doherty, N. M. and Bercaw, J. E., *J. Am. Chem. Soc.*, **1985**, *107*, 2670-2682. c) Sullivan, B. P.

and Meyer, T. J., *Organometallics*, **1986**, *7*, 1500-1502. d) Kubas, G. J.; Wasserman, H. J.; Ryan, R. R., *Organometallics*, **1985**, *4*, 2012-2021.

10) a) Bäckvall, J., *J. Organometallic Chem.*, **2002**, *652*, 105-111. b) Larionov, E.; Li, H.; Mazet, C., *Chem. Commun.*, **2014**, *50*, 9816-9826. c) Halpern, J., *Annals of the New York Academy of Sciences*, **1983**, *415*, 244-252.

11) Hieber, W. and Leutert, F., *Naturwisenschaften*, **1931**, *19*, 360-361.

12) Wilkinson, G. and Birmingham, J. M., *J. Am. Chem. Soc.*, **1955**, *77*, 3421-3422.

13) a) Crabtree, R. H., *The Organometallic Chemistry of the Transition Metals*, 4th ed.; Hoboken, New Jersey, **2005**. b) Kaesz, H. D. and Saillant, R. B., *Chem. Rev.*, **1972**, *72*, 231-281 and references therein.

14) a) Heinekey, D. M. and Michel, S. T., *Organometallics*, **1989**, *8*, 1241-1246.

15) Chatt, J. and Coffey, R. S., *J. Chem. Soc. A,* **1969**, 1963-1972.

16) Vaska, L. and Rhodes, R. E., *J. Am. Chem. Soc.*, **1965**, *87*, 4970-4971.

17) Desrosiers, P. J.; Cai, L.; Lin, Z.; Richards, R.; Halpern, J., *J. Am. Chem. Soc.*, **1991**, *113*, 4173-4184.

18) a) Mutterties, E. L., *Transition Metal Hydrides.* New York: M. Dekker, **1971**. 244-246. Print. b) Moore, D. S. and Robinson, S. D., *Chem. Soc. Rev.*, **1983**, *12*, 415-452. c) Heinekey, D. M.; Voges, M. H.; Barnhard, D. M., *J. Am. Chem. Soc.,* **1996**, *118*, 10792-10802. d) Frost, B. J. and Mebi, C. A., *Organometallics*, **2004**, *23*, 5317-5323.

19) a) Kinney, R. J.; Jones, W. D.; Bergman, R. G., *J. Am. Chem. Soc.*, **1978**, *100*, 635-637. b) Walling, C.; Cooley, J. H.; Ponaras, A. A.; Racah, E. J., *J. Am. Chem. Soc.*, **1966**, *88*, 5361-5363. c) Kuivila, H. G., *Acc. Chem. Res.*, **1968**, *1*, 299-305.

20) Kubas, G. J.; Ryan, R. R.; Swanson, B. I.; Vergamini, P. J.; Wasserman, H. J., *J. Am. Chem. Soc.*, **1984**, *106*, 451-452.

21) Kubas, G. J., *Chem. Rev.*, **2007**, *107*, 4152-4205 and references therein.

22) Mingos, D. M. P., *J. Organomet. Chem.*, **2001**, *635*, 1-8 and references therein.

23) Walker, H. W.; Kresge, C. T.; Ford, P. D.; Pearson, R. G., *J. Am. Chem. Soc.*, **1979**, *101*, 7428-7429.

24) a) Walker, H. W.; Pearson, R. G.; Ford, P. C., *J. Am. Chem. Soc.*, **1983**, *105*, 1179-1186. b) Jia, G. and Morris, R. H., *J. Am. Chem. Soc.*, **1991**, *113*, 875-883. c) Moore, E. J.; Sullivan, J. M.; Norton, J. R., *J. Am. Chem. Soc.*, **1986**, *108*, 2257-2263.

25) Kristjánsdóttir, S. S. and Norton, J. R. Acidity of Hydrido Transition Metal Complexes in Solution. In *Transition Metal Hydrides*; Dedieu, A., Eds.; VCH Publishers, Inc.: New York, New York, **1992**; pp. 309-359.

26) Heinekey, D. M. and Oldham, W. J., *Chem. Rev.*, **1993**, *93*, 913-926.

27) a) Wiersma, A.; van de Sandt, E. J. A. X.; den Hollander, M. A.; van Bekkum, H.; Makkee, M.; Mouljin, J. A., *J. Catal.*, **1998**, *177*, 29-39. b) Wiersma, A.; ten Cate, A.; van de Sandt, E. J. A. X.; Makkee, M., *Ind. Eng. Chem. Res.*, **2007**, *46*, 4158-4165. c) Imamura, S.; Matsuba, Y.; Yamada, E.; Takai, K.; Utani, K., *Ind. Eng. Chem. Res.*, **1997**, *36*, 3978-3981. d) Manzer, L. E. and Nappa, M. J., *Appl. Catal., A*, **2001**, *221*, 267-274.

28) Simon, O. B. and Sisak, A., *Appl. Catal., A*, **2008**, *342*, 131-136.

29) a) Cho, O.-J.; Lee, I.-M.; Park, K.-Y.; Kim, H.-S., *J. Fluorine Chem.*, **1995**, *71*, 107-109. b) Kim, H.-S.; Cho, O.-J.; Lee, I.-M.; Hong, S.-P.; Kwag, C.-Y.; Ahn, B. S., *J. Mole. Catal. A: Chem.*, **1996**, *111*, 49-65.

30) Xie, S.; Georgiev, E. M.; Roundhill, D. M., *J. Organometallic Chem.*, **1994**, *482*, 39-44.

31) Van Roon, M., *Structure, Dynamics, and Reactivity of Hydride Complexes of the Cobalt and Iron Group Metals.* Diss. U of Washington, **1997**. Print.

32) Szymczak, N. K.; Braden, D. A.; Crossland, J. L.; Turov, Y.; Zakharov, L. N.; Tyler, D. R., *Inorg. Chem.* **2009**, *48*, 2976-2984.

Chapter 2

Reaction of Transition Metal Hydride Complexes with Halocarbons and pK_a Studies

2.1 Work Towards Catalysis with a Water Soluble $Ru(PP)_2H_2$ Species

2.1.1 *Introduction*

Previous work in our group focused on the investigation of $Ru(dppe)_2H_2$ (dppe = 1,2-bis(diphenylphosphino)ethane) as a catalyst for the hydrogenolysis of halocarbons.[1] Using DCM as a model solvent for chlorofluorocarbons (CFCs), each step of the proposed catalytic cycle (Scheme 1-6) was performed (Scheme 2-1). Unfortunately, when $Ru(dppe)_2H_2$ was tested for hydrogenolysis of CF_2Cl_2, it was found to have extremely limited solubility in neat CFC. As a result, a system with greater solubility was investigated.

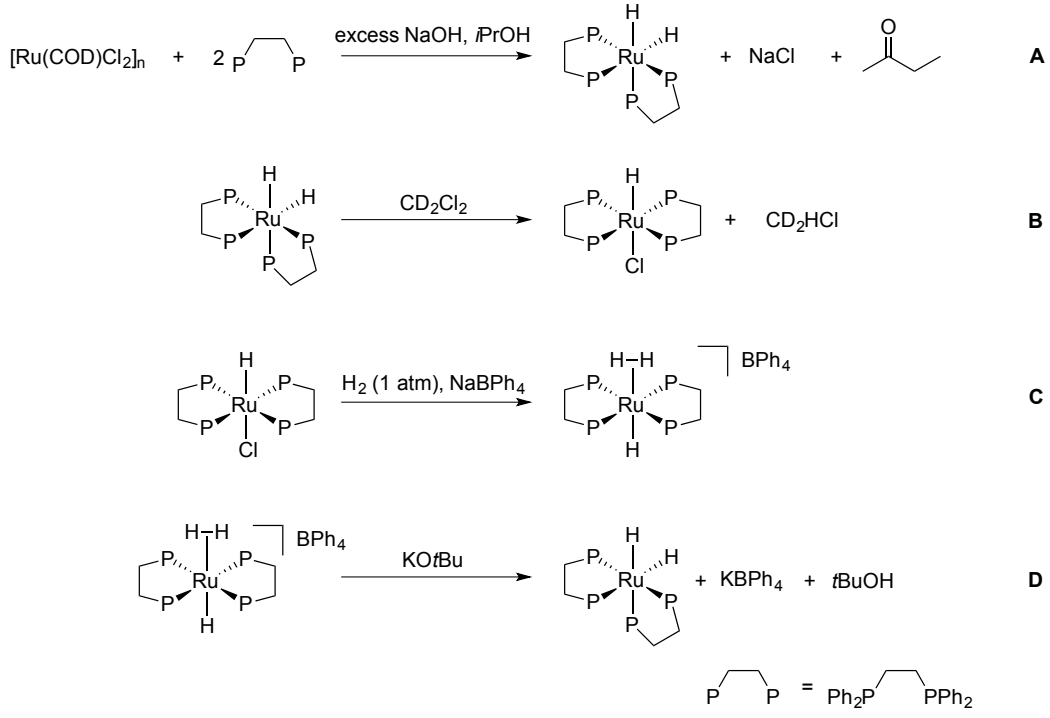

Scheme 2-1. Individual reactions performed to show the competency of $Ru(dppe)_2H_2$ as a catalyst for hydrogenolysis of CFCs.

Tyler and coworkers developed the water-soluble PP ligand for N_2 reduction to ammonia (PP = 1,2-bis[di(methoxypropyl)phosphino]ethane).[2] It was found that Ru complexes containing the PP ligand are not only soluble in water but also in organic non-polar solvents, which is attractive for CFC hydrogenolysis. Iron analogues of the Ru complex have been reported and well characterized, which is an important feature, as eventual use of an earth abundant transition metal is desired.[3] It is also reported that *trans*-$Ru(PP)_2HCl$ (**1**) can react with H_2 under mild pressures to form $[Ru(PP)_2H(H_2)]^+$ (**2**).[4] The facile formation of **2**, again, is attractive due to the previously discussed lack of reactivity between $[Fe(PP_3)Cl]Cl$ and H_2.

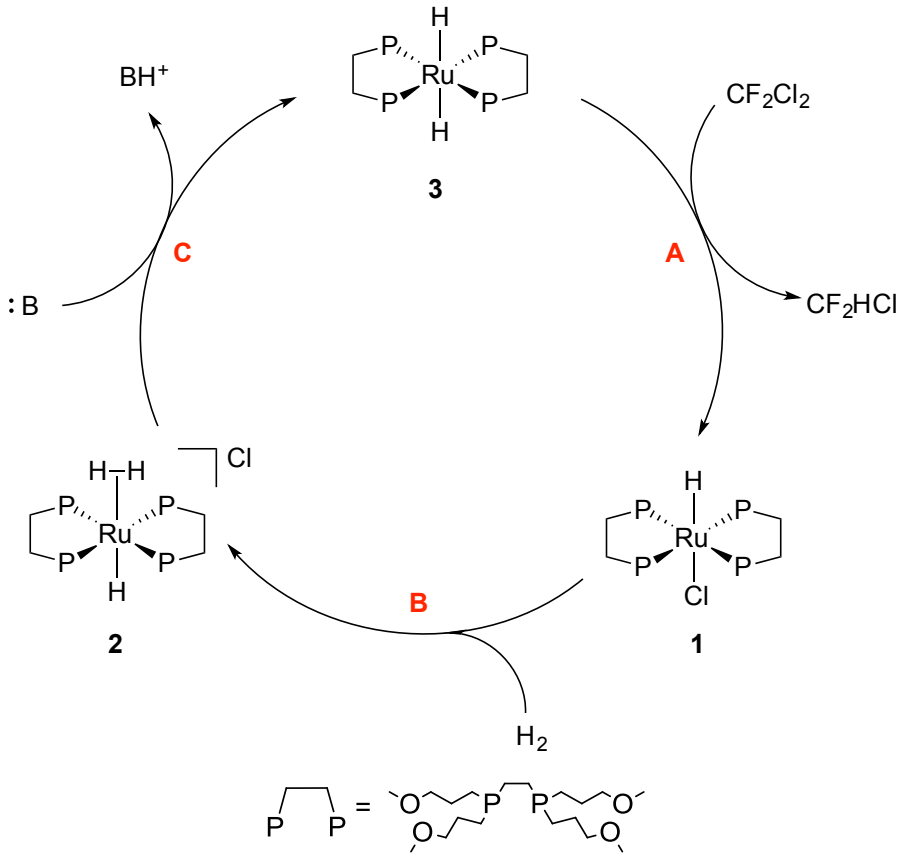

Scheme 2-2. Targeted catalytic cycle utilizing $Ru(PP)_2H_2$ (**3**) as a catalyst.

Scheme 2-2 outlines the desired reactivity of $Ru(PP)_2H_2$ (**3**) as a catalyst for hydrogenolysis of CFCs. In step A, **3** reduces a chlorinated solvent and forms **1**. While exposed to a constant atmosphere of H_2, $Ru(PP)_2HCl$ can react to form **2** (step B). Since

catalysis will be performed in basic media, **2** will immediately be deprotonated to regenerate **3** (step C). While catalysis is stoichiometric in base, we envision that utilizing a cheap base (*e.g.* sodium hydroxide) will result in benign byproducts (*i.e.* sodium chloride).

Industrial grade CF_2Cl_2 was obtained for testing catalysis, however it was found to contain an NMR silent, chlorine containing impurity. In addition to the impurity, CF_2Cl_2 has a high vapor pressure (5.6 atm at room temperature) and low boiling point (243 K). We found it practical to initially screen all potential catalysts with CD_2Cl_2 as a model solvent due to the ease of handling. If compounds are shown to react with CD_2Cl_2, $CDFCl_2$ could be used as another model solvent. $CDFCl_2$ was synthesized from $CDCl_3$ and distilled to purity to suppress side reactions.[5] The vapor pressure (1.6 atm at room temperature) and higher boiling point (282 K) of $CDFCl_2$ make the solvent much easier to work with. The hydrogenated product (CDHFCl) is diagnostically convenient, as it appears as a doublet at 5.9 ppm ($^2J_{HF}$ = 48 Hz) in the ^{1}H NMR spectrum. We envisioned developing and testing a catalyst with $CDFCl_2$ with sufficient longevity to consume the chlorinated impurity in the CF_2Cl_2, then continue to react with the substrate.

2.1.2 *Synthesis of $Ru(PP)_2H_2$*

Isopropyl alcohol (IPA) and sodium metal were added to a THF solution of $Ru(PP)_2Cl_2$ (**4**). The yellow solution turned colorless. After removal of solvent and extracting into pentane, the product, $Ru(PP)_2H_2$ (**3**) was obtained as a waxy, colorless solid.

The ^{1}H NMR spectrum of the resulting product displayed a multiplet for the methoxypropyl groups on the phosphines. The high field region displays two signals for both the *cis*- and *trans*-isomers of **3**. A pentet is present at -10.1 ppm ($^2J_{HP}$ = 20 Hz) for the *trans*-isomer, as all four phosphines are chemically and magnetically equivalent. A multiplet representative of the *cis*-isomer is found at -10.4 ppm. The *cis*-isomer of **3** gives rise to a complicated AA'XX'YY' spin system (Figure 2-1). The $^{31}P\{^1H\}$ NMR spectrum displays a singlet and two triplets (Figure 2-2). The singlet at 78.5 ppm represents *trans*-**3** (four equivalent phosphines), while the two triplets are for the two sets of two inequivalent phosphines in *cis*-**3**, which are coupled to each other. Based on integrations

of the $^{31}P\{^{1}H\}$ spectrum, the solution exists as a mixture of 62% *cis*-**3** and 38% *trans*-**3**. Due to the high solubility of the PP complex in a multitude of solvents, crystals suitable for X-ray diffraction were unattainable.

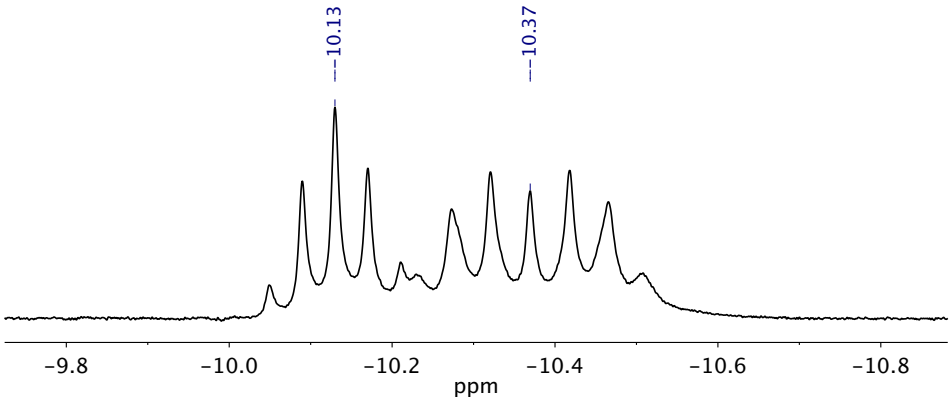

Figure 2-1. ^{1}H NMR spectrum (C_6D_6) of **3**. High field region is displayed to show hydride signals.

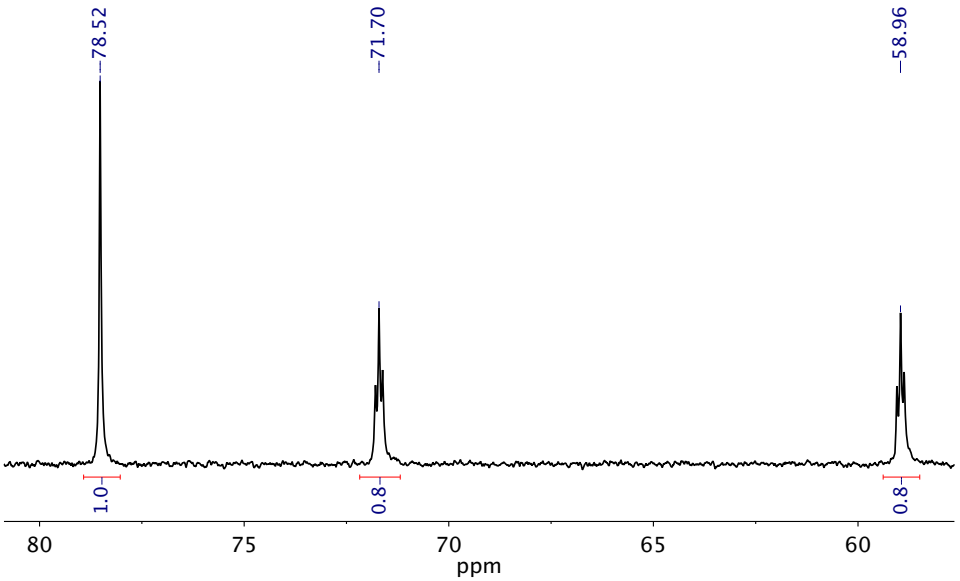

Figure 2-2. $^{31}P\{^{1}H\}$ NMR spectrum (C_6D_6) of *cis*- and *trans*-**3**.

2.1.3 *Reactivity with Carbon-Chlorine Bonds*

Compound **3** was dissolved in neat $CDFCl_2$, and monitored by ^{1}H and $^{31}P\{^{1}H\}$ NMR spectroscopies (step A, Scheme 2-2). Within an hour, CDHFCl was observed by ^{1}H NMR spectroscopy, indicated by a doublet at 5.9 ppm ($^{2}J_{HF}$ = 48 Hz) and a pentent for **1** (-21.5 ppm; $^{2}J_{HP}$ = 20 Hz). The $^{31}P\{^{1}H\}$ NMR spectrum was also consistent, revealing **1** and small amounts of *cis*- and *trans*-**4** (in a 4:1 ratio respectively) (Figure 2-3). Formation

of *cis*- and *trans*-**4** is due to the continued reactivity of **1** with $CDFCl_2$ (Scheme 2-3). Clean reactivity between **3** and $CDFCl_2$ prompted us to test reactivity with CF_2Cl_2, the target substrate. While **3** was soluble in $CDFCl_2$ and a number of other organic solvents, it had limited solubility in CF_2Cl_2. An existing CHF_2Cl (the desired product) impurity in the industrial grade CF_2Cl_2 made it difficult to track small changes in CHF_2Cl concentration by ^{19}F NMR spectroscopy due to dynamic range issues.[6] Attempts to use mass spectrometry also resulted in problems with dynamic range. While reactivity studies between $Ru(PP)_2H_2$ and CF_2Cl_2 were unsuccessful, reactions of the Ru complex with $CDFCl_2$ resulted in clean formation of the dehalogenated product. $Ru(PP)_2H_2$ reacts completely with $CDFCl_2$ to generate CDHFCl, $Ru(PP)_2HCl$, and $Ru(PP)_2Cl_2$ at room temperature. These results indicate the Tyler system *can* react with (nominally inert) chlorinated solvents to generate the desired products if optimized for catalysis.

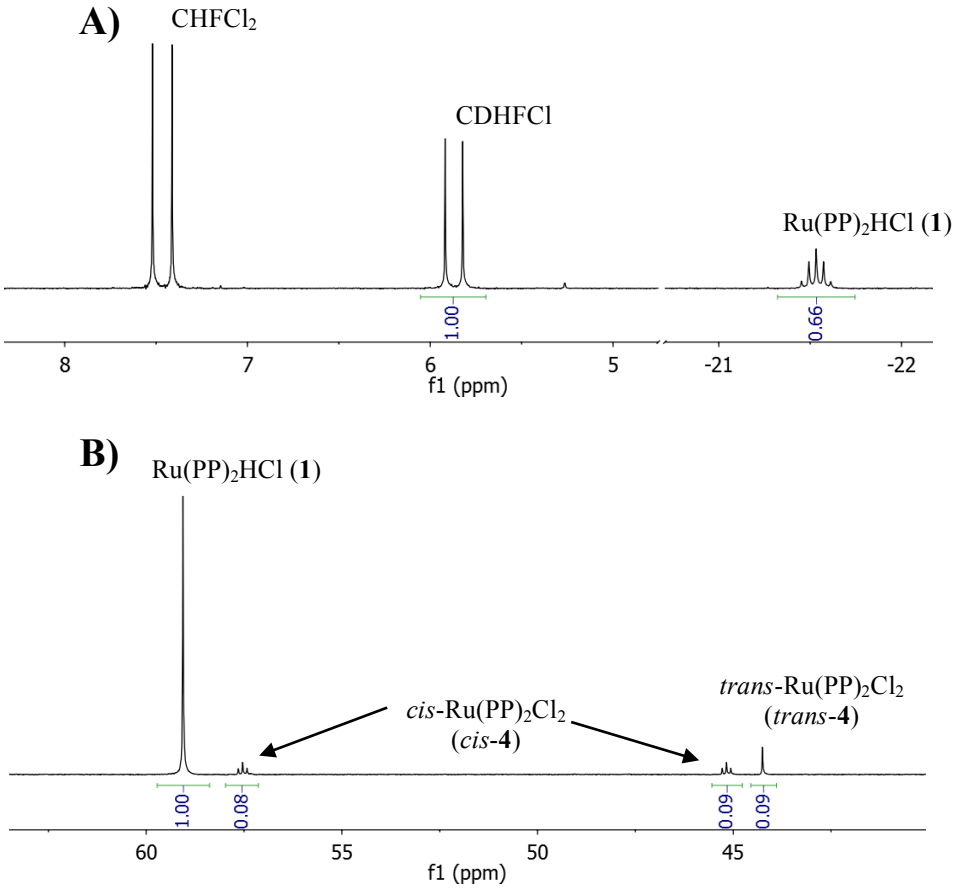

Figure 2-3. A) ^{1}H NMR data (500 MHz) of **3** reacting with $CDFCl_2$. Formation of CDHFCl and **1** are indicated. B) $^{31}P\{^{1}H\}$ NMR data (202.5 MHz) of **3** reacting with $CDFCl_2$. Formation of **1** and *cis*- and *trans*-**4** are indicated.

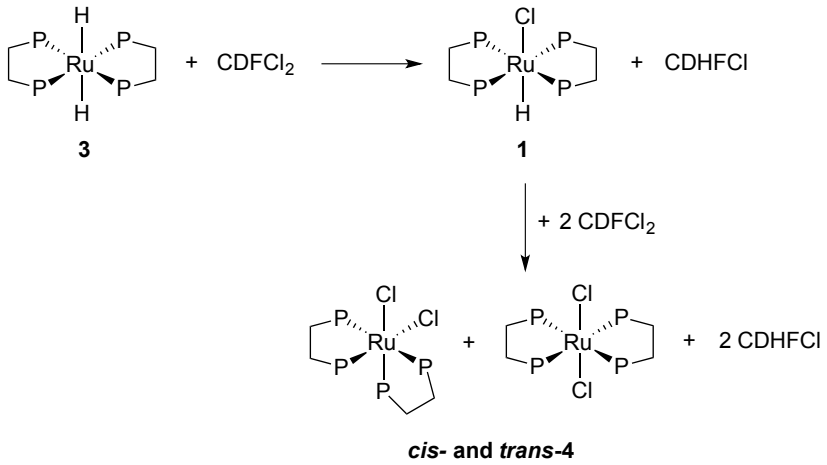

Scheme 2-3. Reactivity of **3** with $CDFCl_2$ to form **1** and CDHFCl. Further reactivity of **1** with $CDFCl_2$ forms *cis*- and *trans*-**4** and CDHFCl.

2.1.4 *Formation of Dihydrogen Complexes*

Metal-dihydrogen complexes can be formed by protonation of a metal-hydride complex or by halide abstraction from the metal-halide under H_2.[7] The targeted catalytic cycle in Scheme 2-2 (step B) aims to exploit the lability of the chloride ligand in **1** to form the dihydrogen complex with H_2 under mild conditions rather than with a stoichiometric chloride abstracting agent. Tyler and coworkers report facile quantitative formation of **2** from **4** under 24 atm of H_2 in pH 7 buffered water at 80 °C.[4,8] Based on mechanistic studies, the reaction was proposed to proceed first by chloride displacement by hydrogen on **4** to form $[Ru(PP)_2(H_2)Cl]Cl$. Water deprotonates the acidic dihydrogen complex to form **1**, which reacts with another equivalent of H_2 to form the desired $[Ru(PP)_2(H_2)H]Cl$ complex.[4]

Our catalytic cycle (Scheme 2-2) requires transformation of $Ru(PP)_2HCl$ to $[Ru(PP)_2(H_2)H]Cl$ with the addition of H_2. We observed that this reaction proceeds under much milder conditions than reported by Tyler and coworkers.[8] A CD_2Cl_2 solution of **1** with 1 atm H_2 results in 2% conversion to **4** (Scheme 2-4, Figure 2-4). Here, we treat CD_2Cl_2 as a model solvent for CF_2Cl_2. This reaction shows that solvation of the chloride ion occurs in a relatively non-polar solvent in order to form **2** under an atmosphere of H_2. While the conversion is low (2%), our target cycle (Scheme 2-2) occurs in basic media leading to immediate deprotonation to regenerate **3**. Keeping the reaction mixture with a constant atmosphere for H_2 regenerates the catalytic cycle. This is a vast improvement compared to the previously mentioned $[Fe(PP_3)Cl]Cl$ compound. The strong *trans*-effect

of the hydride ligand aids in the lability of the chloride ligand to allow small conversion to the desired material.

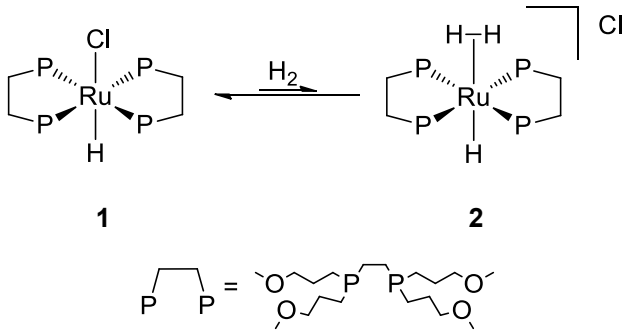

Scheme 2-4. Displacement of chloride ligand in **1** with 1 atm H_2 to form **2**.

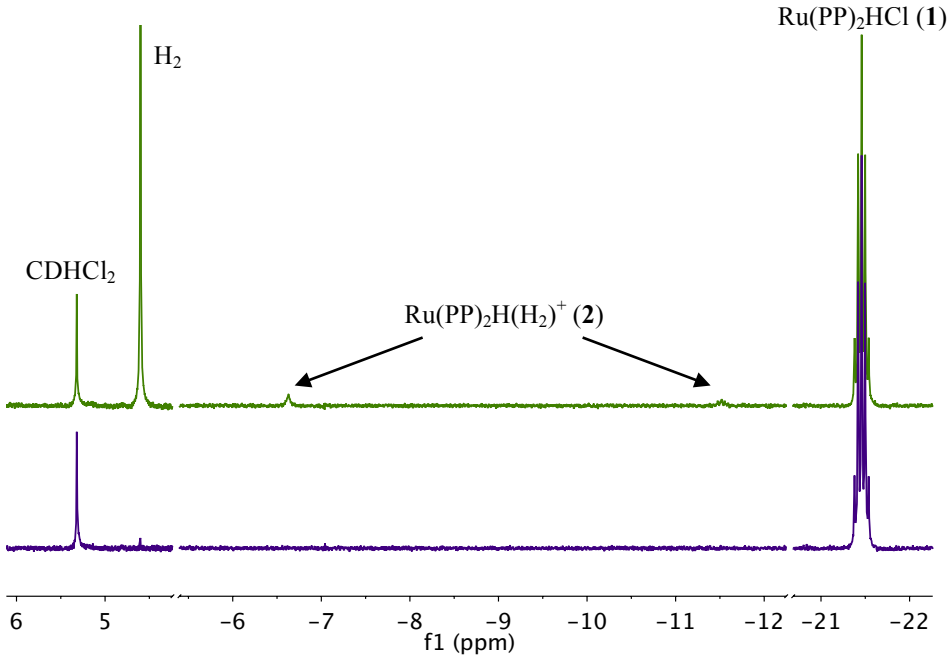

Figure 2-4. ^{1}H NMR spectra (500 MHz, CD_2Cl_2). Bottom: **1** in CD_2Cl_2. Top: Spectrum after addition of 1 atm of H_2. 2% formation of **2** is indicated.

2.1.5 *Acidity of Dihydrogen Complexes*

Based on the electronic similarity of depe versus PP (Figure 2-5), the pK_a values for the dihydrogen ligand on $[Ru(depe)_2(H_2)H]^+$ (depe = 1,2-bis-diethylphosphinoethane) and $[Ru(PP)_2(H_2)H]Cl$ were hypothesized to be very similar. Morris and coworkers report that the pK_a of the dihydrogen ligand in $[Ru(depe)_2(H_2)H]^+$ is 16.5 (THF),[9] implying that DBU (1,8-diazabicyclo[5.4.0]undec-7-ene; pK_a(THF) = 16.6) [10] can deprotonate $[Ru(PP)_2(H_2)H]Cl$. However, our studies show that the dihydrogen ligand on **2** is much

less acidic than hypothesized. While **4** is fully deprotonated with strong bases such as potassium *tert*-butoxide (KO^{t}Bu) and the phosphazene P$_4$-*t*Bu (1-*t*-butyl-4,4,4,-tris(dimethylamino)-2,2-bis[tris(dimethylamino)-phosphoranylidenamino]-2λ^5,4λ^5-catenadi(phosphazene); pK_a(DMSO) = 30.2)[11] DBU was found to deprotonate **4** to 20% completion. This reactivity suggests an approximate pK_a of 18 in DCM.

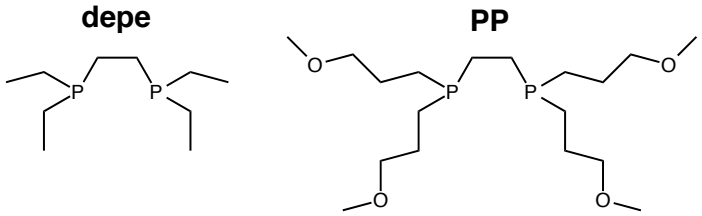

Figure 2-5. 1,2-Bis-diethylphosphinoethane (depe; left) and 1,2-bis[di(methoxypropyl)phosphino]ethane (PP; right).

Strong bases (such as NaOH) have been shown to deprotonate CHF_2Cl to form difluorocarbenes.[12] Since DBU was found to be a suitable base for our targeted catalysis (Scheme 2-2) and is a much weaker base than hydroxide, we attempted to use stoichiometric DBU in our catalytic reactions. However, control reactions revealed that the addition of DBU to a sample of $CDFCl_2$ led to the observation of multiple species by ^{1}H NMR spectroscopy. Protonated DBU is observed amongst the products, indicating that DBU is indeed deprotonating the $CDFCl_2$. This suggests that $CDFCl_2$ has a pK_a could be lower than protonated DBU, however an exact value is difficult to ascertain due to solvent effects. This is an unfortunate conclusion, as it shows that DBU (and other stronger bases) will likely react with CHF_2Cl, the desired product from catalytic CF_2Cl_2 hydrogenolysis. Further control reactions revealed that the strongest base showing no reactivity with $CDFCl_2$ is NEt_3 ($HNEt_3^+$; pK_a(THF) = 12.5).[10] Reactions of **2** with NEt_3 revealed no deprotonation.

2.1.6 *Summary*

Preliminary work with $Ru(PP)_2H_2$ revealed that it is not a competent catalyst for hydrogenolysis of CFCs due to the weak acidity of $[Ru(PP)_2(H_2)H]Cl$. We have found clean conversion of $CDFCl_2$ to CDHFCl with $Ru(PP)_2H_2$ (step A, Scheme 2-2). Additionally, $Ru(PP)_2HCl$ is reactive with only 1 atm of H_2 in CD_2Cl_2 to form

$[Ru(PP)_2(H_2)H]Cl$ (2%; step B, Scheme 2-2). These findings bode well for our proposed catalysis. However, $[Ru(PP)_2(H_2)H]^+$ was not acidic enough to be deprotonated without any resulting side reactions with HCFCs. DBU can deprotonate $[Ru(PP)_2(H_2)H]Cl$ to 20% completion, but DBU reacts with $CHFCl_2$ to generate unwanted species. The study of this system has revealed the necessary requirements for a competent catalyst: reactivity of a metal hydride with chlorinated solvents, facile transformation from the metal chloride to a metal dihydrogen complex, and a metal dihydrogen complex acidic enough to be deprotonated with NEt_3.

2.2 Work with Piano Stool Compounds

2.2.1 *Introduction*

Perutz and coworkers reported a piano-stool Noyori-type catalyst for transfer hydrogenation of ketones with a triethylamine-formic acid mixture (2:5, respectively) as a hydrogen source.[13] Cp*Rh(TsPDA) (**5**) was synthesized *via* the combination of $[Cp^*RhCl_2]_2$, $TsPDAH_2$, and 2 equiv. NEt_3, in DCM (Scheme 2-5) ($TsPDAH_2$ = $CH_3(C_6H_4)SO_2)NH(C_6H_4)NH_2$; Cp* = pentamethylcyclopentadiene). The synthesis was proposed to proceed *via* an intermediate, Cp*Rh(TsPDAH)Cl (**6**), where addition of NEt_3 leads to formation of $[HNEt_3]Cl$ and compound **5**. Scheme 2-6 outlines the proposed hydrogenolysis of CFCs with **5**. Since **6** (an intermediate in the proposed catalysis) can be deprotonated with NEt_3, as demonstrated through the synthesis of **5**, this system addresses the weak acidity issues observed with the Tyler system.

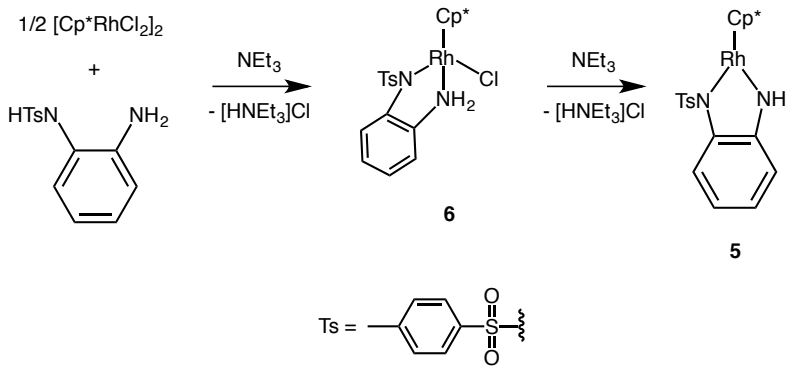

Scheme 2-5. Reported synthesis of **5** where compound **6** is an intermediate.

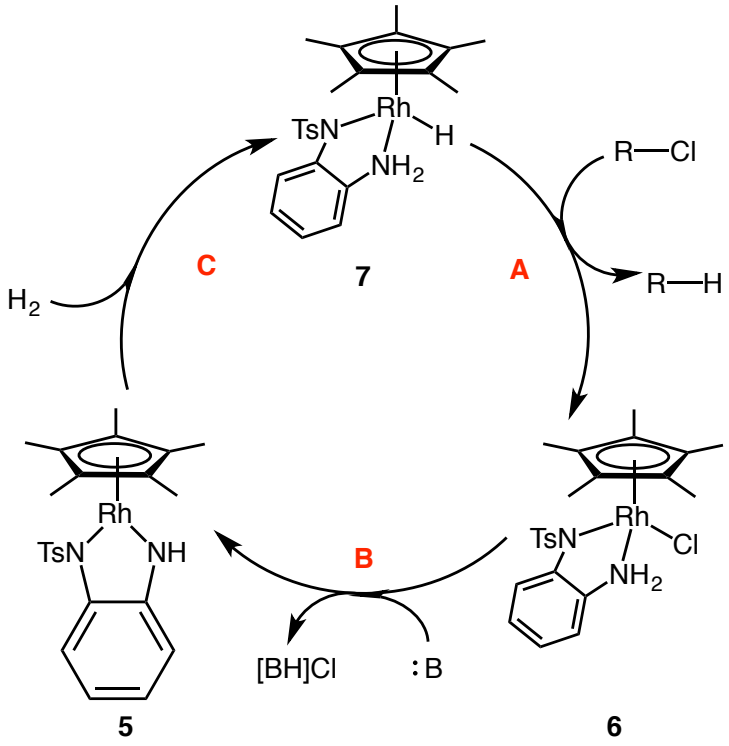

Scheme 2-6. Targeted catalytic cycle utilizing Cp*Rh(TsPDA) (**5**) as a catalyst.

In the proposed catalysis, the coordinatively-unsaturated, formally 16 e^- Rh(III) starting material **5** coordinates dihydrogen to form the rhodium hydro-hydride complex (step C, Scheme 2-6). Precedent for this step is suggested by work from Perutz and coworkers where Cp*Rh(TsPDAH)H (**7**) is observed at 233K after addition of formic acid (Scheme 2-7); upon warming the solution to room temperature dihydrogen is released and **5** is regenerated.[13] Based on microscopic reversibility, we hypothesized that complex **5** under high pressures of H_2 at room temperature would form **7** and react with chlorinated solvents to form **6** (step A, Scheme 2-6). As shown through the synthesis of **5**, complex **6** can be deprotonated with NEt_3 to regenerate the coordinatively-unsaturated complex **5** (step B, Scheme 2-6).

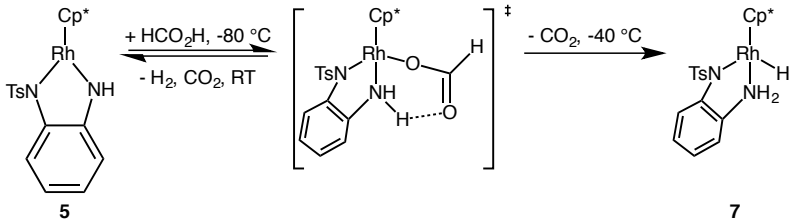

Scheme 2-7. Proposed intermediate after addition of formic acid to **5** to form **7**.

2.2.2 *Reactivity of Cp*Rh(PDA) Compounds*

Complex **6** was synthesized *via* addition of HCl to **5**.[13] As expected, addition of 1 equiv. of NEt_3 resulted in complete deprotonation of **6**. Weaker bases were used in order to measure the pK_a. In CD_2Cl_2, **5** and pyridinium chloride ([PyH][Cl]; pK_a(THF) = 5.5)[10] (1:1.1) were combined. The resulting ^{1}H NMR spectrum was used to calculate the K_a of the reaction. The pK_a of **7** was calculated to be 5.8 ± 0.2 (CH_2Cl_2). We found this value to be consistent with the value derived from the addition of pyridine to **6**. The calculated pK_a of **7** is based on an assumption that the pK_a of [PyH][Cl] is the same in THF and DCM. Based on the similar dielectric constants of THF and DCM, this is a fair assumption. This pK_a study shows that **6** is acidic enough to be deprotonated with pyridine (step B, Scheme 2-6) while not reacting with any HCFCs.

In order to explore the reactivity of **7** with chlorinated solvents (step A, Scheme 2-6), CD_2Cl_2 was utilized as a model solvent. Complex **5**, CD_2Cl_2, and 50 bar of H_2 were combined in a steel autoclave (Parr) reactor and stirred for 18 hours at room temperature. If **7** is formed under high pressures of H_2 and reacting with the bulk solvent, the resulting reaction mixture would contain compound **6**. A ^{1}H NMR spectrum was obtained of the resulting mixture showing no reaction had occurred, as a clean spectrum of **5** was observed.

Previous work from Ikariya and coworkers suggested an alcohol assisted H_2 activation to form metal-hydrides from the heterolytic cleavage of H_2 (Scheme 2-8).[14] With this in mind, an excess of IPA (approx. 7 equiv.) was added to the reaction mixture in the Parr reactor. After 18 hours of stirring under 50 bar of H_2 at room temperature, the color of the solution turned from dark purple to dark orange. A ^{1}H NMR spectrum of the solution indicated that a reaction had occurred. However, neither compound **6** nor

CD_2HCl were observed, suggesting that the desired reaction did not occur. A triplet in the ^1H NMR spectrum was observed at -11.6 ppm (J = 24 Hz). The identity of this species is still undetermined, but based on the multiplicity of the signal we propose a hydride bridged Rh-dimer. However, the reported spectrum of **7** shows a doublet in the hydride region with $^1J_{RhH}$ = 22 Hz. We speculate that the coupling constant of a bridged species would be smaller than the mono-hydride species due to both metal centers having a weaker interaction with the shared hydrogen atom. However, the coupling constant and chemical shift is within the range of other reported $Rh_2(\mu$-H) species.[15]

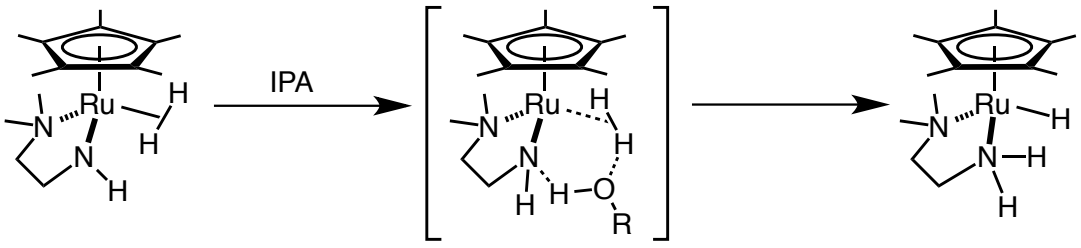

Scheme 2-8. The mechanism for alcohol assisted H_2 activation with piano-stool Noyori-type complexes.

While the ^1H NMR spectra of Parr reactor reactions indicate multiple species formed during the reaction, we were interested in observing formation of CD_2HCl to prove that the piano-stool Noyori-type motif can indeed react with chlorinated solvents. Due to the low boiling point of chloromethane (249 K) it is unlikely to be observed in ^1H NMR spectra after venting the Parr reactors. Specialty high-pressure NMR spectroscopy tubes were used to pressurize NMR spectroscopy scale reactions up to 100 psig (Chapter 4). These high-pressure tubes can remain sealed during the reaction time to ensure that if CD_2HCl is formed, it can be observed by ^1H NMR spectroscopy. A high-pressure tube containing **5**, IPA, CD_2Cl_2, and 90 psig H_2 was monitored over time by ^1H NMR spectroscopy. Over a span of two months, trace amounts of CD_2HCl formed. While a reaction did occur, the ^1H NMR spectra show the loss of all Cp* signals. Although the reaction does not proceed as anticipated, it still sets the precedent for our work. The formation of CD_2HCl over time shows that compound **5** could be reducing CD_2Cl_2, albeit not cleanly or in high yield.

Cp*Rh(TsPDAH)Cl has proven to be sufficiently acidic to be deprotonated by pyridine, an essential characteristic for our proposed catalysis. The pK_a of

Cp*Rh(TsPDAH)Cl has been measured in CD_2Cl_2. However, this system has not shown reactivity towards step A or C of catalysis (Scheme 2-6). Reactivity of complex **7** with chlorinated solvents has been complicated and convoluted. Reactions observed over months where **5** was reacted with H_2 (90 psig) and CD_2Cl_2 indicate paths to decomposition. However, a trace amount of CD_2HCl was observed in the reaction mixtures, indicating reduction of CD_2Cl_2.

2.2.3 *Reactivity of (*p*-cym)Ru(TsDPEN) Compounds*

Given the unproductive reactivity of the Perutz system with H_2, our focus shifted to a new compound. Noyori and coworkers reported the facile formation of (*p*-cym)Ru(TsDPENH)H (*p*-cym = *para*-$(CH_3)(C_6H_4)(CH(CH_3)_2)$; TsDPEN = $(CH_3(C_6H_4)SO_2)NCH(C_6H_5)CH(C_6H_5)NH$) (**8**) by reacting the coordinatively-unsaturated 16 e^- complex, (*p*-cym)Ru(TsDPEN) (**9**; Figure 2-6), with IPA at room temperature in minutes.[16] While the work from Perutz and coworkers exhibited the desired acidity for our catalysis, it lacked a stable hydride analogue making complex **9** a desirable target.

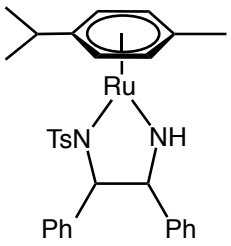

Figure 2-6. Compound **9**, (*p*-cym)Ru(TsDPEN).

Complex **8** was synthesized using reported methods[16] and combined with CD_2Cl_2. After 18 hours at room temperature under an atmosphere of N_2 the hydride signal in the ^1H NMR spectrum (located at -5.8 ppm) was no longer present and a signal for CD_2HCl was present. The reaction is clean, as the final spectrum shows the presence of only CD_2HCl and (*p*-cym)Ru(TsDPENH)Cl (**10**). As a proof of concept, this again shows that this piano-stool metal-hydride motif is viable for reactions with chlorinated solvents to form a metal chloride and the reduced product. In conjunction with the observed

reactivity from compound **8**, this bolsters our hypothesis that these compounds can serve as competent catalysts.

Noyori and coworkers reported that compound **9** is protonated to **10** with $[HNEt_3][Cl]$.[16] However, the percent conversion is never explicitly stated. In the event that there is an equilibrium, we attempted to deprotonate **10** with NEt_3. This resulted in no reaction. Water was added to the previously mentioned deprotonation reaction in hopes of solvating the chloride ion and facilitating deprotonation. 10 μL of argon sparged H_2O was added to a reaction mixture containing **10** and NEt_3 in CD_2Cl_2. An immediate reaction did not occur, and stirring overnight generated no change in the spectrum. An orange solid crashed out of the solution; efforts towards identifying this solid were unsuccessful. However, it is unlikely to be the desired compound as **9** is very soluble in CD_2Cl_2 and dark purple.

Although it has been reported by Noyori that deprotonation of **10** to **9** proceeds *via* a dissociative conjugate base mechanism (D_{cb}), where deprotonation *precedes* chloride loss, there is no evidence of this.[16,17] We believe that the mechanism of deprotonation could proceed *via* initial chloride loss, then deprotonation of the acidic amino proton (Scheme 2-9). The previously mentioned experiment suggests that either the chloride is not very labile, therefore preventing deprotonation, or deprotonation indeed occurs *via* a D_{cb} mechanism and NEt_3 is simply not basic enough to deprotonate the amino proton. Again, the amino proton on the TsDPEN ligand of **10** mimics benzyl ammonium (free benzyl ammonium pK_a(DMSO) = 10.2) which *cannot* be deprotonated by NEt_3 ($[HNEt_3]^+$ pK_a(DMSO) = 9),[18] however it is expected that when bound to the metal center, the benzyl amine moiety would be more acidic.

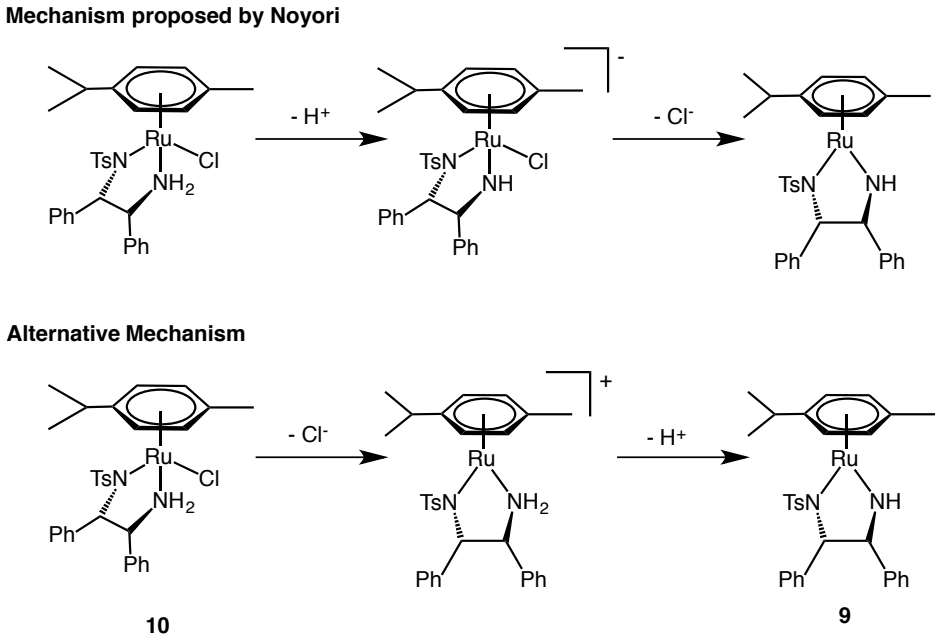

Scheme 2-9. Proposed mechanisms for deprotonation.

Noyori's (*p*-cym)Ru(TsDPEN) system has proven to have reactivity with IPA to form (*p*-cym)Ru(TsDPENH)H at room temperature within minutes. This is an ideal feature as we could envision performing catalysis in a biphasic CFC/IPA reaction mixture as opposed to pressurizing the reaction with H_2 gas. (*p*-cym)Ru(TsDPENH)H can react with chlorinated solvents, however, (*p*-cym)Ru(TsDPENH)Cl lacks the necessary acidity to turnover catalytic reactions with CFCs.

Our studies have shown that while Cp*Rh(TsPDAH)Cl possesses the acidity necessary for the desired catalysis, it lacks the necessary reactivity with IPA or H_2. The independent synthesis of the metal hydride has been difficult. On the other hand, (*p*-cym)Ru(TsDPEN) reacts with IPA to form compound **8** and possesses the reactivity desired with CD_2Cl_2. Compound **10** lacks the acidity to be deprotonated with NEt_3. Therefore, we envision a catalyst with the acidity of **6**, but the reactivity of **9** and **10** with a hydrogen source and chlorinated solvents, respectively.

We hypothesized that the more acidic nature of Cp*Rh(TsPDAH)Cl over (*p*-cym)Ru(TsDPENH)Cl is due to the nature of the chelating amine. In an over-simplified analysis, TsDPENH and TsPDAH are analogous to benzyl ammonium and anilinium, respectively (Figure 2-7). In DMSO, anilinium is more acidic by approximately 6 pK_a

units, loosely explaining the increased acidity of **6** over **10**.[18] As reported, **6** is sufficiently acidic since it can be partially deprotonated by pyridine (*vide supra*). Therefore, a metal complex with an anilinium moiety or something with a similar pK_a is ideal.

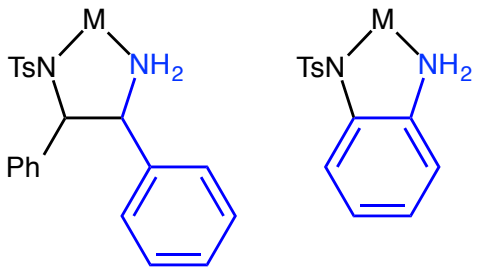

TsDPEN **TsPDA**

Figure 2-7. TsDPEN bound to metal (M), benzyl amine is highlighted in blue (left). TsPDA bound to metal (M), aniline is highlighted in blue (right).

We wanted to probe two factors in the aforementioned systems: (i) the different reactivity between Cp*Rh(TsPDA) and (*p*-cym)Ru(TsDPEN) with H_2 and IPA, and (ii) the markedly different stabilities of Cp*Rh(TsPDAH)H and (*p*-cym)Ru(TsDPENH)H. The known crystal structures of Cp*Rh(TsPDA), Cp*Rh(TsPDAH)Cl, (*p*-cym)Ru(TsDPEN), and (*p*-cym)Ru(TsDPENH)Cl were examined and compared.[13,16,19] The solid-state structure of **5** indicates a plane of symmetry between Rh, the two nitrogens, and the phenyl ring. Once protonated with HCl, the ring flips up to accommodate the formation of a three-legged piano stool complex. The rigid nature of the TsPDA moiety is likely to be the reason behind this large conformational change and a large energy barrier to form a three-legged piano stool. The flexibility in the saturated backbone of TsDPEN is likely to help lower the energy barrier from a two-legged piano stool to three-legged. The solid-state structure of **9** indicates a distortion in the plane of Ru, TsN, NH, and the ethylene linker (Figure 2-8).[16] The solid-state structure of **10** indicates a dihedral angle of 49.35° and no major changes in the angle between the Rh-TsN-NH_2 plane and the TsN-NH_2-ethylene linker plane (Figure 2-8).[19] The flexibility in the chelating ligand of (*p*-cym)Ru(TsDPEN) results in a lower energy barrier between two-legged and three-legged piano stool structures. Therefore, (*p*-cym)Ru(TsDPENH)H is easily formed from IPA, isolable, and thermally stable. On the other hand, there is a large energy barrier when converting Cp*Rh(TsPDA) to Cp*Rh(TsPDAH)Cl, which is a

result of the rigid nature of the TsPDA ligand. Cp*Rh(TsPDAH)H is only stable at 233 K and not isolable.

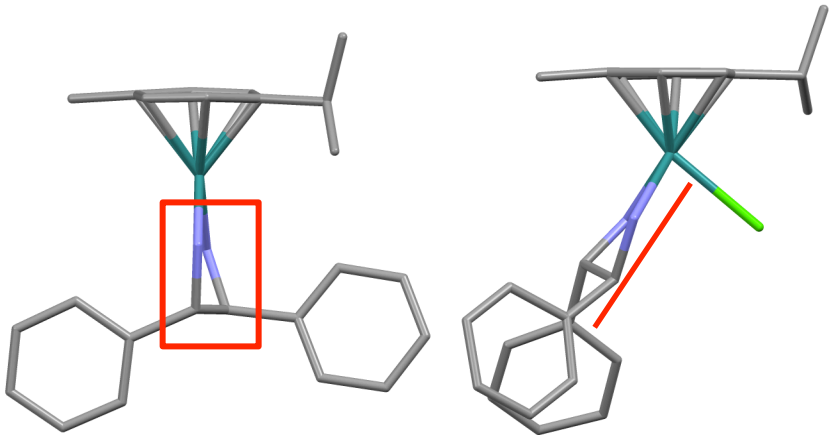

Figure 2-8. Crystal structure of **9** (left). Crystal structure of **10** (right). The tosyl groups and hydrogen atoms have been omitted for clarity. Angles and planes of interest are highlighted. Conformational change from two to three leg piano stool (left to right) maintains the Ru—N—N—ethylene linker plane.[19]

2.2.4 *Initial Results with (*p*-cym)Ru(TsABA)*

Based on the hypotheses about acidity and reactivity of these compounds, we proposed a new ligand that combines both attractive aspects of DPEN and PDA. Use of 1,2-aminobenzylamine as a chelating ligand was explored (Figure 2-9). The non-tosylated nitrogen of the ligand is similar to aniline, so it is likely to have the proper acidity. The methylene linker on the tosylated nitrogen allows for flexibility in the metallocycle, much like the TsDPEN complex. Tosylation of 1,2-aminobenzylamine was performed following literature reports to generate 2-(tosylaminomethyl)aniline ($TsABAH_2$).[20] Reported procedures for similar compounds were adapted for the metallation of $TsABAH_2$. Brown crystals were isolated after layering a DCM solution with hexanes.

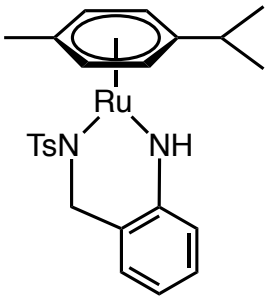

Figure 2-9. Proposed structure for (*p*-cym)Ru(TsABA) (ABA = 2-aminobenzylamine).

The solid-state structure of the brown crystals reveal a dimeric core, [(*p*-cym)Ru(TsABA)]$_2$ (**11**) (Figure 2-10). Compound **11** contains two Ru(II), 18 e$^-$ centers, where the non-tosylated nitrogen (NH) donates to a second Ru center as an L-type ligand. The structure indicates TsN—Ru bond lengths of 2.148(2) and 2.141(2) Å. Despite the bond having imine-like characteristics, the elongation is likely due to the electron withdrawing nature of the tosyl group. This bond length is similar to other TsN—Ru bonds in monomeric species (2.145(8) Å for **10** and 2.065(7) Å for **9**).[19,16] The length of the HN—Ru bonds in **11** are 2.104(2) and 2.115(2) Å, indicating an amine-like bond.[19] HN—Ru bonds with imine-like character have shorter bond lengths; for example, in the 16 e$^-$ coordinatively-unsaturated compound **9** the HN—Ru bond is 1.897(6) Å.[16] To our knowledge, this is the first example of a ruthenium Noyori-type complex forming a dimer. We hypothesize that the ruthenium center of the coordinatively-unsaturated 16 e$^-$ compound (*p*-cym)Ru(TsABA) is electron deficient causing the compound to dimerize and form **11**. A disadvantage of this feature would be the potential increase in acidity due to the electron deficient metal center. However, the electron deficiency could be used to our advantage as well. The increased Lewis acidity of the metal center could increase the reactivity of the metal center with H_2.

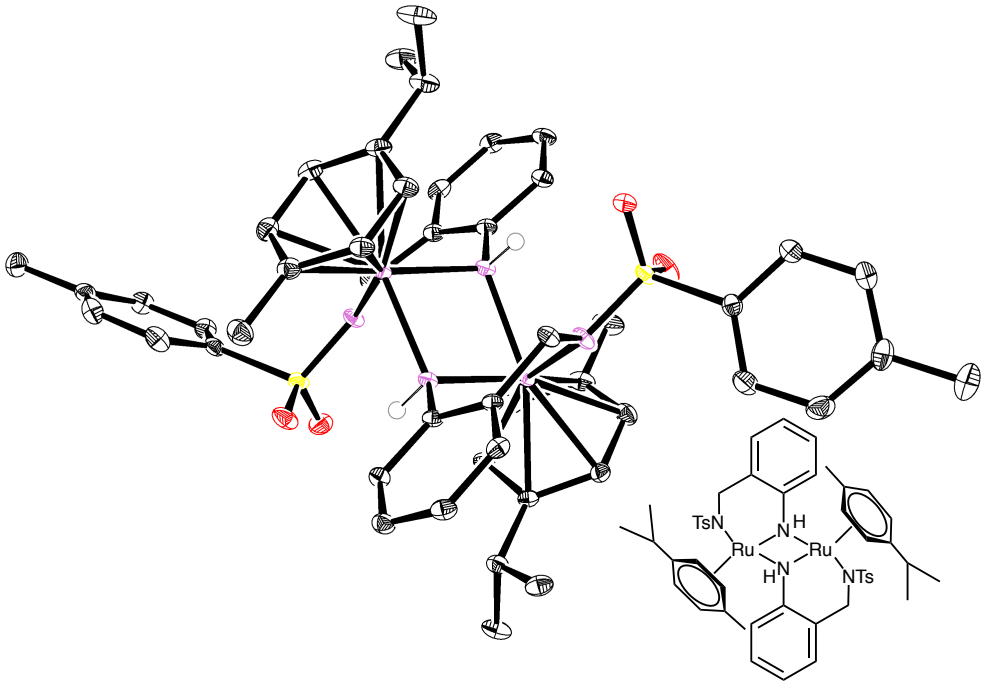

Figure 2-10. ORTEP[21] of **11** with thermal ellipsoids at the 50% probability level. Solvent and some hydrogen atoms omitted for clarity.

Attempts to isolate the monomeric form of **11** have been unsuccessful. Addition of excess HCl to **11** resulted in formation of multiple products, opposed to a clean reaction to form (*p*-cym)Ru(TsABAH)Cl, as expected. Furthermore, **11** was combined with CD_2Cl_2 and 50 bar H_2 stirred at room temperature in a Parr reactor in an attempt to form (*p*-cym)Ru(TsABAH)H *in situ* to react with CD_2Cl_2. If successful, the resulting reaction mixture would contain (*p*-cym)Ru(TsABAH)Cl. The reaction mixture was inspected by ^{1}H NMR spectroscopy and the spectrum was largely identical to ^{1}H NMR spectra of **11** with the addition of IPA. It is likely that IPA was introduced into the reaction from the headspace of the Parr reactor. Owing to the apparent lack of reactivity of **11**, it was no longer pursued for catalysis.

2.3 Conclusions

Work with $Ru(PP)_2H_2$ (**3**), has proven to be unsuccessful as a catalyst for CFC hydrogenolysis. Studies with this system revealed desirable catalyst properties. First and foremost, the base assisted catalysis must utilize a base like NEt_3 or weaker. Stronger

bases have been proven to lead to deprotonation of the desired product ($CHFCl_2$) to form difluorocarbene. $Ru(PP)_2H(H_2)^+$ (**2**) proved to lack the necessary acidity for catalysis. Only 20% deprotonation was observed upon use of DBU as a base. The chloride in $Ru(PP)_2HCl$ (**1**) has proven to be quite labile in halocarbons. Addition of 1 atm of H_2 to a solution in **1** leads to formation of **2**. Also, complex **3** reacts cleanly and quantitatively to **1** within an hour.

In order to address the acidity issues discovered in the $Ru(PP)_2H_2$ system, a new motif was investigated. Based on the synthesis of Cp*Rh(TsPDA) (**5**), we know that Cp*Rh(TsPDAH)Cl (**6**) can be deprotonated completely with NEt_3. pK_a studies revealed that pyridine can be used to partially deprotonate **6** in catalysis. However, it has been found that even with high pressures of H_2, Cp*Rh(TsPDAH)H (**7**) has seemingly poor stability. Reactions performed over months revealed that while reduced halocarbons were observed *in situ*, the reaction was not clean. This prompted the use of a known stable metal hydride with a similar piano stool motif. (*p*-cym)Ru(TsDPEN) (**9**) was shown to react with IPA in minutes to cleanly form (*p*-cym)Ru(TsDPENH)H (**8**), which is isolable and stable at room temperature. Our studies showed the clean reactivity of **8** with CD_2Cl_2 to form CD_2HCl in trace amounts and the formation of (*p*-cym)Rh(TsDPENH)Cl (**10**). Compound **10**, however, cannot be deprotonated with NEt_3. The lack of acidity in **10** and the lack of reactivity of the Cp*Rh(TsPDA) system led to the synthesis of a novel compound, $[(p\text{-cym})Ru(TsABA)]_2$ (**11**). However, reaction of **11** with acid and hydrogen did not lead to formation of the monomeric form of **11** .

2.4 Experimental

General considerations. All experiments and manipulations were performed using standard Schlenk techniques under an argon atmosphere or in an argon- or nitrogen-filled glovebox. Glassware and diatomaceous earth were dried in an oven maintained at 140 °C for at least 24 h. CD_2Cl_2, $CDCl_3$, and C_6D_6 were dried with CaH_2 and distilled prior to use. THF-d_8 was dried with Na/K and distilled prior to use. Protio solvents were passed through columns of activated alumina and molecular sieves. All other reagents were used as received. ^1H NMR spectra were referenced to residual protio solvents: methylene

chloride (5.32 ppm), chloroform (7.26 ppm), benzene (7.16 ppm), THF (1.72, 3,58 ppm).[22] $^{31}P\{^{1}H\}$ NMR shifts were referenced to an 85% H_3PO_4 external standard (0 ppm). ^{19}F NMR shifts were reference to a CF_3COOH external standard (-76.55 ppm). NMR spectra were recorded on either a Bruker AV-500, DRX-500, or AV-300 NMR instrument. X-ray data were collected at −173 °C on a Bruker APEX II single-crystal X-ray diffractometer, with Mo radiation. $[Ru(COD)Cl_2]_n$,[23] 1-methoxy-3-chloropropane,[24] 1,2-bis[dimethoxypropyl)phosphino]ethane (PP), [25] *trans*-$Ru(PP)_2HCl$,[4] $Ru(PP)_2Cl_2$,[8] Cp*Rh(TsPDA),[13] (*p*-cym)Ru(TsDPEN), [26] (*p*-cym)Ru(TsDPENH)H,[16] and 2-(tosylaminomethyl)aniline[20] were synthesized according to published procedures.

Synthesis of $[Ru(PP)_2H(H_2)][B(C_6H_3(CF_3)_2)_4]$ (2):

An NMR tube with a J. Young style Teflon valve was charged with 13.5 mg (0.015 mmole) $Ru(PP)_2HCl$ and 0.5 mL THF-d_8. 14.5 mg (0.016 mmole) $Na(B(C_6H_3(CF_3)_2)_4)$ was added in a nitrogen-filled glovebox. On a Schlenk line, the sample was freeze-pump-thawed and placed under 1 atm H_2. ^{1}H NMR (THF-d_8, 500 MHz, ppm): 9.7-9.1 (m, $B(C_6H_3(CF_3)_2)_4$), 5.3-4.7 (m, ethylene linker), 3.7-3.0 (m, methoxypropyl) -5.0 (br s, $Ru(H_2)$), -9.9 (pent., $^{2}J_{HP}$ = 20 Hz, Ru*H*). $^{31}P\{^{1}H\}$ NMR (THF-d_8, 202 MHz, ppm): 64.1 (s).

Synthesis of $Ru(PP)_2H_2$ (3):

In a nitrogen-filled glovebox, a 100 mL Schlenk flask was charged with 0.099 mg (0.11 mmole) $Ru(PP)_2Cl_2$ and capped with a rubber septum. 10 mL THF was distilled into a second Schlenk flask, then cannula transferred to the flask containing $Ru(PP)_2Cl_2$. 0.3 mL IPA (3.9 mmole) was added to the solution *via* syringe and stirred. Under a heavy flow of argon, the rubber septum was removed and 0.69 mg Na^0 (29.9 mmole) was added to the flask and left to react for 4 hr. Solvent was removed *in vacuo*. The off-white film was extracted 3x20 mL pentane. Solvent was removed *in vacuo*. The off-white solid was redissolved in 20 mL benzene and washed with 10 mL H_2O, dried over $MgSO_4$, and solvent removed *in vacuo*. The reaction mixture resulted in a mixture of *cis*- and *trans*-isomers. ^{1}H NMR (C_6D_6, 500 MHz, ppm): 3.5-3.0 (m, ethylene linker), 2.4-1.1 (m, methoxypropyl), -10.1 (pent., $^{2}J_{HP}$ = 20.1 Hz, *trans*-RuH_2), -10.4 (m, *cis*-RuH_2). $^{31}P\{^{1}H\}$

NMR (C_6D_6, 202 MHz, ppm): 78.0 (s, *trans*-RuH_2), 71.2 (t, $^2J_{PP}$ = 18 Hz, P_a), 58.4 (t, $^2J_{PP}$ = 18 Hz, P_b).

Synthesis of Cp*Rh(TsPDAH)Cl (6):

An NMR tube was charged with 15 mg Cp*Rh(TsPDA) (0.03 mmole) and 0.5 mL CD_2Cl_2 in air. 3 μL 1M HCl in diethyl ether (0.03 mmole) was added to the tube resulting in a dark brown solution. ^{1}H NMR (CD_2Cl_2, 500 MHz, ppm): 8.0 (d, $^3J_{HH}$ = 15 Hz, 2H; tosyl Ar-*H*), 7.4 (d, $^3J_{HH}$ = 10 Hz, 1H; Ar-*H*), 7.1 (d, $^3J_{HH}$ = 10 Hz, 2H; tosyl Ar-*H*), 7.0 (d, $^3J_{HH}$ = 15 Hz, 1H; Ar-*H*), 6.8 (t, $^3J_{HH}$ = 8 Hz, 1H; Ar-*H*), 6.5 (t, $^3J_{HH}$ = 8 Hz, 1H; Ar-*H*), 5.2 (br s, 1H; NH_a), 4.5 (br s, 1H; NH_b), 2.3 (s, 3H; tosyl-CH_3), 1.7 (s, 15H; $C_5(CH_3)_5$).

Synthesis of [(p-cym)Rh(TsABA)]$_2$ (11):

A 25 mL round bottom flask was charged with 101 mg [(*p*-cym)$RuCl_2]_2$ (0.17 mmole), 91 mg TsABA (0.33 mmole), and 95 mg potassium hydroxide (1.7 mmole). The round bottom flask was capped with a rubber septum and sparged with argon. 5.0 mL CH_2Cl_2 was transferred to the round bottom flask *via* syringe. The reaction was stirred at room temperature for 1 hr resulting in a dark green solution. The reaction mixture was washed 3x1mL H_2O then dried with $MgSO_4$. Solvent was removed *via* rotary evaporation resulting in a green film. X-ray quality crystals were grown from a CH_2Cl_2 solution layered with hexane.

2.5 Notes for Chapter 2

1) Work by Jean-Philippe Porcher, Heinekey lab, 2011.
2) Gilbertson, J. D.; Szymczak, N. K.; Tyler, D. R., *J. Am. Chem. Soc.,* **2005**, *127*, 10184-10185.
3) a) Miller, W. K.; Gilbertson, J. D.; Leiva-Paredes, C.; Bernatis, P. R.; Weakley, T. J. R.; Lyon, D. K.; Tyler, D. R., *Inorg. Chem.,* **2002**, *41*, 5453-5465. b) Gilbertson, J. D.; Szymczak, N. K.; Crossland, J. L.; Miller, W. K.; Lyon, D. K.; Foxman, B. M.;

Davis, J.; Tyler, D. R., *Inorg. Chem.,* **2007**, *46*, 1205-1214. c) Crossland, J. L.; Young, D. M.; Zakharov, L. N.; Tyler, D. R., *Dalton Trans.,* **2009**, *42*, 9253-9259.

4) Szymczak, N. K.; Braden, D. A.; Crossland, J. L.; Turov, Y.; Zakharov, L. N.; Tyler, D. R., *Inorg. Chem.,* **2009**, *48*, 2976-2984.
5) Siegel, J. S. and Anet, F. A. L., *J. Org. Chem.,* **1988**, *53*, 2629-2630.
6) Jacobsen, N. E., *NMR Spectroscopy Explained: Simplified Theory, Applications and Examples for Organic Chemistry and Structural Biology*, 1st ed.; John Wiley & Sons, Inc.: New Jersey, 2007.
7) Heinekey, D. M. and Oldham Jr., W. J., *Chem. Rev.,* **1993**, *93*, 913-926.
8) Szymczak, N. K.; Zakharov, L. N.; Tyler, D. R., *J. Am. Chem. Soc.*, **2006**, *128*, 15830-15835.
9) Cappellani, E. P.; Drouin, S. D.; Jia, G.; Maltby, P. A.; Morris, R. H.; Schweitzer, C. T., *J. Am. Chem. Soc*., **1994**, *116*, 3375-3388.
10) Rodima, T.; Kaljurand, I.; Pihl, A.; Mäemets, V.; Leito, I.; Koppel, I. A., *J. Org. Chem.,* **2002**, *67*, 1873-1881.
11) Schwesinger, R.; Schlemper, H.; Hasenfratz, C.; Willaredt, J.; Dambacker, T.; Breuer, T.; Ottaway, C.; Fletschinger, M.; Boele, J.; Fritz, H.; Putzas, D.; Rotter, H. W.; Bordwell, F. G.; Satish, A. V.; Ji, G.; Peters, E.; Peters, K.; von Schnering, H. G.; Walz, L., *Liebigs Annalen,* **1996**, *7*, 1055-1081.
12) a) Brahms, D. L. S. and Dailey, W. P., *Chem. Rev.,* **1996**, *96*, 1585-1632. b) Hine, J. and Dowell Jr., A. M., *J. Am. Chem. Soc.,* **1954**, *76*, 2688-2692. c) Hine, J. and Burske, N. W., *J. Am. Chem. Soc.,* **1956**, *78*, 3337-3339. d) Hine, J., *J. Am. Chem. Soc.,* **1950**, *72*, 2438-2445. e) Hine, J.; Peek, R. C.; Oakes, B. D., *J. Am. Chem. Soc.,* **1954**, *76*, 827-829. f) Hine, J.; Dowell Jr., A. M.; Singley Jr., J. E., *J. Am. Chem. Soc.,* **1956**, *78*, 479-482.
13) Blacker, A. J.; Clot, E.; Duckett, S. B.; Eisenstein, O.; Grace, J.; Nova, A.; Perutz, R. N.; Taylor, D. J.; Whitwood, A. C., *Chem. Commun.,* **2009**, *44*, 6801-6803.
14) Ito, M.; Hirakawa, M.; Murata, K.; Ikariya, T., *Organometallics*, **2001**, *20*, 379-381.
15) a) Fryzuk, M. D.; Jones, T.; Einstein, F. W. B., *Organometallics*, **1984**, *3*, 185-191. b) Carmona, D.; Oro, L. A.; Lamata, M. P.; Puebla, M. P.; Ruiz, J.; Maitlis, P. M., *J.*

Chem. Soc., Dalton Trans., **1987**, 639-645. c) White, C.; Oliver, A. J.; Maitlis, P. M., *J. Chem. Soc., Dalton Trans.,* **1973**, 1901-1907.

16) Haack, K.; Hashiguchi, S.; Fujii, A.; Ikariya, T.; Noyori, R., *Angew. Chem. Int. Ed.,* **1997**, *36*, 285-288.

17) Sandoval, C. A.; Ohkuma, T.; Muñiz, K.; Noyori, R., *J. Am. Chem. Soc.,* **2003**, *125*, 13490-13503.

18) Crampton, M. R. and Robotham, I. A., *J. Chem. Res.,* **1997**, 22-23.

19) Uematsu, N.; Fujii, A.; Hashiguchi, S.; Ikariya, T.; Noyori, R., *J. Am. Chem. Soc.,* **1996**, *118*, 4916-4917.

20) Sanmartín, J.; Novio, F.; García-Deibe, A. M.; Fondo, M.; Bermejo, M. R., *New J. Chem.,* **2007**, *31*, 1605-1612.

21) Farrugia, L. J., Ortep-3 for Windows, *J. Appl. Cryst.*, **1997**, *30***,** 565-566.

22) Fulmer, G. R.; Miller, A. J. M.; Sherden, N. H.; Gottlieb, H. E.; Nudelman, A.; Stoltz, B. M.; Bercaw, J. E.; Goldberg, K. I., *Organometallics*, **2010**, *29*, 2176-2179.

23) Albers, M. O; Ashworth, T. V.; Oosthuizen, H. E.; Singleton, E., *Inorg. Synth.,* **1989**, *26*, 68-77.

24) Letsinger, R. L. and Schnizer, A. W., *J. Org. Chem.,* **1951**, *16*, 704-707.

25) Herbowski, A. and Deutsch, E. A., *J. Organomet. Chem.,* **1993**, *460*, 19-23.

26) Giuffredi, G. T.; Purser, S.; Sawicki, M.; Thompson, A. L.; Gouverneur, V., *Tetrahedron: Asymmetry*, **2009**, *20*, 910-920.

Chapter 3

Pincer Complexes of Rhodium

3.1 Introduction

3.1.1 *General Introduction to Pincer Chemistry*

Moulton and Shaw first reported the synthesis of a novel set of ligands known as "pincers" owing to their crab-like coordination to metal centers.[1] Pincer ligated compounds are typically robust due to the *tris*-chelating nature of the ligand to coordinate in a meridional fashion. Due to the high stability of pincer complexes and ease of electronic and steric tunability there has been widespread use in inorganic and organometallic chemistry.[2] While the literature on these ligands has expanded in the past decades to include different motifs and atoms bound to the metal center, the classic PCP and POCOP ligands are still widely used (PCP = C_6H_3-1,3-$[CH_2P(R)_2]_2$; POCOP = C_6H_3-1,3-$[OP(R)_2]_2$; R = aryl or alkyl; Figure 3-1).

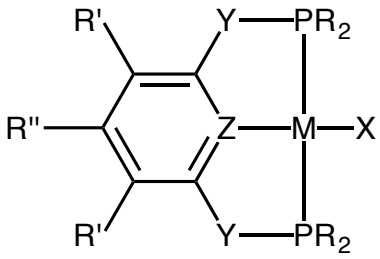

Figure 3-1. A generalized illustration of pincer ligands. M = metal; R = alkyl or aryl group; Z = C or N, commonly; Y = O or CH_2, commonly; X = halide; R' and R'' = placement of electronically or sterically tunable groups.

The mechanism of metallation in pincer compounds, such as those containing PCP and POCOP, has been extensively studied.[3] Metallation of such ligands usually proceeds *via* metal coordination to the phosphorus atoms followed by C—H activation at the *ipso*-carbon leading to oxidative addition. There are, however, limited examples in the literature of complexes that may resemble intermediates in this process.[4] This chapter

describes the isolation of a (POCOP)Rh compound with a strong C_{ipso}—H agostic interaction as indicated by X-ray crystallography.

3.1.2 *Proposed Catalysis of Chlorofluorocarbons with Rhodium Pincer Compounds*

Rhodium pincer compounds were investigated for catalysis towards hydrogenolysis of chlorofluorocarbons. Work in the literature has highlighted the exceptional acidity of dihydrogen ligands on certain pincer compounds, which could be advantageous for our targeted catalysis. Prior work from our lab approximated the pK_a of an Ir-dihydrogen species; $[Cp^*Ir(dmpm)(H_2)]^{2+}$ ($Cp^* = C_5(CH_3)_5^-$; dmpm = bis(dimethylphosphino)-methane) is deprotonated with triflate, a very weak base.[5,6] While the species has a much different ligand scaffold, it illustrates that Ir-dihydrogen compounds can be highly acidic. Recently, work from our group has shown that *trans*-(^{tBu}POCOP)Ir(CO)H_2 can be formed from (^{tBu}POCOP)Ir(CO) by addition of low pressures of H_2 and a catalytic amount of acid (Scheme 3-1).[7] (^{tBu}POCOP)Ir(CO) is protonated to form [(^{tBu}POCOP)Ir(CO)H]$^+$. Dihydrogen can coordinate to the metal to form [(^{tBu}POCOP)Ir(CO)(H_2)H]$^+$; the dihydrogen ligand becomes very acidic and is easily deprotonated to form (^{tBu}POCOP)Ir(CO)H_2. Lao *et al.* demonstrated this by reacting (^{tBu}POCOP)Ir(CO) with H_2 and a catalytic amount of anilinium tetrafluoroborate in THF. (^{tBu}POCOP)Ir(CO)H_2 is not observed without addition of acid. The pK_a of anilinium is 10.62 (MeCN), indicating that aniline is a much weaker base than triethyl amine (pK_a of triethyl ammonium ($HNEt_3^+$) (MeCN) = 18.82).[8] As previously discussed, NEt_3 is the strongest base that can be used in our targeted catalysis. Unpublished results from our group show that pyridinium can be used in a reaction analogous to that of Lao *et al*. Here the conjugate base is pyridine, which is again a weaker base than NEt_3.[8]

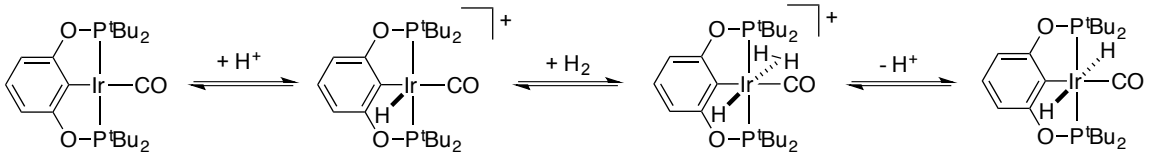

Scheme 3-1. Acid catalyzed formation of (^{tBu}POCOP)Ir(CO)H_2 species.

In closely related work, Brookhart and coworkers report the acid catalyzed formation of (^{tBu}PONOP)Ir(CH_3)H_2 from (^{tBu}PONOP)Ir(CH_3) (^{tBu}PONOP = κ^3-2,6-bis(di-*tert*-butylphosphinito)pyridine).[9] Water acts as an acid to protonate the neutral (^{tBu}PONOP)Ir(CH_3) species. Addition of H_2 forms *trans*-[(^{tBu}PONOP)Ir(CH_3)H(H_2)]$^+$, water then deprotonates the dihydrogen-hydride to form *trans*-(^{tBu}PONOP)Ir(CH_3)H_2. In this study, the *trans*-dihydrogen-hydride species is observed *in situ* at -90 °C in methylene chloride-d_2 (CD_2Cl_2) and was deprotonated with 10 equiv. of NEt_3. It is proposed that water can act as the acid and base in this transformation.

Based on the previous findings of both Heinekey and Brookhart, we propose a catalytic cycle that could proceed *via* one of two routes (Scheme 3-2). (i) (^{R}POCOP)Rh(CO) (R = *t*Bu or *i*Pr) oxidatively adds H_2 and isomerizes to form *trans*-(^{R}POCOP)Rh(CO)H_2, which reacts with the chlorinated substrate. The resulting *trans*-(^{R}POCOP)Rh(CO)HCl can lose HCl to regenerate (^{R}POCOP)Rh(CO). (ii) (^{R}POCOP)Rh(CO) is protonated with HCl to form *trans*-(^{R}POCOP)Rh(CO)HCl. Dihydrogen can displace chloride to form *trans*-[(POCOP)Rh(CO)(H_2)H]$^+$. As discussed, this dihydrogen ligand is likely to be acidic and easily deprotonated to form *trans*-(^{R}POCOP)Rh(CO)H_2. The dihydride species would react with the metal-chloride to regenerate *trans*-(POCOP)Rh(CO)HCl. While we targeted the use of compounds like those shown in Scheme 3-2 for catalytic hydrogenolysis of CFCs, during our studies we isolated a novel rhodium species with an η^2-C—H interaction. This chapter outlines the characterization of this compound, followed by initial studies towards catalysis.

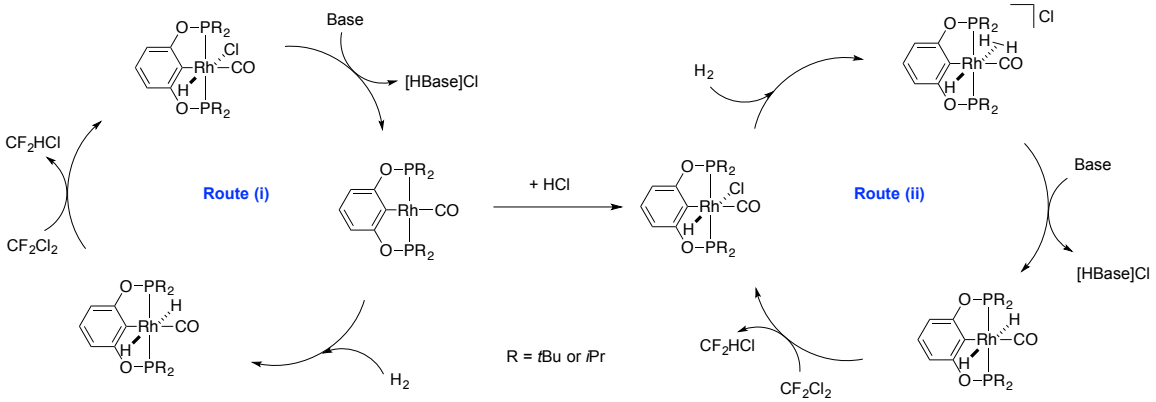

Scheme 3-2. Proposed catalysis using Rh-pincer compounds. Left, route (i); right, route (ii).

3.1.3 *Previous Work with Rhodium Pincer Complexes*

Limited examples of complexes that resemble intermediates in pincer metallation reactions exist in the literature. Milstein has isolated two PCP ligated systems with an aromatic agostic interaction (Figure 3-2).[10] Milstein's naphthyl-based PCP system (A, Figure 3-2) is formed by reaction of (*nap*-PCP)Rh(CO) with $[HEt_2O][BF_4]$ (HBF_4) or $[H(Et_2O)_2][B(C_6H_3(CF_3)_2)_4]$. The product is isolable and the room temperature ^1H NMR spectrum displays a signal at *ca*. 3.9 ppm in CD_2Cl_2 for the *ipso*-proton. [(*nap*-PCP)Rh(CO)H]$^+$ has not been characterized by X-ray diffraction.[10b] However, [(^{tBu}PCP)Rh(CO)H]$^+$ (Figure 3-2, compound B) has been isolated and characterized by X-ray diffraction. [(^{tBu}PCP)Rh(CO)H][OTf] (**12**) is synthesized *via* metallation of (^{tBu}PCP) with $[Rh(C_2H_4)(CO)(solv)_n][OTf]$ (n = 1, 2).[10a] [(^{iPr}PCP)Rh(CO)H]$^+$ is synthesized *via* addition of excess CO to [(^{iPr}PCP)Rh(acetone)$_2$H][BF_4].[11] Both *i*Pr and *t*Bu analogues have been characterized by X-ray crystallography. The *ipso*-proton is located at *ca*. 4 ppm in the ^1H NMR spectrum.

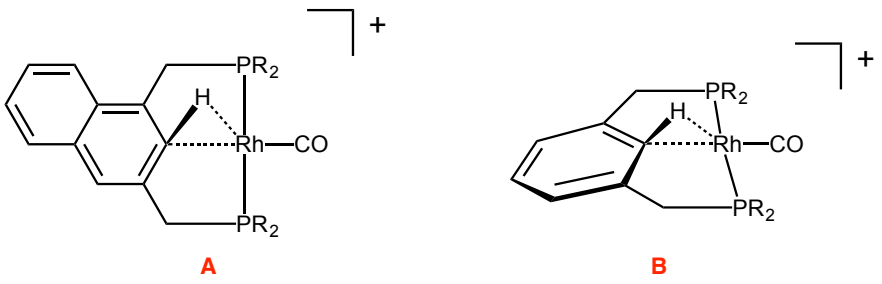

Figure 3-2. Previously reported examples of agostic interactions in Rh pincer complexes reported by Milstein and coworkers.[10]

3.2 Synthesis and Characterization of [(^{tBu}POCOP)Rh(CO)H][$B(C_6F_5)_4$]

3.2.1 *Synthesis*

(^{tBu}POCOP)Rh(CO) (**13**) was synthesized and isolated *via* reported methods.[12] Addition of 1 eq. of $[H(Et_2O)_2][B(C_6F_5)_4]$ ($HBArF_{20}$) to a fluorobenzene solution of **13** affords [(^{tBu}POCOP)Rh(CO)(H)][$BArF_{20}$] (**14**) (Scheme 3-3). X-ray quality crystals were obtained by layering with pentane.

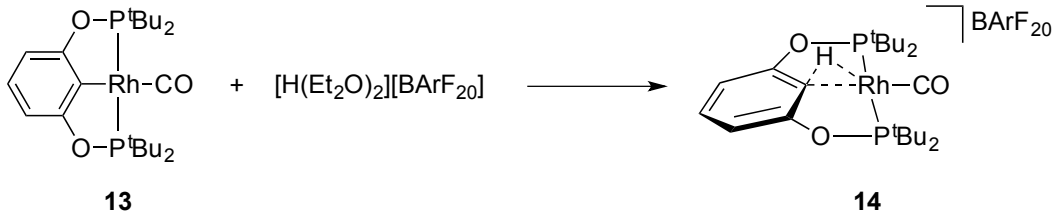

13 **14**

Scheme 3-3. Synthesis of **14**.

3.2.2 *Solid State Characterization*

The molecular structure of **14** (Figure 3-3) reveals the POCOP aryl ring bent out of the Rh—P—(CO) plane as a result of protonation at the *ipso*-carbon. The hydrogen atom on the *ipso*-carbon has been explicitly located in the electron density map. The Rh metal center in **14** is best described as square planar, indicating a formal oxidation state of Rh(I). While Milstein and coworkers have published multiple examples of PCP-ligated systems exhibiting agostic interactions in the solid state, compound **14** is, to the best of our knowledge, the first example of protonation at the *ipso*-carbon of a POCOP ligated compound.[4,10,11] Selected bond lengths and angles have been listed in Table 3-1 for **14**, Milstein's previously reported [(^{tBu}PCP)Rh(CO)H]OTf (**12**), and the respective Rh(I) carbonyl analogues.[10a] Figure 3-4 depicts two angles used to describe the deviation of C_{ipso}—H from sp^2 hybridization and the aryl ring from the square plane of the metal center. As indicated by angle **B**, the C_{ipso}—H bond in **14** deviates more from planarity than **12**, indicating that C(1) is *less* sp^2-like in **14** than **12**. The aryl ring in **12** is bent *less* out of the square plane of the metal center. Moreover, the difference in Rh—C_{ipso} bond length is greater in the PCP system than with POCOP. This points towards a stronger agostic interaction in **14**, possibly nearing oxidative addition of the C_{ipso}—H bond to Rh.

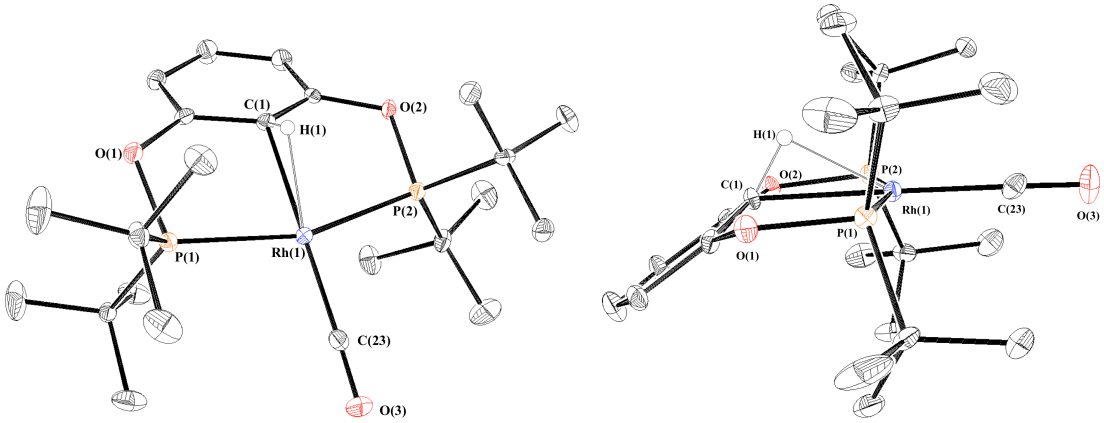

Figure 3-3. a) ORTEP[13] diagram for **14** shown with 30% thermal ellipsoids. Counter ion and all hydrogens except H(1) have been omitted for clarity. b) Side view of **14** displaying the orientation of the aryl ring, Rh center, and H(1).

	(^{tBu}POCOP)Rh(CO)H$^+$(14)	(^{tBu}PCP)Rh(CO)H$^+$(12)	(^{tBu}POCOP)Rh(CO) (13)	(^{tBu}PCP)Rh(CO)
Angle A	36.17	44.24	---	---
Angle B	22.86	14.34	---	---
P(1)—Rh(1)—P(2)	161.09(4)	167.32(5)	157.32(3)	163.7(1)
Rh(1)—H(1)—C(1)	91(3)	97.57	---	---
Rh(1)—C(1)—H(1)	59(3)	58.28	---	---
Rh(1)—C(1)	2.148(4)	2.273(5)	2.043(3)	2.08(1)
Rh(1)—C(23)	1.862(5)	1.820(5)	1.887(3)	1.848(16)
Rh(1)—P(1)	2.314(1)	2.330(2)	2.2816(9)	2.283(3)
Rh(1)—P(2)	2.313(1)	2.325(2)	2.2829(11)	2.292(3)
C(23)—O(3)	1.138(6)	1.146(6)	1.133(4)	1.128(16)

Table 3-1. Select bond lengths (Å) and angles(°) for **14**, **12**, **13**, and (^{tBu}PCP)Rh(CO).[10a,14,15]

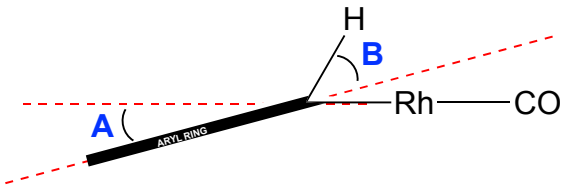

Figure 3-4. A side-on view of **12** and **14**; the linker arms are omitted for clarity. Angles **A** and **B** are highlighted.

3.2.3 *Solution State Characterization*

The agostic interaction indicated by the solid state molecular structure has been probed in the solution state by both NMR and IR spectroscopy. ^{1}H NMR spectroscopy of **14** revealed a doublet centered at -6.50 ppm where J_{RhH} = 34.8 Hz (CD_2Cl_2). The large J_{RhH} value suggests a strong Rh—(C-H) bond interaction, especially compared to **12**

where J_{RhH} = 18.1 Hz.[10a,16] The $^{31}P\{^{1}H\}$ NMR spectrum of **14** exhibited a doublet centered at 202 ppm with $^{1}J_{RhP}$ = 107 Hz. This coupling is relatively small compared to compound **13** ($^{1}J_{RhP}$ = 157 Hz) which indicates a less electron rich metal center, possibly suggesting more Rh(III) character versus Rh(I). ^{13}C NMR spectroscopy data reveals a doublet at 105.2 ppm for the *ipso*-carbon with $^{1}J_{CH}$ = 76 Hz. This diminished coupling constant is consistent with a high degree of activation of the C—H bond. A hydrogen bound to an sp^2 carbon atom, as in benzene, has a coupling constant of *ca.* 159 Hz.[17] For complex **12**, Milstein and coworkers report $^{1}J_{CH}$ = 123 Hz for the *ipso*-carbon. The significant decrease in coupling constant indicates a weaker C—H bond, and possibly a stronger agostic interaction in compound **14**. The increased agostic interaction in **14** is due to the general weaker σ-donation capabilities of POCOP versus PCP. This leads to a less electron rich metal center, which favors stronger agostic interactions.[18]

Low temperature ^{1}H NMR spectroscopy suggests an equilibrium between an agostic species (**14a**) and 5-coordinate Rh-hydride (**14b**) (Scheme 3-4). Lowering the temperature of the sample to -60 °C shifted the C_{ipso}—*H* doublet upfield by 0.72 ppm and J_{RhH} increased by 0.8 Hz (Figure 3-5). Based on other similar species, we expect **14b** to have a signal at -25 ppm or further upfield.[12,19,20] Similar pincer compounds with aromatic agostic interactions, similar to **14a**, have low field ^{1}H NMR signals (*ca.* 3-6 ppm)[4a,10] and the C_{ipso}—*H* of non-ligated ^{tBu}POCOP has a proton signal at 7.0 ppm. Thus, the room temperature ^{1}H NMR signal at -6.50 ppm is an average of the ^{1}H NMR signals of **14a** and **14b**. The high field shift at lower temperature suggests a shift in equilibrium towards **14b**, suggesting **14b** is the thermodynamically more stable species. Reported five-coordinate Rh(III) hydride species resembling **14b** have J_{RhH} of *ca*. 55 Hz, while agostic species similar to **14a** have coupling constants near 18 Hz.[10,15] Thus, the room temperature coupling constant of 34.8 Hz is a reasonable value for the population weighted average. The increase in J_{RhH} at lower temperatures is consistent with the equilibrium outlined in scheme 3-4. As the equilibrium is shifted towards a five-coordinate Rh(III)-hydride, the coupling constant is expected to increase in magnitude.

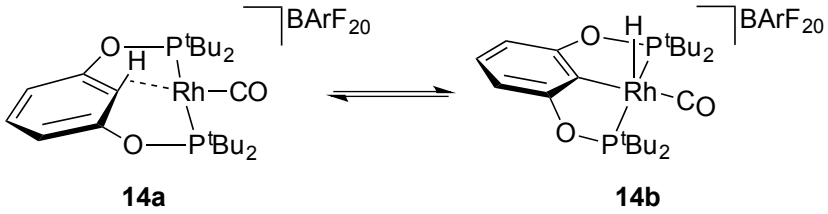

Scheme 3-4. Proposed equilibrium of **14** where the hydrogen goes from an agostic interaction (**14a**) to a Rh—H species (**14b**).

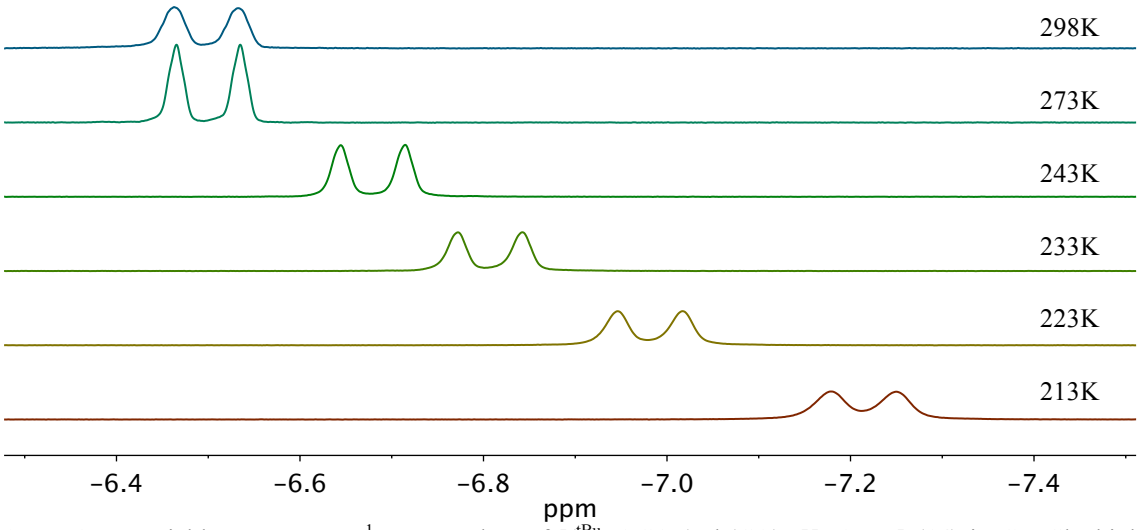

Figure 3-5. Variable temperature ^{1}H NMR data of [(^{tBu}POCOP)Rh(CO)H][BArF$_{20}$] (**14**) in CD_2Cl_2, high field region is shown.

A partially deuterated sample of **14** was prepared by combining **13** and [D(Et$_2$O)$_2$][BArF$_{20}$] in fluorobenzene to form **14-***d*$_1$.[21] The ^{2}H NMR spectrum of the resulting reaction mixture showed a broad singlet at -4.6 ppm, 2.5 ppm downfield of the corresponding proton signal in **14**. This observation suggests that there is an isotopic perturbation of an equilibrium between two structures. The isotopic perturbation shifts the relative concentrations of **14a-***d*$_1$ and **14b-***d*$_1$ towards **14a-***d*$_1$ due to the relatively stronger C—D *versus* Rh—D bonds, thus shifting the averaged chemical shift downfield.[16]

Previous reports indicate that, generally, Rh(I)-carbonyl compounds have CO stretching frequencies near 1900 cm^{-1} and Rh(III) compounds have frequencies of 2000 cm^{-1} or higher.[22] Compound **14** exhibits two IR bands, which we have assigned as compounds **14a** and **14b**. While on the NMR spectroscopy time scale the equilibrium

between compounds **14a** and **14b** is too fast to observe even at -80 °C, we find that on the IR spectroscopy time scale both compounds **14a** and **14b** are observed individually (Figure 3-6). The band assigned to **14b** (2083 cm^{-1}) is consistent with other Rh(III)(CO) species, including (^{iPr}POCOP)Rh(CO)HCl (2064 cm^{-1}) which has been independently synthesized, *vide infra* (Table 3-2). The band assigned to **14a** (2024 cm^{-1}) is higher in energy than other Rh(I)(CO) species in the literature such as **13** and (^{tBu}PCP)Rh(CO) (1956 and 1925 cm^{-1}, respectively). However, reported cationic Rh(I)(CO) species in the literature have υ_{CO} at or higher than 2000 cm^{-1}.[23]

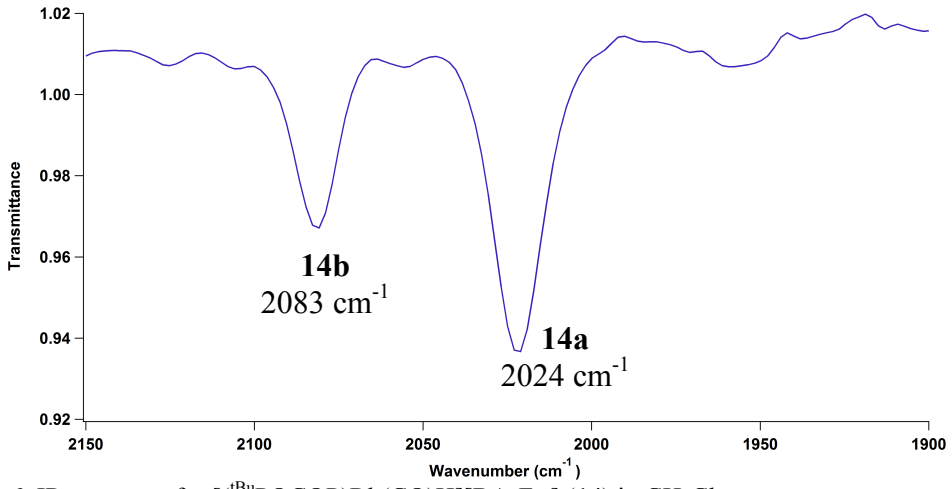

Figure 3-6. IR spectrum for [(^{tBu}POCOP)Rh(CO)H][$BArF_{20}$] (**14**) in CH_2Cl_2.

	υ_{CO} (cm^{-1})
13	1956
14a	2024
14b	2083
[(^{tBu}PCP)Rh(CO)H]$^+$ [10a]	1981[a]
(^{tBu}PCP)Rh(CO)[1]	1925[a]
(^{iPr}POCOP)Rh(CO)HCl	2064

Table 3-2. Selected IR data for rhodium pincer complexes. Data was collected in solution cells with CH_2Cl_2. [a]Obtained as a film.

3.3 Synthesis and Reactivity of (^{iPr}POCOP)Rh(CO)

Milstein has reported the synthesis of (^{iPr}POCOP)Rh(CO) (**15**) by reacting a mixture of (^{iPr}POCOP)Rh(N_2) and [(^{iPr}POCOP)Rh]$_2$(μ-N_2) with CO in C_6D_6.[24] A modified synthesis is reported herein. (^{iPr}POCOP)RhHCl was prepared according to reported methods.[19a] The reaction mixture was sparged with CO, transforming the red solution to bright orange. $^{31}P\{^1H\}$ NMR spectroscopy of this reaction mixture reveals the formation of **15** and (^{iPr}POCOP)Rh(CO)HCl (**16**) in a 1:0.7 ratio. In contrast, sparging (^{tBu}POCOP)RhHCl with CO leads to complete conversion to **13** (*vide infra*). The orange product mixture was passed through neutral alumina, resulting in a yellow solution and pure **15**. The independent synthesis of **16** was achieved by reacting **15** with HCl. The hydride region of the ^1H NMR spectrum exhibits a doublet of triplets at -14.5 ppm ($^1J_{RhH}$ = 24 Hz; $^2J_{HP}$ = 10 Hz; C_6D_6) and the $^{31}P\{^1H\}$ NMR spectrum exhibited a doublet at 200 ppm ($^1J_{RhP}$ = 104 Hz).

To form [(^{iPr}POCOP)Rh(CO)H]$^+$ (**17**), HBF_4 was combined with a benzene solution of **15**. The resulting ^1H NMR spectrum contained a broad signal at -21.6 ppm (J_{RhH} = 32 Hz) and a corresponding doublet at 199 ppm ($^1J_{RhP}$ = 106 Hz, C_6D_6) in the $^{31}P\{^1H\}$ NMR spectrum. The high field signal in the ^1H NMR spectrum is indicative of a five-coordinate species, however broadness of the signal suggests a fluxional process—perhaps similar to **14a**/**14b** or binding of BF_4^- coordination to the open site. Protonation of **15** with $HBArF_{20}$ in fluorobenzene resulted in a $^{31}P\{^1H\}$ NMR signal (196 ppm, $^1J_{RhP}$ = 106 Hz) nearly identical to the $^{31}P\{^1H\}$ NMR spectrum when using HBF_4. This suggests that there is no BF_4^- coordination, as $BArF_{20}$ is too bulky to bind. However the ^1H NMR signal is different; a broad doublet is observed at -17.6 ppm (J_{RhH} = 34 Hz).

Low temperature ^1H NMR spectroscopy was used in order to probe any possible agostic interaction in compound **17** (Figure 3-7) Due to the high freezing point of C_6D_6 and fluorobenzene, CD_2Cl_2 was utilized in the experiment. Upon lowering the temperature of the sample to -80 °C, the proton signal for **17** (at -17.6 ppm) moves downfield slightly (0.1 ppm). The signal at -17.8 ppm moves upfield as the temperature is lowered. At -40 °C the signal splits into two, which move further apart as the temperature decreases. The identity of the two species at -40 °C has not been determined. Unexpected

reactivity was observed upon prolonged exposure of **17** to CD_2Cl_2 (18 h). Two new hydride signals at -9.1 ppm (multiplet) and -17.8 ppm (J = 26 Hz) were recorded in the ^{1}H NMR spectrum. We hypothesize that the signal at -17.8 ppm is due to a solvent coordinated species, [(^{iPr}POCOP)Rh(CO)H(CD_2Cl_2)]$^+$. This observation would be consistent with a less sterically encumbered sixth coordination site.

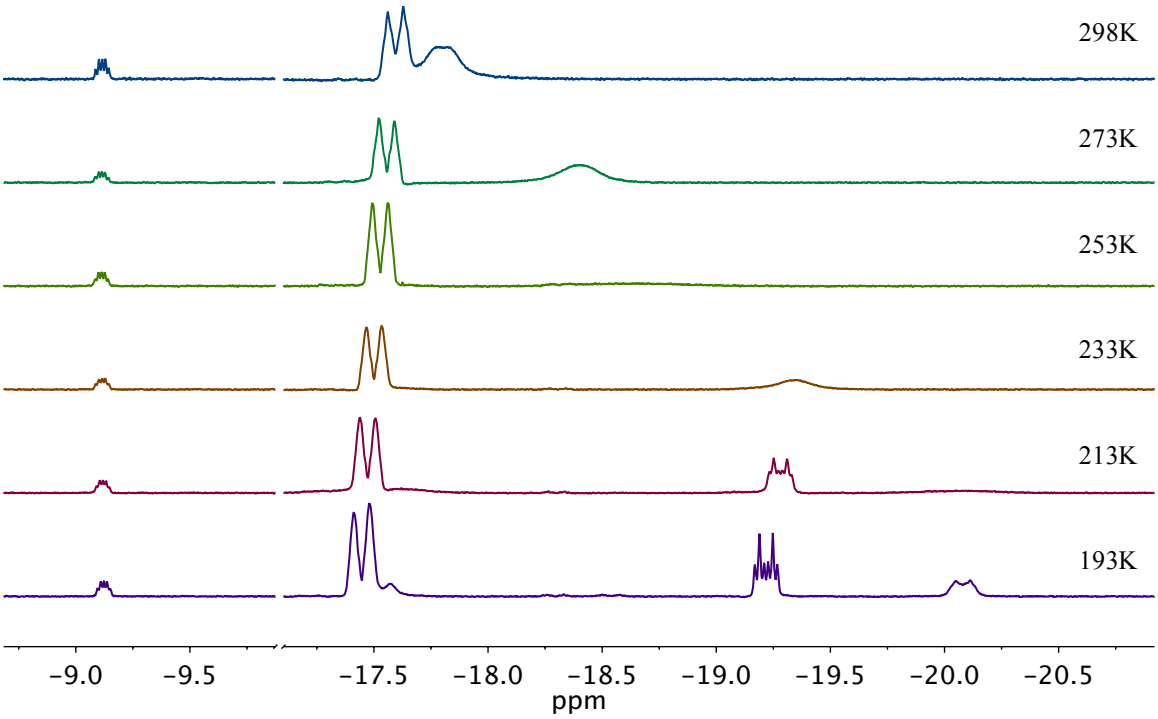

Figure 3-7. Variable temperature ^{1}H NMR spectra of **17** in CD_2Cl_2.

Deuterium incorporation was explored by combining $DBArF_{20}$ and **15** in fluorobenzene. ^{2}H NMR spectra exhibited a deuterium signal at -12 ppm ($\Delta\nu_{½}$ = 13 Hz). This is a downfield shift of ~5 ppm from the ^{1}H NMR spectrum. This is consistent with what was observed with [(^{tBu}POCOP)Rh(CO)H]$^+$, and suggests that there is in fact an equilibrium where there is an agostic species involved.

While it seems protonation of **15** to **17** similarly forms an agostic species like **13** to **14**, increased reactivity at the metal center makes characterization in the solution state non-trivial. The increased reactivity is likely due to a more open coordination site with (^{iPr}POCOP) versus the bulkier (^{tBu}POCOP).

3.4 pK_a Studies of (^{tBu}POCOP)Rh(CO)H$^+$ and (^{iPr}POCOP)Rh(CO)H$^+$ Species

Milstein and coworkers have reported that due to the acidity of the C_{ipso}—*H* bond, addition of D_2O leads to deuterium incorporation into **12** in THF.[10a] Presumably, D_2O deprotonates **12** to form D_2HO^+ which protonates the neutral carbonyl species, leading to deuterium incorporation. Greater than 28.6 eq. of water per metal center led to deprotonation of **12** to form (^{tBu}PCP)Rh(CO). Similarly, we find that treatment of a DCM solution of **14** with ~5 eq. of D_2O gives deuterium incorporation, as indicated by the corresponding signal in the ^{2}H NMR. We however find that upon addition of 10.5 eq of water deprotonation of **14** is observed, implying that **14** is *more* acidic than **12**. This is expected as the C—H bond is more activated in **14** than in **12**.

Reaction of $HBArF_{20}$ and **13** (1:1) results in complete conversion to **14**. Unsurprisingly, a large excess of Et_2O leads to deprotonation of **14**. Upon addition of 40 equiv. of Et_2O to a fluorobenzene solution of **14**, the $^{31}P\{^1H\}$ spectrum exhibits a 3:7 ratio of compounds **13**:**14**. From this established equilibrium and the reported pK_a value of Et_2OH^+ (pK_a (H_2O) = -3.6),[25] we approximate a pK_a value of -1.2 for **14**. A second pK_a study was performed by protonation of **13** with *para*-nitroanilinium ($PNAH^+$, pK_a (MeCN) = 6.22).[8] Stoichiometric amounts of **13**, PNA, and $HBArF_{20}$ were combined in fluorobenzene and observed by NMR spectroscopy. The $^{31}P\{^1H\}$ NMR spectrum was integrated to find the relative concentrations of **13** and **14**. Using the pK_a of $PNAH^+$ in MeCN, 1.3 is the calculated pK_a value for **14**. The discrepancy in the two measured pK_a values could be due to solvent effects. The pK_a measurement of **14** was performed in fluorobenzene, but the known pK_a values used in calculations were reported in H_2O and MeCN. As previously discussed, ion pairing is greatly affected by the properties of the solvent. Additionally, we hypothesize that the solution structure of **14** is not as straightforward as initially expected. The observed ^{1}H NMR signal for the *ipso*-proton of **14** is a broad doublet ($\Delta\nu_{½}$ = ~11 Hz). Originally, this was proposed to be due to the equilibrium outlined in Scheme 3.4. Based on the discussed pK_a studies, we hypothesize that the broadening in the ^{1}H NMR spectrum could also be due to hydrogen bonding with Et_2O (Scheme 3-5). If in fact this hydrogen bonding network is present, it would account

for the lower pK_a value in the presence of excess Et_2O. Due to this proposed interaction, obtaining the pK_a value of **14** is non-trivial.

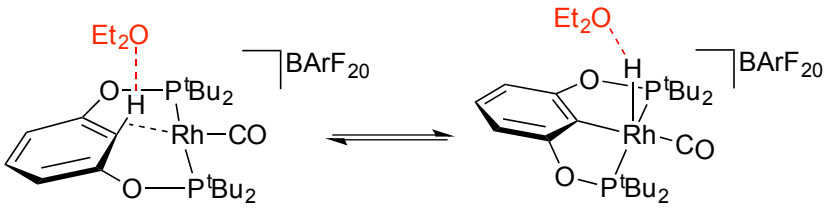

Scheme 3-5. Proposed equilibrium for compound **14** where hydrogen bonding to free Et_2O occurs.

(^{iPr}POCOP)Rh(CO), (^{tBu}POCOP)Rh(CO), and $HBArF_{20}$ were combined in fluorobenzene in a 1.4 : 1.0 : 1.1 ratio, respectively (Figure 3-8, red trace). The resulting $^{31}P\{^1H\}$ spectrum was recorded after equilibrium was established. Based on integrations, we can conclude that the pK_a values of **14** and **17** are very similar. In other words, the *thermodynamic* acidity of the compounds are similar. The signals for the (^{iPr}POCOP) containing species broaden from *ca.* $\Delta\nu_{½}$ = 5 Hz (Figure 3-8, purple trace) to $\Delta\nu_{½}$ = 35-50 Hz (Figure 3-8, red trace). To the same sample, additional acid was added to fully protonate both Rh-species (Figure 3-8, green trace). The peaks sharpen to *ca*. $\Delta\nu_{½}$ = 5 and 20 Hz ([(^{tBu}POCOP)Rh(CO)H]$^+$ and [(^{iPr}POCOP)Rh(CO)H]$^+$, respectively). Next, 5.8 equiv. of Et_2O was added to the reaction mixture to observe any potential deprotonation of either species (Figure 3-8, blue trace). This resulted in visibly broader peaks in the $^{31}P\{^1H\}$ spectrum (*ca.* $\Delta\nu_{½}$ = 20 (**17**) and 50 (**14**) Hz). Deprotonation was not observed. The broader signals for **15** and **17** suggest that **17** is in fact *kinetically* more acidic than the analogous *t*Bu compounds. This is likely due to the steric constraints around the metal center with (^{tBu}POCOP) *versus* (^{iPr}POCOP). Furthermore, broadening of signals after Et_2O addition suggests that the pK_a of [(^{iPr}POCOP)Rh(CO)H][$BArF_{20}$] is similar to $[HOEt_2]^+$.

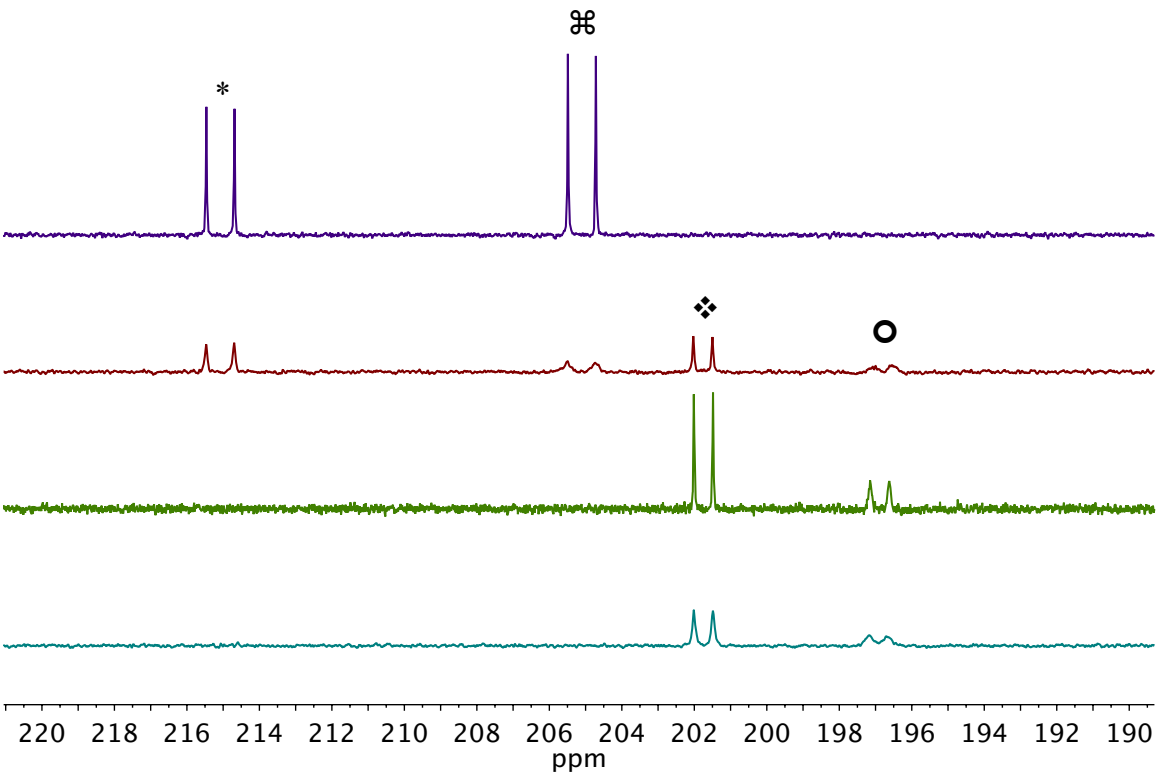

Figure 3-8. $^{31}P\{^{1}H\}$ NMR spectra. (i) *Purple spectrum*: (^{iPr}POCOP)Rh(CO) (**15**) (⌘) and (^{tBu}POCOP)Rh(CO) (**13**) (*). (ii) *Red spectrum*: after addition of 1.1 equiv. $HBArF_{20}$. [(^{tBu}POCOP)Rh(CO)H]$^{+}$ (**14**) (❖) and [(^{iPr}POCOP)Rh(CO)H]$^{+}$ (**17**) (O). (iii) *Green spectrum*: after addition of $HBArF_{20}$ for full protonation of both species. (iv) *Blue spectrum*: after addition of 5.8 equiv. Et_2O.

3.5 Steric Effects at the Rhodium Center

3.5.1 *Previous Reports of Steric Effects in Pincer Complexes*

Previous work in our group outlined the importance of steric effects on reactivity in Ir-pincer compounds.[19] Data has shown that iridium and rhodium have identical atomic radii (1.35 Å).[26] Moreover, crystallographic data has shown Rh(I) and Ir(I) PCP and POCOP ligated compounds have nearly identical M—C and M—P bond lengths (Table 3-3) supporting the notion that the steric effects around the metal center in Rh and Ir complexes should be very similar.[14,15,27] Thus, it is anticipated that the reactivity directed by steric effects in Ir and Rh pincer complexes would be analogous. However, our observations indicate that Lewis acidity of the metal center is likely to dictate the

reactivity of (^{tBu}POCOP)Rh(CO) and (^{iPr}POCOP)Rh(CO) more so than sterics. A comparison of differing reactivity of analogous Ir and Rh compounds will be discussed.

3.5.2 *Reactivity of and Coordination to the Sixth Coordination Site*

The reactivity of **15** with HCl to form **16** is consistent with the analogous (^{iPr}POCOP)Ir(CO) species. However, addition of excess HCl (in diethyl ether) to (^{tBu}POCOP)Rh(CO) results in no reaction. This is unexpected, as (^{tBu}POCOP)Ir(CO)HCl can be formed quantitatively upon addition of excess HCl. Further, Koridze and coworkers report the synthesis of **13** by sparging a solution of (^{tBu}POCOP)RhHCl with CO.[12] We find that pressurizing the solution of (^{tBu}POCOP)RhHCl with CO results in no conversion to **13**. A plausible mechanism invokes chloride dissociation followed by deprotonation of the intermediate five-coordinate protonated species by chloride, a weak base. Sparging the solution drives off HCl and drives the reaction forward. We hypothesize that the facile loss of chloride is facilitated by the steric bulk of the *t*Bu groups. These observations suggest that the Rh—H bond is strongly acidic, especially compared to the analogous Ir—H species. We hypothesize that (^{tBu}POCOP)Rh(CO)HCl is unable to form due to the steric constraint at the metal center imparted by the *tert*-butyl groups and the weaker Rh—H bond relative to Ir—H. It is clear that the Rh—H bond weakness relative to Ir—H bonds plays a greater role in reactivity at the metal center than expected.[28]

	M—P(1)	M—P(2)	M—C_{Aryl}	M—(CO)
(^{tBu}POCOP)Ir(CO)	2.2822(9)	2.2825(8)	2.046(3)	1.880(4)
(^{tBu}POCOP)Rh(CO)	2.2816(9)	2.2829(11)	2.043(3)	1.887(3)
(^{tBu}PCP)Ir(CO)	2.291(2)	2.298(2)	2.102(8)	1.873(10)
(^{tBu}PCP)Rh(CO)	2.283(3)	2.292(3)	2.084(9)	1.848(16)

Table 3-3. Select bond distances (Å) of Ir and Rh pincer complexes.

Unlike [(^{tBu}POCOP)Ir(CO)H]$^+$, which is observed *in situ* and isolated as a five-coordinate species, [(^{iPr}POCOP)Ir(CO)H][BF_4] is observed *in situ*, but only isolated in the solid state as [(^{iPr}POCOP)Ir(CO)(H_2O)H][BF_4].[19] Upon addition of water to **14**, three species are observed by $^{31}P\{^1H\}$ NMR spectroscopy. Based on relative integrations, 24% of **13**, 62% of **14**, and 14% of a new species (d, 187.9 ppm, $^1J_{RhP}$ = 120 Hz) are observed

in solution. The $^{31}P\{^{1}H\}$ NMR signals of **13** and **14** are broadened to the point where the $^{1}J_{RhP}$ is no longer observable ($\Delta\nu_{½}$ = 332 (**13**) and 279 (**14**) Hz). The signal at 187.9 ppm corresponds to a new ^{1}H NMR signal at -27.2 ppm ($^{1}J_{RhH}$ = 55 Hz; $^{2}J_{PH}$ = 10 Hz). We have tentatively assigned this as an aquo species, [(^{tBu}POCOP)Rh(CO)H(H_2O)][$BArF_{20}$] (**18**). Based on the formation of **18**, as well as the facile deprotonation of **14** to **13**, we propose an equilibrium outlined in Scheme 3-6.

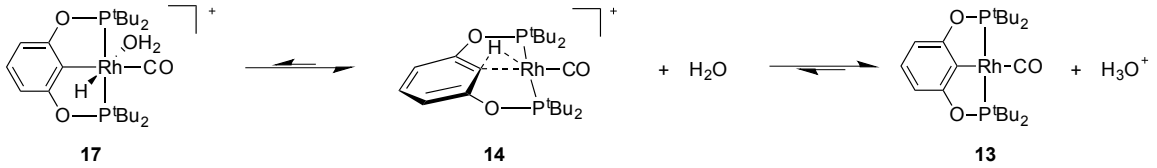

Scheme 3-6. Proposed reactivity of **14** with water where association of water in the open coordination or deprotonation by water (at high enough concentrations) can occur.

Milstein has reported that the addition of 1 eq. of CO to a precooled chloroform solution of [(^{tBu}POCOP)Rh(acetone)H][BF_4] resulted in the observation of [(^{tBu}POCOP)Rh(CO)H][BF_4], at -40°C with a hydride signal at -12.4 ppm ($^{1}J_{RhH}$ = 41 Hz) and a $^{31}P\{^{1}H\}$ signal at 203.6 ppm ($^{1}J_{RhP}$ = 106 Hz).[15] Upon warming to room temperature, this species is deprotonated to yield **13**. Milstein and coworkers mention the possibility of acetone or BF_4^- coordination but conclude that this complex is best formulated as a five-coordinate species. Based on our observations, we propose that [(^{tBu}POCOP)Rh(CO)H][BF_4] is in fact the BF_4^- coordinated species, (^{tBu}POCOP)Rh(CO)(BF_4)H (**19**). We find that addition of HBF_4 (5 eq.) to a fluorobenzene solution of **13** at room temperature gives a light yellow solution with an NMR spectrum exhibiting a hydride signal at -12.8 ppm ($^{1}J_{RhH}$ = 36 Hz) and a $^{31}P\{^{1}H\}$ chemical shift at 204 ppm ($^{1}J_{RhP}$ = 109 Hz). This is very similar to data reported by Milstein and coworkers. The ^{19}F NMR spectrum also displays a broad signal at -151 ppm ($\Delta\nu_{½}$ = 275 Hz) which is indicative of a bound BF_4^- anion.[15,29] In contrast to these results, it has been shown that protonation of (^{tBu}POCOP)Ir(CO) with HBF_4 affords [(^{tBu}POCOP)Ir(CO)H][BF_4]. There is no evidence of anion or water coordination to Ir. Thus, evidence of compound **19** is surprising. The concentration of **19** observed *in situ* has poor reproducibility in dilute solutions, which is likely due to adventitious water deprotonating **19**, or water exchanging with coordinated BF_4^-. Addition of **13** to neat

HBF_4 results in similar spectroscopic data. Attempts to crystallize the species have been unsuccessful.

3.6 Attempted Catalysis

In order to explore the potential catalytic properties of the (^{tBu}POCOP)Rh(CO) system, compound **14** was pressurized with H_2 in hopes of observing [(^{tBu}POCOP)Rh(CO)(H_2)H]$^+$. A fluorobenzene solution of **14** was added to a high pressure NMR tube (see Chapter 4) and pressurized to 100 psig of H_2. The reaction mixture was observed over days with no change. The reaction was heated to 100 °C for 10 hours, again with no change.

[(^{iPr}POCOP)Rh(CO)H][BF_4] was also evaluated for catalysis. A C_6D_6 solution of **17** was pressurized with 100 psig of H_2 and observed by ^{1}H and ^{31}P{^{1}H} NMR spectroscopy. After 24 hrs at room temperature, 36% deprotonation to **15** was observed. Continuing to heat the reaction at 100 °C for two days lead to complete deprotonation and no formation of [(^{iPr}POCOP)Rh(CO)(H_2)H][BF_4] or (^{iPr}POCOP)Rh(CO)H_2. The deprotonation is likely due to the introduction of adventitious water while pressurizing with H_2.

3.7 Summary

A novel Rh compound with an η^2-aromatic C—H agostic interaction has been isolated and fully characterized, [(^{tBu}POCOP)Rh(CO)H][$BArF_{20}$]. The hybridization of the *ipso*-carbon has been examined and found to have less s-character than previously reported PCP-ligated species. This is due to the weak σ-donating capabilities of POCOP. The strong agostic interaction leads to an equilibrium between an agostic species and Rh—H; this interaction has been probed by isotopic perturbation and variable temperature NMR spectroscopy. Unexpected results were encountered, as coordination to the sixth coordination site at rhodium is observed with bulky ligands while this type of interaction is not observed in analogous iridium species. Further work with less sterically encumbered (^{iPr}POCOP)Rh(CO) has been examined. Increased reactivity at the sixth coordination site is likely due to the increased Lewis acidity of Rh—H bonds *versus* Ir—

H bonds. The increased reactivity has made characterization problematic. However, initial studies have suggested a similar agostic interaction to **14** when (^{iPr}POCOP)Rh(CO) is protonated.

3.8 Experimental

General Considerations. All experiments and manipulations were performed using standard Schlenk techniques under an argon atmosphere or in an argon- or nitrogen-filled glovebox. Glassware and diatomaceous earth were dried in an oven maintained at 140 °C for at least 24 h. Deuterated solvents methylene chloride-d_2, benzene-d_6, and protio-fluorobenzene for NMR spectroscopy were dried over calcium hydride and stored over 4 Å activated molecular sieves. Protio solvents were passed through columns of activated alumina and molecular sieves. All other reagents were used as received. ^{1}H NMR spectra were referenced to residual protio solvents: methylene chloride (5.32 ppm), benzene (7.16 ppm).[30] ^{1}H NMR spectra in protio-fluorobenzene were referenced to silicon grease (0.24 ppm). ^{13}C NMR shifts were referenced to solvent signals: methylene chloride (54.00 ppm). ^{31}P{^{1}H} NMR shifts were referenced to an 85% H_3PO_4 external standard (0 ppm). ^{19}F NMR shifts were reference to a CF_3COOH external standard (-76.55 ppm). Infrared spectra were recorded on a Bruker Tensor 27 FTIR instrument. NMR spectra were recorded on either a Bruker AV-800, AV-500, DRX-500, or AV-300 NMR instrument. X-ray data were collected at −173 °C on a Bruker APEX II single-crystal X-ray diffractometer, with Mo radiation. Elemental analyses were performed under air-free conditions at Atlantic Microlabs. $[Rh(COE)_2Cl]_2$, [31] (^{tBu}POCOP), [32] (^{iPr}POCOP),[19] (^{tBu}POCOP)Rh(CO),[12] (^{iPr}POCOP)RhHCl,[19a] were synthesized according to published procedures. $[H(Et_2O)_2][B(C_6F_5)_4]$[33] was synthesized *via* modified published procedures.

Synthesis of [(^{tBu}POCOP)Rh(CO)H][BArF$_{20}$] (14):

An NMR tube fitted with a J. Young style Teflon valve was charged with 13 mg (^{tBu}POCOP)Rh(CO) (0.025 mmole), 21 mg $HBArF_{20}$ (0.025 mmole), and 0.5 mL fluorobenzene resulting in an orange solution. The solution was layered with pentane resulting in crystals suitable for diffraction. Anal. Calcd for $C_{47}H_{40}BF_{20}O_3P_2Rh$: C, 46.71;

H, 3.34. Found: C, 46.59; H, 3.15. ^{1}H NMR (CD_2Cl_2, 300 MHz, ppm): 7.6 (t, $^{3}J_{HH}$ = 7 Hz, 1H; *para* Ar-*H*), 6.8 (d, $^{3}J_{HH}$ = 7 Hz, 2H; *meta* Ar-*H*), 1.3 (vt, $^{3}J_{PH}$ + $^{5}J_{PH}$ = 8 Hz, 18H; PC(CH_3)$_3$), 1.2 (vt, $^{3}J_{PH}$ + $^{5}J_{PH}$ = 8 Hz, 18H; PC(CH_3)$_3$), -6.6 (br d, J_{RhH} = 36 Hz, 1H; Rh*H*). ^{31}P{^{1}H} NMR (CD_2Cl_2, 121.5 MHz, ppm): 201.9 (d, $^{1}J_{RhP}$ = 107 Hz). ^{13}C NMR (CD_2Cl_2, 201.2 MHz, ppm): 188.9 (d, $^{1}J_{RhC}$ = 75 Hz; Rh-*C*O), 172.1 (s; *ortho* C_{Ar}), 142.2 (d, $^{1}J_{CH}$ = 162 Hz, C_{Ar}), 111.1 (d, $^{1}J_{CH}$ = 170 Hz, C_{Ar}), 105.2 (d, $^{1}J_{CH}$ = 76 Hz, C_{ipso}), 42.8 (s, *C*$(CH_3)_3$), 40.2 (s, *C*$(CH_3)_3$), 27.9 (m, C(*C*$H_3)_3$). IR (solution, CH_2Cl_2, cm^{-1}) υ_{CO} = 2083 and 2024.

Synthesis of (^{iPr}POCOP)Rh(CO) (15):

10 mL of a 0.06 M solution of (^{iPr}POCOP)RhHCl in toluene was placed in a 50 mL reaction vessel with a Teflon stopper. The solution was sparged with CO for 10 minutes, resulting in a color change from red to bright orange. In an O_2 free environment, the solution was passed through a neutral alumina plug, resulting in a yellow solution. The solvent was removed *in vacuo*. Spectroscopic data matched the literature.[34,24]

Synthesis of (^{iPr}POCOP)Rh(CO)HCl (16):

27 mg (^{iPr}POCOP)Rh(CO) (0.06 mmole) and 10 mL CH_2Cl_2 were added to a 100 mL Schlenk flask. 0.3 mL of a 2.0 M HCl in diethyl ether solution (0.6 mmole) was added to the Schlenk flask *via* syringe. The yellow solution immediately turned colorless. The solvent was removed *in vacuo* resulting in an off-white solid. Anal. Calcd for $C_{19}H_{32}ClO_3P_2Rh$: C, 44.86; H, 6.34. Found: C, 44.74; H, 6.44. ^{1}H NMR (C_6D_6, 300 Hz, ppm): 6.8 (t, $^{3}J_{HH}$ = 8 Hz, 1H; *para* Ar-*H*), 6.7 (d, $^{3}J_{HH}$ = 8 Hz, 2H; *meta* Ar-*H*), 3.5 (sept, $^{3}J_{HH}$ = 7 Hz, 2H; PC*H*$(CH_3)_2$), 2.1 (m, 2H; PC*H*$(CH_3)_2$), 1.4 (m, 3H; PCH(CH_3)(CH_3)), 1.2 (m, 3H; PCH(CH_3)(CH_3)), 0.9 (m, 3H; PCH(CH_3)(CH_3)), 0.8 (m, 3H; PCH(CH_3)(CH_3)), -14.5 (dt, $^{1}J_{RhH}$ = 24 Hz, $^{2}J_{HP}$ = 10 Hz, 1H; Rh*H*). ^{31}P{^{1}H} NMR (C_6D_6, 121.5 MHz, ppm): 200.1 (d, $^{1}J_{RhP}$ = 104 Hz). ^{13}C{^{1}H} (C_6D_6, 125.8 MHz, ppm): 191 (dt, $^{2}J_{PC}$ = 8 Hz, $^{1}J_{RhC}$ = 42 Hz; Rh(*C*O)), 164 (s; Ar), 106 (t, $^{2}J_{PC}$ = 6 Hz; *ipso*-Ar), other aromatic signals obstructed by C_6D_6 signal, 30 (t, $^{1}J_{CP}$ = 14 Hz; P*C*(CH_3)), 28 (t, $^{1}J_{CP}$ = 13 Hz; P*C*$(CH_3)_2$), 18.2 (s; PC(*C*$H_3)_2$), 17.9 (s; PC(*C*$H_3)_2$), 15.7 (s; PC(*C*$H_3)_2$), 1.4 (s; PC(*C*$H_3)_2$). IR (solution, CH_2Cl_2, cm^{-1}) υ_{CO} = 2064 cm^{-1}.

Synthesis of [(^{iPr}POCOP)Rh(CO)H][BF_4] (17):

An NMR tube fitted with a J. Young style Teflon valve was charged with 13.5 mg (^{iPr}POCOP)Rh(CO) (0.03 mmole) and 0.5 mL C_6D_6. Under a heavy flow of argon, 4.0 μL HBF_4 was added *via* micropipette. The product was not isolated and was characterized by NMR spectroscopy *in situ*. ^{1}H NMR (C_6D_6, 300 Hz, ppm): 7.0 (t, $^3J_{HH}$ = 8 Hz, 1H; *para* Ar-*H*), 6.7 (d, $^3J_{HH}$ = 8 Hz, 2H; *meta* Ar-*H*), 3.1 (m, 2H; PC*H*$(CH_3)_2$), 2.1 (m, 2H; PC*H*$(CH_3)_2$), 1.4 (m, 3H; PCH(C*H*$_3$)(CH_3)), 1.3 (m, 3H; PCH(C*H*$_3$)(CH_3)), 1.2 (m, 3H; PCH(C*H*$_3$)(CH_3)), 0.8 (m, 3H; PCH(C*H*$_3$)(CH_3)), -21.6 (br d, $^1J_{RhH}$ = 32 Hz,; Rh*H*). ^{31}P{^{1}H} NMR (C_6D_6, 121.5 MHz, ppm): 199 (d, $^1J_{RhP}$ = 106 Hz).

Synthesis of (^{tBu}POCOP)Rh(CO)H(BF_4) (19):

An NMR tube fitted with a J. Young style Teflon valve was charged with 10 mg (0.02 mmole) and 0.5 mL [H(Et_2O)][BF_4] resulting in an orange solution. ^{1}H NMR ([H(Et_2O)][BF_4], externally reference with CD_3Cl, 300.1 MHz, ppm): 7.8 (t, $^3J_{HH}$ = 7 Hz; *para* Ar-*H*), 7.1 (d, $^3J_{HH}$ = 8 Hz; *meta* Ar-*H*), *t*Bu signals are obstructed by Et_2O signals , -12 (br d, J_{RhH} = 40 Hz; Rh*H*). ^{31}P{^{1}H} NMR ([H(Et_2O)][BF_4], 121.5 MHz, ppm): 204 (d, $^1J_{RhP}$ = 106 Hz). ^{13}C{^{1}H} NMR ([H(Et_2O)][BF_4], not referenced, 75.5 MHz, ppm): 189.4 (d, $^1J_{RhC}$ = 76 Hz; Rh-*C*O), 171.2 (s; *ortho* C_{Ar}), 139.2 (s; C_{Ar}), 116.6 (s, C_{Ar}), 109.9 (s; C_{ipso}), 42.7 (s; *C*$(CH_3)_3$), 39.9 (s; *C*$(CH_3)_3$), 27.5 (s; C(*C*H$_3$)$_3$), 26.8 (s, C(*C*H$_3$)$_3$). ^{19}F NMR (obtained from a dilute fluorobenzene solution, 470.55 MHz, ppm): 146 (free BF_4^-), 151 (bound BF_4^-, $\Delta\nu_{½}$ = 275 Hz).

3.9 Notes for Chapter 3

1) Moulton, C. J. and Shaw, B. L., *J. Chem. Soc., Dalton Trans.,* **1976**, *11*, 1020-1024
2) a) *Organometallic Pincer Chemistry*; Topics in Organometallic Chemistry; van Koten, G. and Milstein, D., Eds.; Springer: Heidelberg, **2013**; Vol. *40*. b) van der Boom, M. E. and Milstein, D., *Chem. Rev.*, **2003**, *103*, 1759-1792. c) O'Reilly, M. E. and Veige, A. S., *Chem. Soc. Rev.*, **2014**, *43*, 6325-6369. d) Henning, J.; Schubert, H.; Eichele, K.; Winter, F.; Pöttgen, R.; Mayer, H. A.; Wesemann, L., *Inorg. Chem*., **2012**, *51*, 5787-5794.
3) *PCP*: a) Rimml, H. and Venanzi, L. M., *Phosphorus Sulfur Relat. Elem.*, **1987**, *30*, 297-300. b) van der Boom, M. E.; Gozin, M.; Ben-David, Y.; Shimon, L. J. W.; Frolow, F.; Kraatz, H.; Milstein, D., *Inorg. Chem.*, **1996**, *35*, 7068-7073. c) Albrecht, M. and van Koten, G., *Angew. Chem. Int. Ed.*, **2001**, *40*, 3750-3781. *POCOP*: d) Vabre, B.; Lambert, M. L.; Petit, A.; Ess. D. H.; Zargarian, D., *Organometallics*, **2012**, *31*, 6041-6053. e) Vabre, B.; Spasyuk, D. M.; Zargarian, D., *Organometallics*, **2012**, *31*, 8561-8570.
4) *Other similar known agostic species*: a) Connelly, S. J.; Chanez, A. G.; Kaminsky, W.; Heinekey, D. M., *Angew. Chem. Int. Ed.,* **2015**, *54*, 5915-5918. b) Dani, P.; Karlen, T.; Gossage, R. A.; Smeets, W. J. J.; Spek, A. L.; van Koten, G., *J. Am. Chem. Soc.*, **1997**, *119*, 11317-11318. c) Dani, P.; Toorneman, M. A. M.; van Klink, G. P. M.; van Koten, G., *Organometallics*, **2000**, *19*, 5287-5296. d) Kelley, P.; Lin, S.; Edouard, G.; Day, M. W.; Agapie, T., *J. Am. Chem. Soc.*, **2012**, *134*, 5480-5483.
5) Pons, V. and Heinekey, D. M., *J. Am. Chem. Soc.*, **2003**, *125*, 8428-8429.
6) Raamat, E.; Kaupmees, K.; Ovsjannikov, G.; Trummal, A.; Kütt, A.; Saame, J.; Koppel, I.; Kaljurand, I.; Lipping, L.; Rodima, T.; Pihl, V.; Koppel, I. A.; Leito, I., *J. Phys. Org. Chem.*, **2013**, *26*, 162-170.
7) Lao, D. B.; Owens, A. C. E.; Heinekey, D. M.; Goldberg, K. I., *ACS Catalysis*, **2013**, *3*, 2391-2396.
8) Kaljurand, I.; Kütt, A.; Sooväli, L.; Rodima, T.; Mäemets, V.; Leito, I.; Koppel, I. A., *J. Org. Chem.*, **2005**, *70*, 1019-1028.

9) Findlater, M.; Bernskoetter, W. H.; Brookhart, M., *J. Am. Chem. Soc.*, **2010**, *132*, 4534-4535.

10) a) Vigalok, A.; Uzan, O.; Shimon, L. J. W.; Ben-David, Y.; Martin, J. M. L.; Milstein, D., *J. Am. Chem. Soc.,* **1998**, *120*, 12539. b) Frech, C. M.; Shimon, L. J. W.; Milstein, D., *Organometallics*, **2009**, *28*, 1900-1908.

11) Montag, M.; Schwartsburd, L.; Cohen, R.; Leitus, G.; Ben-David, Y.; Martin, J. M. L.; Milstein, D., *Angew. Chem. Int. Ed.*, **2007**, *46*, 1901-1904.

12) Polezhaev, A. V.; Kuklin, S. A.; Ivanov, D. M.; Petrovskii, P. V.; Dolgushin, F. M.; Ezernitskaya, M. G.; Koridze, A. A., *Russ. Chem. Bull., Int. Ed.,* **2009**, *58*, 1847-1854.

13) Farrugia, L. J., Ortep-3 for Windows, *J. Appl. Cryst.*, **1997**, *30***,** 565-566.

14) Huang, K.; Grills, D. C.; Han, J. H.; Szalda, D. J.; Fujita, E., *Inorg. Chim. Acta.*, **2008**, *361*, 3327-3331.

15) Montag, M.; Efremenko, I.; Cohen, R.; Shimon, L. J. W.; Leitus, G.; Diskin-Posner, Y.; Ben-David, Y.; Salem, H.; Martin, J. M. L.; Milstein, D. *Chem. Eur. J.*, **2010**, *16*, 328-353.

16) Brookhart, M. and Green, M. L. H., *J. Organomet. Chem.*, **1983**, *250*, 395-408.

17) Weigert, F. J. and Roberts, J. D., *J. Am. Chem. Soc.*, **1967**, *89*, 2967-2969.

18) a) Crabtree, R. H. and Hamilton, D. G., *Adv. Organomet. Chem.*, **1988**, *28*, 299-388. b) Hall, C. and Perutz, R. N., *Chem. Rev.*, **1996**, *96*, 3125-3146.

19) Goldberg, J. M.; Wong, G. W.; Brastow, K. E.; Kaminsky, W.; Goldberg, K. I.; Heinekey, D. M., *Organometallics*, **2015**, *34*, 753-762.

20) a) Salem, H.; Shimon, L. J. W.; Leitus, G.; Weiner, L.; Milstein, D., *Organometallics*, **2008**, *27*, 2293-2299. b) Punji, B.; Emge, T. J.; Goldman, A. S., *Organometallics*, **2010**, *29*, 2702-2709.

21) $[D(Et_2O)_2][BArF_{20}]$ was synthesized by addition of D_2O to PCl_3 to form DCl gas. The gas was vacuum transferred to an diethyl ether solution of $K[BArF_{20}]$.

22) Chatt, J. and Shaw, B. L., *J. Chem. Soc. A: Inorg. Phys. Theor.*, **1966**, 1437-1442.

23) a) Schrock, R. R. and Osborn, J. A., *J. Am. Chem. Soc.,* **1971**, *93*, 2397-2407. b) Mestroni, G.; Camus, A.; Zassinovich, G., *J. Organometallic Chem.*, **1974**, *65*, 119-129.

24) Salem, H.; Ben-David, Y.; Shimon, L. J. W.; Milstein, D., *Organometallics*, **2006**, *25*, 2292-2300.

25) Smith, M. B. and March, J., *March's Advanced Organic Chemistry: Reactions, Mechanisms, and Structure*, 5th ed.; John Wiley & Sons, Inc:.: 2001; pp. 329-331.

26) Slater, J. C., *J. Chem. Phys*., **1964**, *41*, 3199-3204.

27) a) Kuklin, S. A.; Sheloumov, A. M.; Dolgushin, F. M.; Ezernitskaya, M. G.; Peregudov, A. S.; Petrovskii, P. V.; Koridze, A. A., *Organometallics*, **2006**, *25*, 5466-5476. b) Morales-Morales, D.; Redón, R.; Wang, Z.; Lee, D. W.; Yung, C.; Magnuson, K.; Jensen, C. M., *Can. J. Chem.,* **2001**, *79*, 823-829.

28) Martinho Simões, J. A. and Beauchamp, J. L., *Chem. Rev.,* **1990,** *90*, 629-688.

29) *Evidence for broadening in ^{19}F NMR data with PF_6^- coordination*: Honeychuck, R. V. and Hersh, W. H., *Inorg. Chem.*, **1989***, 28*, 2869-2886.

30) Fulmer, G. R.; Miller, A. J. M.; Sherden, N. H.; Gottlieb, H. E.; Nudelman, A.; Stoltz, B. M.; Bercaw, J. E.; Goldberg, K. I., *Organometallics*, **2010**, *29*, 2176-2179.

31) van der Ent, A. and Onderdelinden, A. L, *Inorg. Synth.*, **1990**, *28*, 90-92.

32) Göttker-Schnetmann, I.; White, P.; Brookhart, M., *J. Am. Chem. Soc.*, **2004**, *126*, 1804-1811.

33) Brookhart, M.; Grant, B.; Volpe, A. F., Jr., *Organometallics*, **1992**, 11, 3920-3922.

34) Frech, C. M. and Milstein, D., *J. Am. Chem. Soc.*, **2006**, *128*, 12434-12435.

Chapter 4

Engineering of High Pressure Hydrogen Delivery System and NMR Sample Mixer

4.1 High Pressure Hydrogen Delivery System

4.1.1 *Introduction*

Steel autoclave reactors (Parr reactors) are generally used for high-pressure reactions. Parr reactors can hold a maximum pressure of 200 bar and be heated up to 300 °C. The drawback to using these reactors is the lack of monitoring capabilities of reactions while in the reactor. Additionally, the Parr reactors in our labs have a volume of 45 mL. This can be troublesome, as often times laboratory screening processes are conducted on small scales (*ca.* ≤ 1 mL). The small scale reactions minimize the amount of (often precious) metal compounds. This chapter outlines the design of a high pressure H_2 delivery system adapted to fit Wilmad-LabGlass NMR spectroscopy tubes (Figure 4-1). Figures and specifications are included.

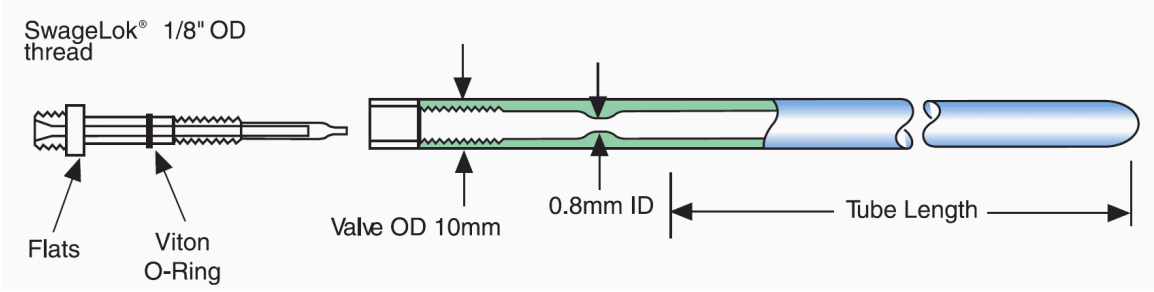

Figure 4-1. Image obtained from Wilmad-LabGlass website depicting high pressure NMR tubes.[1]

4.1.2 *Assembly of High Pressure Setup*

Figure 4-2 is an illustration of the complete hydrogen delivery system. For photos of the system, refer to Section 4.1.4. 3/8" Copper tubing was connected to the H_2 regulator with a compression fitting. A coil was placed in the copper tubing to allow for flexibility. The majority of joints were connected by soldering with 3/8" copper tees and

couplings. 90° joints in copper tubing were achieved by use of compression fittings and Teflon tape to seal the joint. Two needle valves were fitted to the apparatus. One valve is for connecting to a Schlenk line if reduced pressure is necessary. The other needle valve connects to an oil bubbler for purging, checking for leaks, and venting the system. Currently, our system is fitted with a 100 psig (max) pressure gauge, however any gauge with an NPT (national pipe thread) fitting is suitable. If higher pressures are desired, accommodations must be made as current needle valves are only rated to 150 psi.

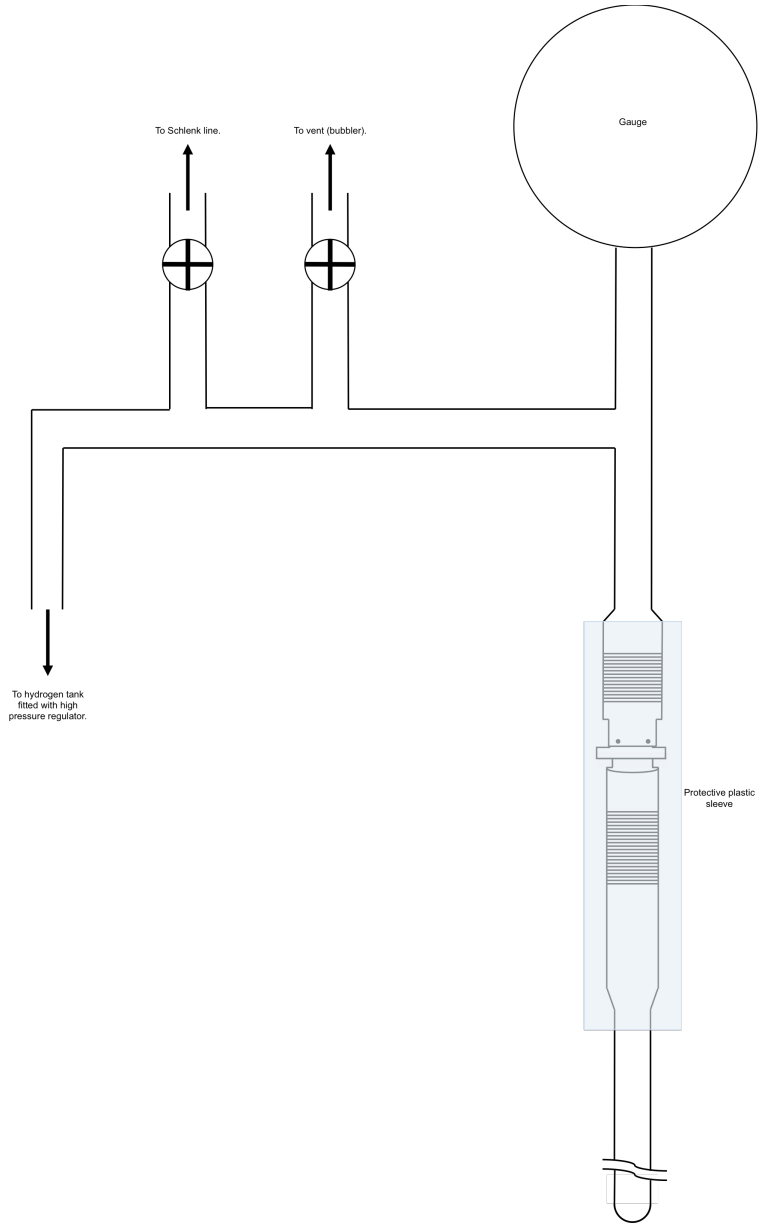

Figure 4-2. Illustration of H_2 delivery system.

Due to the "right-handed" threading of the glass and Teflon pin the connection of Teflon pin to brass fitting is important (Figure 4-3). To prevent loosening the Teflon cap from the brass fitting while attaching and detaching the tube, set screws are used to secure the cap in place. The Teflon pins have been modified after purchase to accommodate the pressurization system. To prevent opening the seal between the glass and Teflon pin while removing the tube from the system, grooves were cut into the Teflon pin and a custom wrench made to fit the groove are used to loosen only the cap from the brass system. This results in removal of the NMR tube without releasing any pressure.

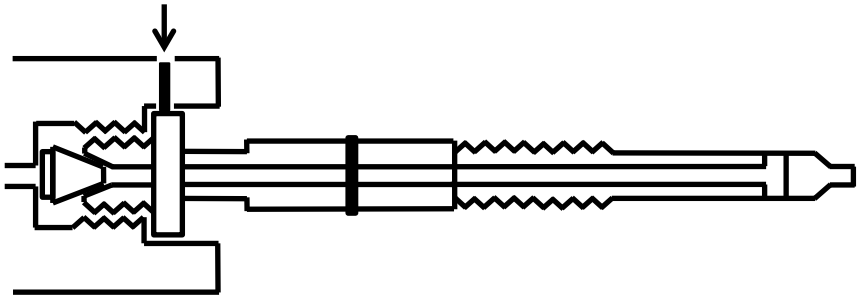

Figure 4-3. Depiction of Teflon fitting for high pressure tubes while attached to the H_2 system. Arrow indicates placement of setscrew to hold Teflon fitting in place. Another setscrew is placed 90° from indicated setscrew.

4.1.3 *How to Pressurize an NMR Tube*

Caution: **Hydrogen is an extremely flammable gas. Remove all open flames while system is in use. While dealing with high pressures, use all safety precautions including but not limited to Kevlar gloves and sleeves, lab coat, facemask, and blast shields. Do not operate system while alone. While transporting tubes, secondary, shatter-proof containment should always be used.**

The NMR sample is degassed by three freeze-pump-thaw cycles by screwing the NMR tube into the custom attachment made to fit a Schlenk line (Figure 4-4). After the sample has been degassed it is ready for pressurization. Twist the tube into the open end of the apparatus (finger tight). Using the custom wrench, tighten the Teflon pin into the brass fitting using the customized grooves and turn clockwise (Figure 4-5 and 4-6; caution, over tightening the cap at this point can lead to disfiguration of the Teflon pin at

the threading as well as the customized groove). With the small allen wrench, tighten both set screws into place (*vide infra*, Figure 4-10). The Teflon pin should be secured and leak free. Raise the plastic protective sleeve around the tube and screw on completely (*vide infra*, Figure 4-8).

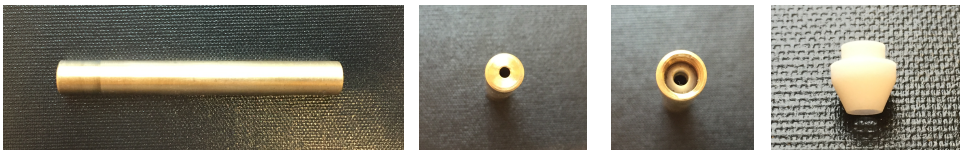

Figure 4-4. From left to right: i) Brass custom piece to fit tubes to Schlenk Line. ii) Top of piece. A small valve for gas and vacuum flow. iii) Bottom of piece. Threading to match Teflon pin and Teflon ferrule to ensure a tight seal to tube. iv) Teflon ferrule. This is affixed to the brass piece with a silicon based sealant.

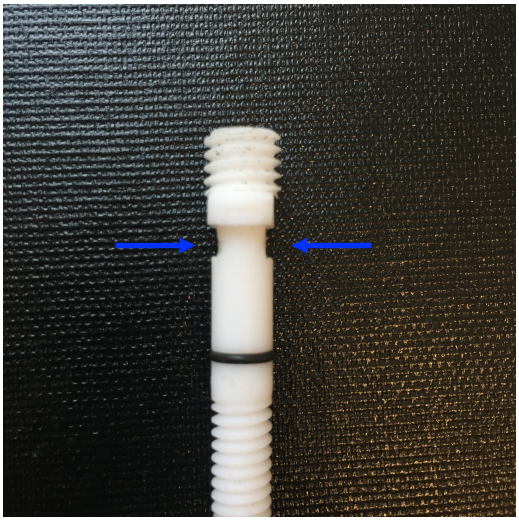

Figure 4-5. Teflon pin after modification. Modification highlighted with blue arrows.

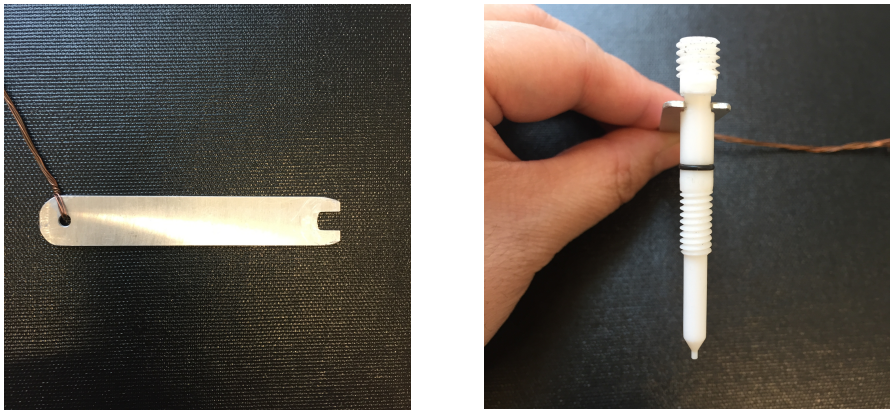

Figure 4-6. Left: Customized wrench for securing and removing NMR tube from system. Right: Wrench positioned in customized grooves on Teflon pin.

With the vacuum needle valve closed and the vent valve open, turn on the hydrogen tank and achieve a moderate flow of hydrogen. Purge the system for approximately 15 minutes. After venting is finished, close the vent valve and carefully raise the pressure to 20 psig. Ensure that the gauge on the pressurization system and the secondary gauge on the regulator are reading the same value. While pressurizing, leaks are more likely to occur from the needle valve, this can be identified by bubbles in the oil. Tighten the needle valve if necessary. Once the system has been checked, the tube can be opened by twisting the neck of the tube (under the plastic protective sleeve) counter-clockwise. With the tube open, raise the pressure delivered from the regulator by controlling the diaphragm to the desired pressure. Once achieved, close the tube by twisting the tube clockwise. Close the H_2 tank at the main valve, ensuring to leave the needle valve on the regulator open. Slowly open the vent valve and release the pressure in the system. Once the pressure is released, close the needle valve on the regulator. Remove the plastic safety sleeve from the system and loosen the allen screws. Using the wrench, carefully remove the tube by twisting counter-clockwise. Place the tube in secondary containment.

4.1.4 *Photographs of Hydrogen Delivery System*

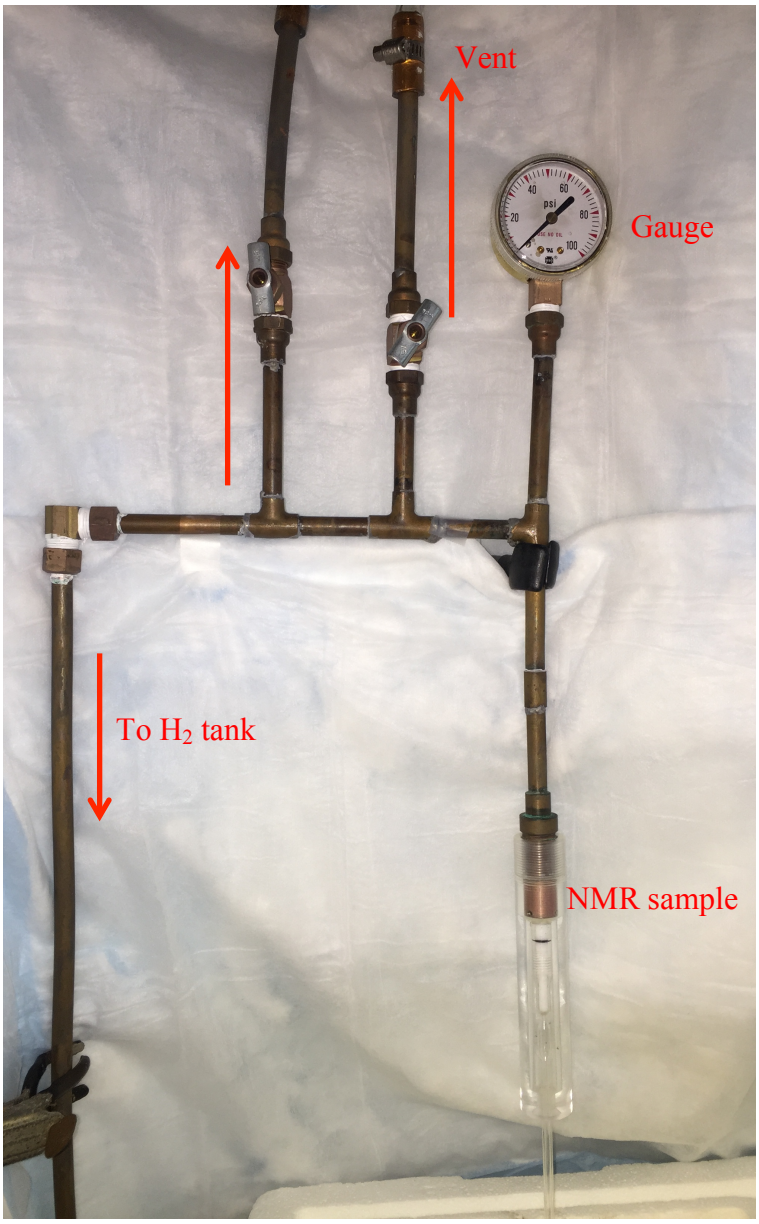

Figure 4-7. H_2 delivery system.

Figure 4-8. Close-up of sample attachment to apparatus.

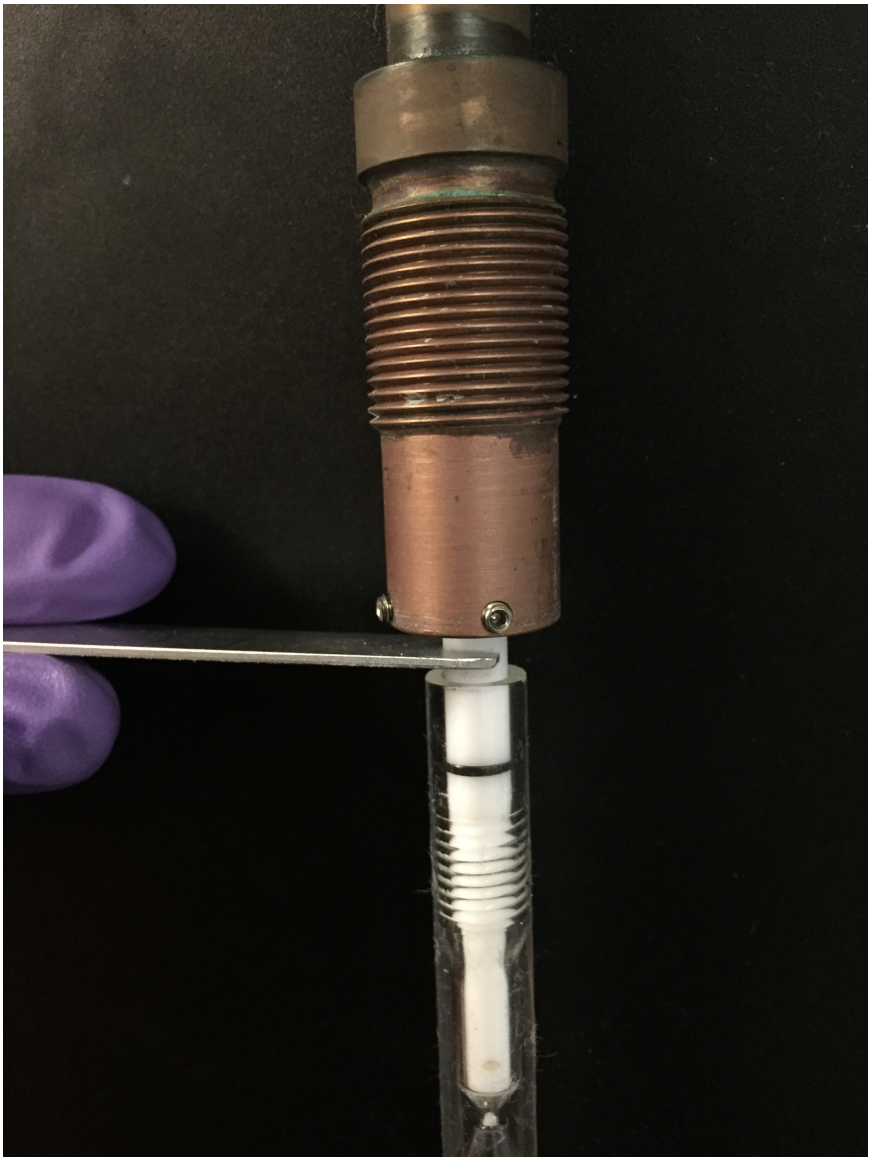

Figure 4-9. Using the custom wrench to tighten sample to copper fitting on H_2 apparatus. It is especially important to use the custom wrench when removing the sample to prevent venting the pressure in the sample.

Figure 4-10. Tightening one of two set screws to secure Teflon pin. By tightening the set screws, the Teflon cap will not be loosened while manipulating sample during pressurization.

Figure 4-11. Both set screws tightened. The sample is ready for the plastic protective sleeve.

4.1.5 *Part Numbers*

The following parts were used to assemble the custom-made pressurization system:

3/8” copper piping
3/8” compression fittings
3/8” copper tees, couplings, and elbows
1/4” NPT fittings

Wilmad-LabGlass:

522-PV-7	5 mm heavy wall precision pressure/vacuum valve NMR sample tube 7” L, 500MHz
OF-70	Polytetrafluoroethylene (PTFE) stepped cone ferrule
PV-ANV	Needle valve
PV-ANV-O	O-Ring for needle valve

VWR (USA):

55850-275	VWR Heavy-duty single-stage gas regulator Delivery pressure: 600 psig; Supply pressure: 4,000 psig
300007-378	Welding and compressed gas gauge, Ametek U.S. gauge

Grainger:

1VPW3	Needle valve, straight, brass, ¼ in., MNPT Maximum pressure limit of 150 psi

4.2 NMR Sample Mixer

4.2.1 *Introduction*

Due to the small inner diameter of the high-pressure tubes, diffusion of H_2 gas is slow. In order to combat this, proper mixing of the sample must take place. In addition to facilitating proper mixing of gases, the NMR sample mixer allows for constant mixing of

inhomogeneous mixtures, like in reactions with poorly soluble reagents (*e.g.* silver salts). The rotary device is controlled by a variac in order to maintain the speed of mixing.

4.2.2 *Figures and Plans*

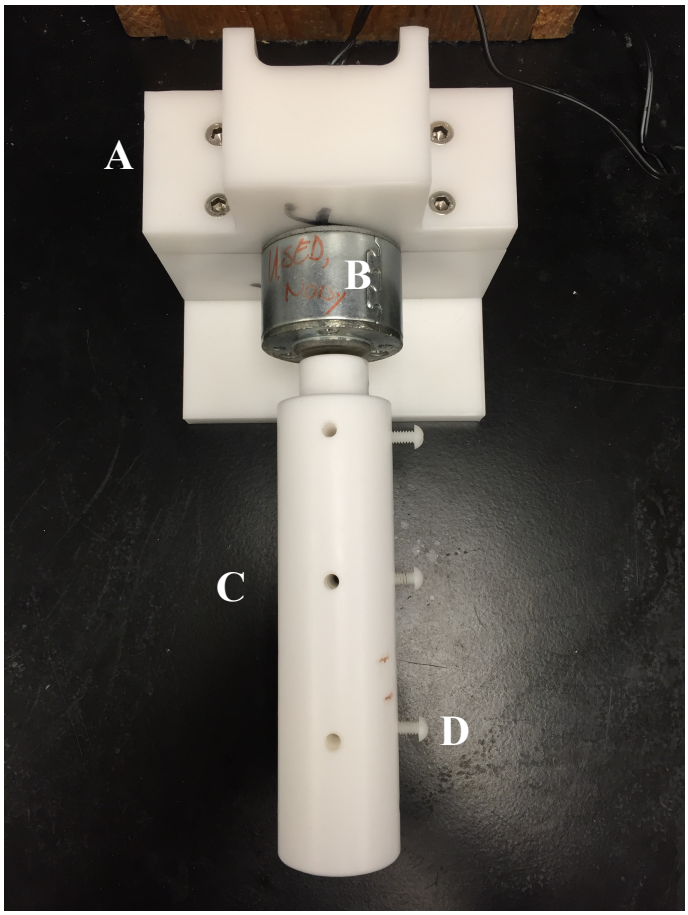

Figure 4-12. Top view of rotary device. A) Heavy base to prevent the device from falling. Electrical plug is fed through the base and plugged into a variac to control speed of rotation. B) Refurbished rotary motor. C) Shaft with 5 mm holes to fit NMR tubes. There are six holes in total; two sets of three with are perpendicular to each other. D) Plastic set screws are placed perpendicular to each hole (C) to set the tube in place to prevent any slippage.

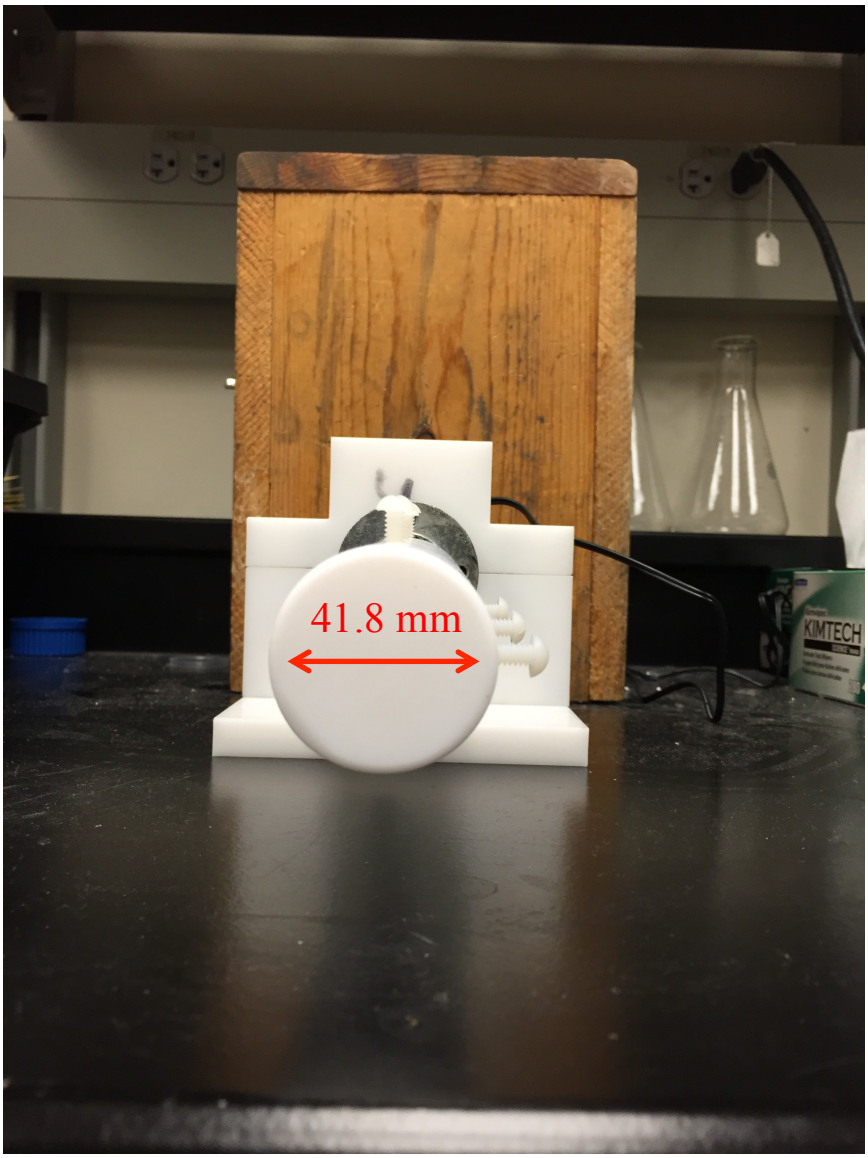

Figure 4-13. Front view of rotary device. The shaft is 41.8 mm in diameter. The two sets of set screws are visible.

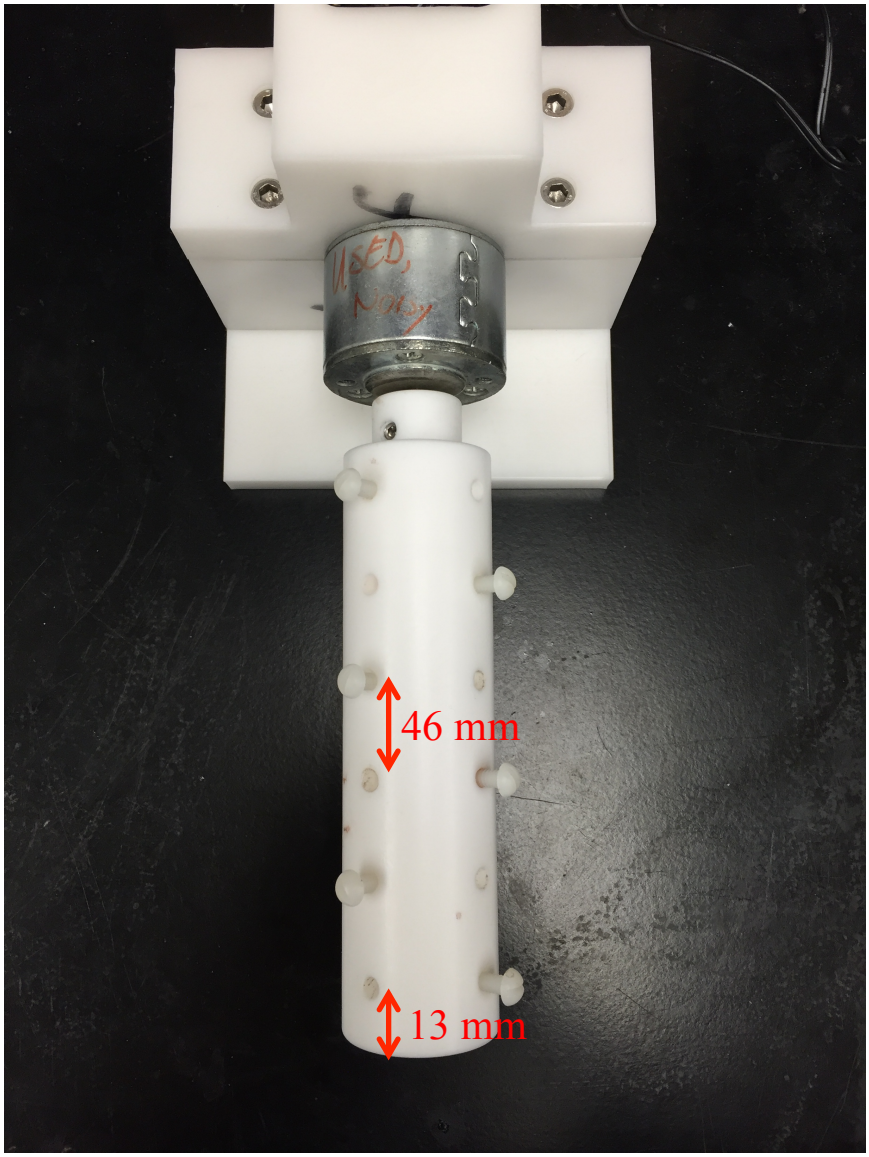

Figure 4-14. Alternate top view. There is a 13 mm gap from the front of the device to the first hole. All other gaps are 46 mm.

4.3 Notes for Chapter 4

1) Wilmad-LabGlass SP Scienceware. http://www.wilmad-labglass.com (Accessed 12 Jan 2015).

Bibliography

Albers, M. O; Ashworth, T. V.; Oosthuizen, H. E.; Singleton, E., *Inorg. Synth.,* **1989**, *26*, 68-77.

Albrecht, M. and van Koten, G., *Angew. Chem. Int. Ed.*, **2001**, *40*, 3750-3781.

Bäckvall, J., *J. Organometallic Chem.*, **2002**, *652*, 105-111.

Blacker, A. J.; Clot, E.; Duckett, S. B.; Eisenstein, O.; Grace, J.; Nova, A.; Perutz, R. N.; Taylor, D. J.; Whitwood, A. C., *Chem. Commun.,* **2009**, *44*, 6801-6803.

Brahms, D. L. S. and Dailey, W. P., *Chem. Rev.,* **1996**, *96*, 1585-1632.

Brookhart, M. and Green, M. L. H., *J. Organomet. Chem.*, **1983**, *250*, 395-408.

Brookhart, M.; Grant, B.; Volpe, A. F., Jr., *Organometallics*, **1992**, 11, 3920-3922.

Cappellani, E. P.; Drouin, S. D.; Jia, G.; Maltby, P. A.; Morris, R. H.; Schweitzer, C. T., *J. Am. Chem. Soc*., **1994**, *116*, 3375-3388.

Carmona, D.; Oro, L. A.; Lamata, M. P.; Puebla, M. P.; Ruiz, J.; Maitlis, P. M., *J. Chem. Soc., Dalton Trans.,* **1987**, 639-645.

Chatt, J. and Coffey, R. S., *J. Chem. Soc. A,* **1969**, 1963-1972.

Chatt, J. and Shaw, B. L., *J. Chem. Soc. A: Inorg. Phys. Theor.*, **1966**, 1437-1442.

Chem. Eng. News, **1996**, *74* (11), 4.

Cho, O.-J.; Lee, I.-M.; Park, K.-Y.; Kim, H.-S., *J. Fluorine Chem.*, **1995**, *71*, 107-109.

Connelly, S. J.; Chanez, A. G.; Kaminsky, W.; Heinekey, D. M., *Angew. Chem. Int. Ed.,* **2015**, *54*, 5915-5918.

Crabtree, R. H. and Hamilton, D. G., *Adv. Organomet. Chem.*, **1988**, *28*, 299-388.

Crabtree, R. H., *The Organometallic Chemistry of the Transition Metals*, 4th ed.; Hoboken, New Jersey, 2005.

Crampton, M. R. and Robotham, I. A., *J. Chem. Res.,* **1997**, 22-23.

Crossland, J. L.; Young, D. M.; Zakharov, L. N.; Tyler, D. R., *Dalton Trans.,* **2009**, *42*, 9253-9259.

Dani, P.; Karlen, T.; Gossage, R. A.; Smeets, W. J. J.; Spek, A. L.; van Koten, G., *J. Am. Chem. Soc.*, **1997**, *119*, 11317-11318.

Dani, P.; Toorneman, M. A. M.; van Klink, G. P. M.; van Koten, G., *Organometallics*, **2000**, *19*, 5287-5296.

Desrosiers, P. J.; Cai, L.; Lin, Z.; Richards, R.; Halpern, J., *J. Am. Chem. Soc.*, **1991**, *113*, 4173-4184.

Doherty, N. M. and Bercaw, J. E., *J. Am. Chem. Soc.*, **1985**, *107*, 2670-2682.

ESLR Global Monitoring Division – Halocarbons and Other Atmospheric Trace Species. http://www.esrl.noaa.gov/gmd/hats/flask/hcfc.html (Accessed October 2014).

ESRL Global Monitoring Division. http://www.esrl.noaa.gov/gmd/hats/publictn/elkins/cfcs.html (accessed January 2016).

Evidence for broadening in ^{19}F NMR data with PF_6^- coordination: Honeychuck, R. V. and Hersh, W. H., *Inorg. Chem.*, **1989***, 28*, 2869-2886.

Farrugia, L. J., Ortep-3 for Windows, *J. Appl. Cryst.*, **1997**, *30***,** 565-566.

Findlater, M.; Bernskoetter, W. H.; Brookhart, M., *J. Am. Chem. Soc.*, **2010**, *132*, 4534-4535.

Fisher, D. A.; Hales, C. H.; Wang, C.; Ko, M. K. W.; Sze, N. D., *Nature*, **1990**, *344*, 513-516.

Frech, C. M. and Milstein, D., *J. Am. Chem. Soc.*, **2006**, *128*, 12434-12435.

Frech, C. M.; Shimon, L. J. W.; Milstein, D., *Organometallics*, **2009**, *28*, 1900-1908.

Frost, B. J. and Mebi, C. A., *Organometallics*, **2004**, *23*, 5317-5323.

Fryzuk, M. D.; Jones, T.; Einstein, F. W. B., *Organometallics*, **1984**, *3*, 185-191.

Fulmer, G. R.; Miller, A. J. M.; Sherden, N. H.; Gottlieb, H. E.; Nudelman, A.; Stoltz, B. M.; Bercaw, J. E.; Goldberg, K. I., *Organometallics*, **2010**, *29*, 2176-2179.

Gilbertson, J. D.; Szymczak, N. K.; Crossland, J. L.; Miller, W. K.; Lyon, D. K.; Foxman, B. M.; Davis, J.; Tyler, D. R., *Inorg. Chem.,* **2007**, *46*, 1205-1214.

Gilbertson, J. D.; Szymczak, N. K.; Tyler, D. R., *J. Am. Chem. Soc.,* **2005**, *127*, 10184-10185.

Giuffredi, G. T.; Purser, S.; Sawicki, M.; Thompson, A. L.; Gouverneur, V., *Tetrahedron: Asymmetry*, **2009**, *20*, 910-920.

Goldberg, J. M.; Wong, G. W.; Brastow, K. E.; Kaminsky, W.; Goldberg, K. I.;

Göttker-Schnetmann, I.; White, P.; Brookhart, M., *J. Am. Chem. Soc.*, **2004**, *126*, 1804-1811.

Haack, K.; Hashiguchi, S.; Fujii, A.; Ikariya, T.; Noyori, R., *Angew. Chem. Int. Ed.,* **1997**, *36*, 285-288.

Hall, C. and Perutz, R. N., *Chem. Rev.*, **1996**, *96*, 3125-3146.

Halpern, J., *Annals of the New York Academy of Sciences*, **1983**, *415*, 244-252.

Heinekey, D. M., *Organometallics*, **2015**, *34*, 753-762.

Heinekey, D. M. and Michel, S. T., *Organometallics*, **1989**, *8*, 1241-1246.

Heinekey, D. M. and Oldham Jr., W. J., *Chem. Rev.,* **1993**, *93*, 913-926.

Heinekey, D. M. and Oldham, W. J., *Chem. Rev.*, **1993**, *93*, 913-926.

Heinekey, D. M.; Voges, M. H.; Barnhard, D. M., *J. Am. Chem. Soc.,* **1996**, *118*, 10792-10802.

Henning, J.; Schubert, H.; Eichele, K.; Winter, F.; Pöttgen, R.; Mayer, H. A.; Wesemann, L., *Inorg. Chem*., **2012**, *51*, 5787-5794.

Herbowski, A. and Deutsch, E. A., *J. Organomet. Chem.,* **1993**, *460*, 19-23.

Hieber, W. and Leutert, F., *Naturwisenschaften*, **1931**, *19*, 360-361.

Hine, J., *J. Am. Chem. Soc.,* **1950**, *72*, 2438-2445.

Hine, J. and Burske, N. W., *J. Am. Chem. Soc.,* **1956**, *78*, 3337-3339.

Hine, J. and Dowell Jr., A. M., *J. Am. Chem. Soc.,* **1954**, *76*, 2688-2692.

Hine, J.; Dowell Jr., A. M.; Singley Jr., J. E., *J. Am. Chem. Soc.,* **1956**, *78*, 479-482.

Hine, J.; Peek, R. C.; Oakes, B. D., *J. Am. Chem. Soc.,* **1954**, *76*, 827-829.

Huang, K.; Grills, D. C.; Han, J. H.; Szalda, D. J.; Fujita, E., *Inorg. Chim. Acta.*, **2008**, *361*, 3327-3331.

Imamura, S.; Matsuba, Y.; Yamada, E.; Takai, K.; Utani, K., *Ind. Eng. Chem. Res.*, **1997**, *36*, 3978-3981.

Ito, M.; Hirakawa, M.; Murata, K.; Ikariya, T., *Organometallics*, **2001**, *20*, 379-381.
Jacobsen, N. E., *NMR Spectroscopy Explained: Simplified Theory, Applications and Examples for Organic Chemistry and Structural Biology*, 1st ed.; John Wiley & Sons, Inc.: New Jersey, 2007.

Jia, G. and Morris, R. H., *J. Am. Chem. Soc.*, **1991**, *113*, 875-883.

Kaesz, H. D. and Saillant, R. B., *Chem. Rev.*, **1972**, *72*, 231-281.

Kaljurand, I.; Kütt, A.; Sooväli, L.; Rodima, T.; Mäemets, V.; Leito, I.; Koppel, I. A., *J. Org. Chem.*, **2005**, *70*, 1019-1028.

Kelley, P.; Lin, S.; Edouard, G.; Day, M. W.; Agapie, T., *J. Am. Chem. Soc.*, **2012**, *134*, 5480-5483.

Kim, H.-S.; Cho, O.-J.; Lee, I.-M.; Hong, S.-P.; Kwag, C.-Y.; Ahn, B. S., *J. Mole. Catal. A: Chem.*, **1996**, *111*, 49-65.

Kinney, R. J.; Jones, W. D.; Bergman, R. G., *J. Am. Chem. Soc.*, **1978**, *100*, 635-637.

Kristjánsdóttir, S. S. and Norton, J. R. Acidity of Hydrido Transition Metal Complexes in Solution. In *Transition Metal Hydrides*; Dedieu, A., Eds.; VCH Publishers, Inc.: New York, New York, 1992; pp. 309-359.

Kubas, G. J., *Chem. Rev.*, **2007**, *107*, 4152-4205 and references therein.

Kubas, G. J.; Ryan, R. R.; Swanson, B. I.; Vergamini, P. J.; Wasserman, H. J., *J. Am. Chem. Soc.*, **1984**, *106*, 451-452.

Kubas, G. J.; Wasserman, H. J.; Ryan, R. R., *Organometallics*, **1985**, *4*, 2012-2021.

Kuivila, H. G., *Acc. Chem. Res.*, **1968**, *1*, 299-305.

Kuklin, S. A.; Sheloumov, A. M.; Dolgushin, F. M.; Ezernitskaya, M. G.; Peregudov, A. S.; Petrovskii, P. V.; Koridze, A. A., *Organometallics*, **2006**, *25*, 5466-5476.

Lao, D. B.; Owens, A. C. E.; Heinekey, D. M.; Goldberg, K. I., *ACS Catalysis*, **2013**, *3*, 2391-2396.

Larionov, E.; Li, H.; Mazet, C., *Chem. Commun.*, **2014**, *50*, 9816-9826.

Letsinger, R. L. and Schnizer, A. W., *J. Org. Chem.,* **1951**, *16*, 704-707.

Manzer, L. E. and Nappa, M. J., *Appl. Catal., A*, **2001**, *221*, 267-274.

Martinho Simões, J. A. and Beauchamp, J. L., *Chem. Rev.,* **1990,** *90*, 629-688.

Mestroni, G.; Camus, A.; Zassinovich, G., *J. Organometallic Chem.*, **1974**, *65*, 119-129.

Miller, W. K.; Gilbertson, J. D.; Leiva-Paredes, C.; Bernatis, P. R.; Weakley, T. J. R.; Lyon, D. K.; Tyler, D. R., *Inorg. Chem.,* **2002**, *41*, 5453-5465.

Mingos, D. M. P., *J. Organomet. Chem.*, **2001**, *635*, 1-8 and references therein.

Montag, M.; Efremenko, I.; Cohen, R.; Shimon, L. J. W.; Leitus, G.; Diskin-Posner, Y.; Ben-David, Y.; Salem, H.; Martin, J. M. L.; Milstein, D. *Chem. Eur. J.*, **2010**, *16*, 328-353.

Montag, M.; Schwartsburd, L.; Cohen, R.; Leitus, G.; Ben-David, Y.; Martin, J. M. L.; Milstein, D., *Angew. Chem. Int. Ed.*, **2007**, *46*, 1901-1904.

Moore, D. S. and Robinson, S. D., *Chem. Soc. Rev.*, **1983**, *12*, 415-452.

Moore, E. J.; Sullivan, J. M.; Norton, J. R., *J. Am. Chem. Soc.*, **1986**, *108*, 2257-2263.

Morales-Morales, D.; Redón, R.; Wang, Z.; Lee, D. W.; Yung, C.; Magnuson, K.; Jensen, C. M., *Can. J. Chem.,* **2001**, *79*, 823-829.

Moulton, C. J. and Shaw, B. L., *J. Chem. Soc., Dalton Trans.,* **1976**, *11*, 1020-1024

Mutterties, E. L., *Transition Metal Hydrides.* New York: M. Dekker, 1971. 244-246. Print.

O'Reilly, M. E. and Veige, A. S., *Chem. Soc. Rev.*, **2014**, *43*, 6325-6369.

Organometallic Pincer Chemistry; Topics in Organometallic Chemistry; van Koten, G. and Milstein, D., Eds.; Springer: Heidelberg, **2013**; Vol. *40*.

Ozone Hole Watch. http://ozonewatch.gsfc.nasa.gov/monthly/monthly_2015-10_SH.html (Accessed December 2015).

Ozone Science: The Facts Behind the Phaseout | Ozone Layer Protection | US EPA. http://www.epa.gov/ozone/science/sc_fact.html (Accessed January 2012).

Polezhaev, A. V.; Kuklin, S. A.; Ivanov, D. M.; Petrovskii, P. V.; Dolgushin, F. M.; Ezernitskaya, M. G.; Koridze, A. A., *Russ. Chem. Bull., Int. Ed.,* **2009**, *58*, 1847-1854.

Pons, V. and Heinekey, D. M., *J. Am. Chem. Soc.*, **2003**, *125*, 8428-8429.

Prinn, R. G. and Golombek, A., *Nature*, **1990**, *344*, 47-49.

Punji, B.; Emge, T. J.; Goldman, A. S., *Organometallics*, **2010**, *29*, 2702-2709.

Raamat, E.; Kaupmees, K.; Ovsjannikov, G.; Trummal, A.; Kütt, A.; Saame, J.; Koppel, I.; Kaljurand, I.; Lipping, L.; Rodima, T.; Pihl, V.; Koppel, I. A.; Leito, I., *J. Phys. Org. Chem.*, **2013**, *26*, 162-170.

Rimml, H. and Venanzi, L. M., *Phosphorus Sulfur Relat. Elem.*, **1987**, *30*, 297-300.

Rodima, T.; Kaljurand, I.; Pihl, A.; Mäemets, V.; Leito, I.; Koppel, I. A., *J. Org. Chem.,* **2002**, *67*, 1873-1881.

Salem, H.; Ben-David, Y.; Shimon, L. J. W.; Milstein, D., *Organometallics*, **2006**, *25*, 2292-2300.

Salem, H.; Shimon, L. J. W.; Leitus, G.; Weiner, L.; Milstein, D., *Organometallics*, **2008**, *27*, 2293-2299.

Sandoval, C. A.; Ohkuma, T.; Muñiz, K.; Noyori, R., *J. Am. Chem. Soc.,* **2003**, *125*, 13490-13503.

Sanmartín, J.; Novio, F.; García-Deibe, A. M.; Fondo, M.; Bermejo, M. R., *New J. Chem.,* **2007**, *31*, 1605-1612.

Schrock, R. R. and Osborn, J. A., *J. Am. Chem. Soc.,* **1971**, *93*, 2397-2407.

Schwesinger, R.; Schlemper, H.; Hasenfratz, C.; Willaredt, J.; Dambacker, T.; Breuer, T.; Ottaway, C.; Fletschinger, M.; Boele, J.; Fritz, H.; Putzas, D.; Rotter, H. W.; Bordwell, F. G.; Satish, A. V.; Ji, G.; Peters, E.; Peters, K.; von Schnering, H. G.; Walz, L., *Liebigs Annalen,* **1996**, *7*, 1055-1081.

Selmeczy, A. D. and Jones, W. D., *Inorg. Chim. Acta.*, **2000**, 138-150.

Siegel, J. S. and Anet, F. A. L., *J. Org. Chem.,* **1988**, *53*, 2629-2630.

Simon, O. B. and Sisak, A., *Appl. Catal., A*, **2008**, *342*, 131-136.

Slater, J. C., *J. Chem. Phys*., **1964**, *41*, 3199-3204.

Smith, M. B. and March, J., *March's Advanced Organic Chemistry: Reactions, Mechanisms, and Structure*, 5th ed.; John Wiley & Sons, Inc:.: 2001; pp. 329-331.

Sullivan, B. P. and Meyer, T. J., *Organometallics*, **1986**, *7*, 1500-1502.

Szymczak, N. K.; Braden, D. A.; Crossland, J. L.; Turov, Y.; Zakharov, L. N.; Tyler, D. R., *Inorg. Chem.* **2009**, *48*, 2976-2984.

Szymczak, N. K.; Zakharov, L. N.; Tyler, D. R., *J. Am. Chem. Soc.*, **2006**, *128*, 15830-15835.

The Alternative Fluorocarbons Environmental Acceptability Study. http://www.afeas.org/overview.php (accessed February 2015).

The Montreal Protocol on Substances that Deplete the Ozone Layer | Ozone Layer Protection | US EPA. http://www.epa.gov/ozone/intpol/index.html (Accessed February 2015).

Tokuhashi, K.; Urano, Y.; Sadashige, H.; Kondo, S., *Combust. Sci. and Tech.* **1990**, *72*, 117-129.

Uematsu, N.; Fujii, A.; Hashiguchi, S.; Ikariya, T.; Noyori, R., *J. Am. Chem. Soc.,* **1996**, *118*, 4916-4917.

Vabre, B.; Lambert, M. L.; Petit, A.; Ess. D. H.; Zargarian, D., *Organometallics*, **2012**, *31*, 6041-6053.

Vabre, B.; Spasyuk, D. M.; Zargarian, D., *Organometallics*, **2012**, *31*, 8561-8570.

van der Boom, M. E. and Milstein, D., *Chem. Rev.*, **2003**, *103*, 1759-1792.

van der Boom, M. E.; Gozin, M.; Ben-David, Y.; Shimon, L. J. W.; Frolow, F.; Kraatz, H.; Milstein, D., *Inorg. Chem.*, **1996**, *35*, 7068-7073.

van der Ent, A. and Onderdelinden, A. L, *Inorg. Synth.*, **1990**, *28*, 90-92.

Van Roon, M., *Structure, Dynamics, and Reactivity of Hydride Complexes of the Cobalt and Iron Group Metals.* Diss. U of Washington, 1997. Print.

Vaska, L. and Rhodes, R. E., *J. Am. Chem. Soc.*, **1965**, *87*, 4970-4971.

Vigalok, A.; Uzan, O.; Shimon, L. J. W.; Ben-David, Y.; Martin, J. M. L.; Milstein, D., *J. Am. Chem. Soc.,* **1998**, *120*, 12539.

Walker, H. W.; Kresge, C. T.; Ford, P. D.; Pearson, R. G., *J. Am. Chem. Soc.*, **1979**, *101*, 7428-7429.

Walker, H. W.; Pearson, R. G.; Ford, P. C., *J. Am. Chem. Soc.*, **1983**, *105*, 1179-1186.

Walling, C.; Cooley, J. H.; Ponaras, A. A.; Racah, E. J., *J. Am. Chem. Soc.*, **1966**, *88*, 5361-5363.

Wallington, T. J.; Hurley, M. D.; Ball, J. C.; Kalser, E. W., *Environ. Sci. Technol.*, **1992**, *26*, 1318-1324.

Weigert, F. J. and Roberts, J. D., *J. Am. Chem. Soc.*, **1967**, *89*, 2967-2969.

White, C.; Oliver, A. J.; Maitlis, P. M., *J. Chem. Soc., Dalton Trans.,* **1973**, 1901-1907.

Wiersma, A.; ten Cate, A.; van de Sandt, E. J. A. X.; Makkee, M., *Ind. Eng. Chem. Res.*, **2007**, *46*, 4158-4165.

Wiersma, A.; van de Sandt, E. J. A. X.; den Hollander, M. A.; van Bekkum, H.; Makkee, M.; Mouljin, J. A., *J. Catal.*, **1998**, *177*, 29-39.

Wilkinson, G. and Birmingham, J. M., *J. Am. Chem. Soc.*, **1955**, *77*, 3421-3422.

Wilmad-LabGlass SP Scienceware. http://www.wilmad-labglass.com (Accessed 12 Jan 2015).

Xie, S.; Georgiev, E. M.; Roundhill, D. M., *J. Organometallic Chem.*, **1994**, *482*, 39-44.

Appendix A: Numbering Scheme for Compounds

(1)

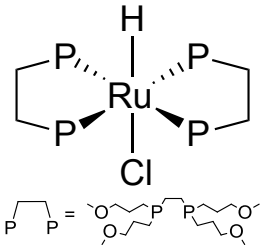

(2)

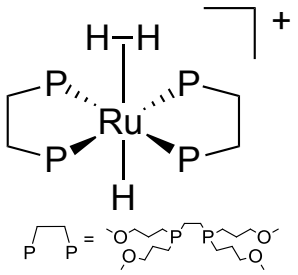

(3)

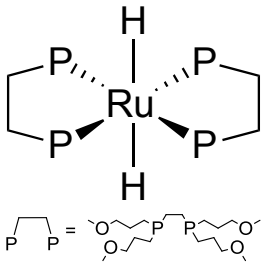

(4)

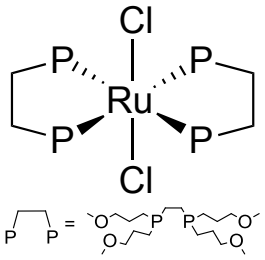

(5)

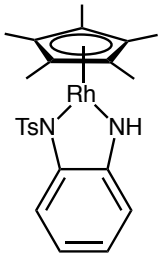

(6)

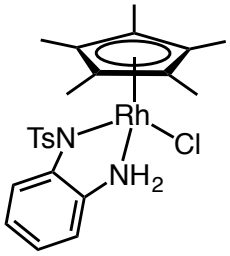

(7)

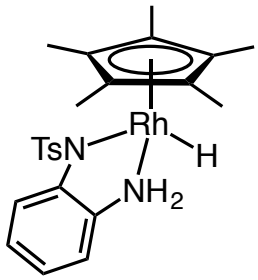

(8)

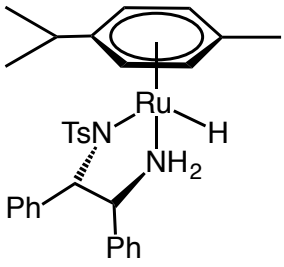

(9)

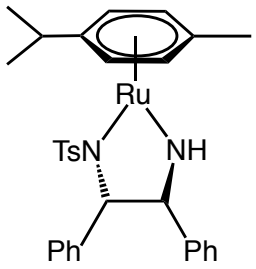

(10)

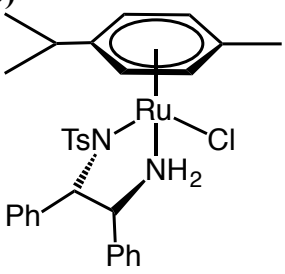

(11)

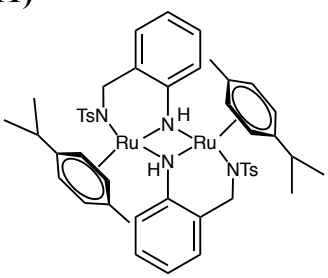

(12)

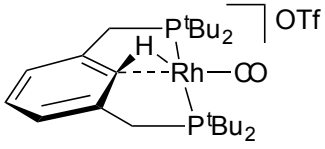

(13)

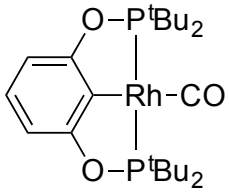

(14)

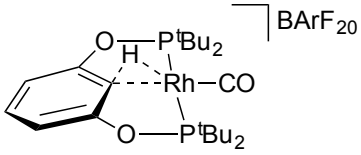

(15)

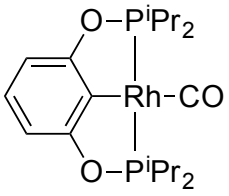

(16)

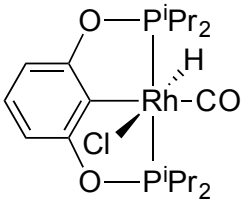

(17)

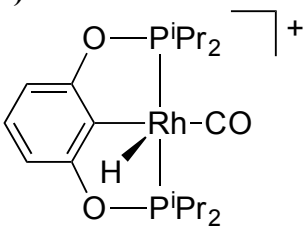

(18)

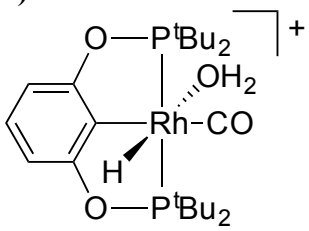

(19)

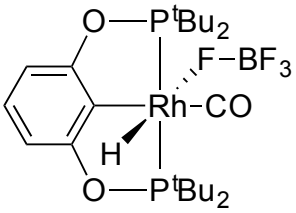

Appendix B: Crystal Structure Data for Chapter 2

*Crystal structure data for **11**, [(p-cym)Ru(TsABA)]$_2$*:

A brown prism, measuring 0.15 x 0.14 x 0.08 mm^3 was mounted on a loop with oil. Data was collected at -183^{o}C on a Bruker APEX II single crystal X-ray diffractometer, Mo-radiation.

Crystal-to-detector distance was 40 mm and exposure time was 5 seconds per frame for all sets. The scan width was 0.5^o. Data collection was 99.9% complete to 25^o in ϑ. A total of 365088 reflections were collected covering the indices, h = -13 to 13, k = -38 to 38, l = -22 to 22. 12473 reflections were symmetry independent and the R_{int} = 0.0763 indicated that the data was of average quality. Indexing and unit cell refinement indicated a primitive monoclinic lattice. The space group was found to be P 2_1/c (No.14).

The data was integrated and scaled using SAINT, SADABS within the APEX2 software package by Bruker.[1]

Solution by direct methods (SHELXS, SIR97[2]) produced a complete heavy atom phasing model consistent with the proposed structure. The structure was completed by difference Fourier synthesis with SHELXL97.[3,4] Scattering factors are from Waasmair and Kirfel.[5] Hydrogen atoms were placed in geometrically idealised positions and constrained to ride on their parent atoms with C-H distances in the range 0.95-1.00 Angstrom. Isotropic thermal parameters U_{eq} were fixed such that they were 1.2U_{eq} of their parent atom Ueq for CH's and 1.5U_{eq} of their parent atom U_{eq} in case of methyl groups. All non-hydrogen atoms were refined anisotropically by full-matrix least-squares.

Solvent analysis discovered a total of 6 CH_2Cl_2 in the unit cells within two infinite channels along [1 0 0] and their contribution to the diffraction pattern was removed with SQUEEZE.[6]

Table B-1. Crystal data and structure refinement for 11.

Empirical formula	$C_{48}\ H_{56}\ N_4\ O_4\ Ru_2\ S_2$	
Formula weight	1019.23	
Temperature	90(2) K	
Wavelength	0.71073 Å	
Crystal system	Monoclinic	
Space group	P 2_1/c	
Unit cell dimensions	a = 10.1910(12) Å	α= 90°.
	b = 28.717(3) Å	β= 99.504(6)°.
	c = 17.115(2) Å	γ = 90°.
Volume	4940.2(10) $Å^3$	
Z	4	
Density (calculated)	1.370 Mg/m^3	
Absorption coefficient	0.740 mm^{-1}	
F(000)	2096	
Crystal size	0.15 x 0.14 x 0.08 mm^3	
Theta range for data collection	2.15 to 28.53°.	
Index ranges	-13<=h<=13, -38<=k<=38, -22<=l<=22	
Reflections collected	365088	
Independent reflections	12473 [R(int) = 0.0763]	
Completeness to theta = 25.00°	99.9 %	
Max. and min. transmission	0.9432 and 0.8971	
Refinement method	Full-matrix least-squares on F^2	
Data / restraints / parameters	12473 / 0 / 550	
Goodness-of-fit on F^2	1.076	
Final R indices [I>2sigma(I)]	R1 = 0.0308, wR2 = 0.0663	
R indices (all data)	R1 = 0.0369, wR2 = 0.0685	
Largest diff. peak and hole	0.895 and -0.721 $e.Å^{-3}$	

Table B-2. Atomic coordinates ($\times 10^4$) and equivalent isotropic displacement parameters ($Å^2 \times 10^3$) for **11**. U(eq) is defined as one third of the trace of the orthogonalized U^{ij} tensor.

	x	y	z	U(eq)
C(1)	-480(2)	1152(1)	6125(1)	21(1)
C(2)	1010(2)	1181(1)	6269(1)	16(1)
C(3)	1802(2)	852(1)	6741(1)	18(1)
C(4)	3219(2)	870(1)	6862(1)	18(1)
C(5)	3876(2)	1226(1)	6518(1)	17(1)
C(6)	3087(2)	1575(1)	6063(1)	15(1)
C(7)	1692(2)	1553(1)	5947(1)	15(1)
C(8)	5378(2)	1250(1)	6573(1)	21(1)
C(9)	5705(2)	1119(1)	5757(1)	29(1)
C(10)	6156(2)	940(1)	7211(1)	26(1)
C(11)	4900(2)	1836(1)	8300(1)	12(1)
C(12)	6182(2)	1999(1)	8236(1)	15(1)
C(13)	7310(2)	1810(1)	8680(1)	17(1)
C(14)	7187(2)	1449(1)	9203(1)	17(1)
C(15)	5935(2)	1291(1)	9277(1)	16(1)
C(16)	4771(2)	1475(1)	8833(1)	14(1)
C(17)	3487(2)	1252(1)	8973(1)	16(1)
C(18)	840(2)	605(1)	8779(1)	15(1)
C(19)	74(2)	357(1)	8176(1)	19(1)
C(20)	2(2)	-125(1)	8223(1)	20(1)
C(21)	665(2)	-367(1)	8874(1)	17(1)
C(22)	1402(2)	-110(1)	9487(1)	17(1)
C(23)	1500(2)	371(1)	9441(1)	16(1)
C(24)	564(2)	-891(1)	8930(1)	23(1)
C(25)	5307(2)	2723(1)	9582(1)	25(1)
C(26)	3847(2)	2788(1)	9285(1)	18(1)
C(27)	2910(2)	2437(1)	9414(1)	16(1)
C(28)	1539(2)	2503(1)	9159(1)	13(1)
C(29)	1034(2)	2918(1)	8745(1)	13(1)
C(30)	1975(2)	3253(1)	8595(1)	14(1)

C(31)	3367(2)	3190(1)	8869(1)	18(1)
C(32)	-449(2)	2978(1)	8502(1)	14(1)
C(33)	-1064(2)	3113(1)	9230(1)	21(1)
C(34)	-846(2)	3330(1)	7839(1)	18(1)
C(35)	257(2)	2344(1)	6873(1)	11(1)
C(36)	-1091(2)	2244(1)	6866(1)	13(1)
C(37)	-2078(2)	2471(1)	6351(1)	15(1)
C(38)	-1729(2)	2798(1)	5821(1)	15(1)
C(39)	-395(2)	2894(1)	5814(1)	13(1)
C(40)	611(2)	2673(1)	6337(1)	11(1)
C(41)	2041(2)	2775(1)	6279(1)	13(1)
C(42)	4245(2)	3623(1)	6582(1)	14(1)
C(43)	3212(2)	3912(1)	6695(1)	20(1)
C(44)	3279(2)	4386(1)	6525(1)	22(1)
C(45)	4379(2)	4572(1)	6252(1)	21(1)
C(46)	5386(2)	4271(1)	6119(2)	26(1)
C(47)	5329(2)	3797(1)	6278(1)	22(1)
C(48)	4485(3)	5088(1)	6101(2)	31(1)
N(1)	3793(2)	2033(1)	7791(1)	12(1)
N(2)	2286(2)	1369(1)	8410(1)	13(1)
N(3)	1222(2)	2125(1)	7449(1)	11(1)
N(4)	2884(2)	2884(1)	7052(1)	13(1)
O(1)	-154(1)	1364(1)	8122(1)	21(1)
O(2)	957(2)	1384(1)	9515(1)	22(1)
O(3)	5219(2)	3058(1)	7673(1)	23(1)
O(4)	4797(2)	2766(1)	6305(1)	20(1)
S(1)	954(1)	1223(1)	8712(1)	15(1)
S(2)	4333(1)	3036(1)	6922(1)	14(1)
Ru(1)	2422(1)	1548(1)	7207(1)	11(1)
Ru(2)	2570(1)	2579(1)	8147(1)	10(1)

Table B-3. Bond lengths [Å] and angles [°] for **11**.

C(1)-C(2)	1.500(3)
C(1)-H(1A)	0.9800
C(1)-H(1B)	0.9800
C(1)-H(1C)	0.9800
C(2)-C(3)	1.408(3)
C(2)-C(7)	1.432(3)
C(2)-Ru(1)	2.234(2)
C(3)-C(4)	1.425(3)
C(3)-Ru(1)	2.204(2)
C(3)-H(3)	0.9500
C(4)-C(5)	1.403(3)
C(4)-Ru(1)	2.225(2)
C(4)-H(4)	0.9500
C(5)-C(6)	1.433(3)
C(5)-C(8)	1.520(3)
C(5)-Ru(1)	2.241(2)
C(6)-C(7)	1.404(3)
C(6)-Ru(1)	2.177(2)
C(6)-H(6)	0.9500
C(7)-Ru(1)	2.163(2)
C(7)-H(7)	0.9500
C(8)-C(10)	1.526(3)
C(8)-C(9)	1.535(3)
C(8)-H(8)	1.0000
C(9)-H(9A)	0.9800
C(9)-H(9B)	0.9800
C(9)-H(9C)	0.9800
C(10)-H(10A)	0.9800
C(10)-H(10B)	0.9800
C(10)-H(10C)	0.9800
C(11)-C(16)	1.400(3)
C(11)-C(12)	1.409(3)
C(11)-N(1)	1.424(2)
C(12)-C(13)	1.381(3)

C(12)-H(12)	0.9500
C(13)-C(14)	1.388(3)
C(13)-H(13)	0.9500
C(14)-C(15)	1.380(3)
C(14)-H(14)	0.9500
C(15)-C(16)	1.402(3)
C(15)-H(15)	0.9500
C(16)-C(17)	1.511(3)
C(17)-N(2)	1.466(3)
C(17)-H(17A)	0.9900
C(17)-H(17B)	0.9900
C(18)-C(19)	1.385(3)
C(18)-C(23)	1.392(3)
C(18)-S(1)	1.782(2)
C(19)-C(20)	1.390(3)
C(19)-H(19)	0.9500
C(20)-C(21)	1.391(3)
C(20)-H(20)	0.9500
C(21)-C(22)	1.395(3)
C(21)-C(24)	1.512(3)
C(22)-C(23)	1.390(3)
C(22)-H(22)	0.9500
C(23)-H(23)	0.9500
C(24)-H(24A)	0.9800
C(24)-H(24B)	0.9800
C(24)-H(24C)	0.9800
C(25)-C(26)	1.503(3)
C(25)-H(25A)	0.9800
C(25)-H(25B)	0.9800
C(25)-H(25C)	0.9800
C(26)-C(31)	1.401(3)
C(26)-C(27)	1.432(3)
C(26)-Ru(2)	2.239(2)
C(27)-C(28)	1.406(3)
C(27)-Ru(2)	2.1767(19)
C(27)-H(27)	0.9500

C(28)-C(29)	1.436(3)
C(28)-Ru(2)	2.1799(19)
C(28)-H(28)	0.9500
C(29)-C(30)	1.412(3)
C(29)-C(32)	1.511(3)
C(29)-Ru(2)	2.2300(19)
C(30)-C(31)	1.430(3)
C(30)-Ru(2)	2.203(2)
C(30)-H(30)	0.9500
C(31)-Ru(2)	2.222(2)
C(31)-H(31)	0.9500
C(32)-C(34)	1.522(3)
C(32)-C(33)	1.535(3)
C(32)-H(32)	1.0000
C(33)-H(33A)	0.9800
C(33)-H(33B)	0.9800
C(33)-H(33C)	0.9800
C(34)-H(34A)	0.9800
C(34)-H(34B)	0.9800
C(34)-H(34C)	0.9800
C(35)-C(36)	1.401(3)
C(35)-C(40)	1.404(3)
C(35)-N(3)	1.420(2)
C(36)-C(37)	1.386(3)
C(36)-H(36)	0.9500
C(37)-C(38)	1.392(3)
C(37)-H(37)	0.9500
C(38)-C(39)	1.389(3)
C(38)-H(38)	0.9500
C(39)-C(40)	1.397(3)
C(39)-H(39)	0.9500
C(40)-C(41)	1.505(3)
C(41)-N(4)	1.487(2)
C(41)-H(41A)	0.9900
C(41)-H(41B)	0.9900
C(42)-C(43)	1.380(3)

C(42)-C(47)	1.390(3)
C(42)-S(2)	1.780(2)
C(43)-C(44)	1.396(3)
C(43)-H(43)	0.9500
C(44)-C(45)	1.389(3)
C(44)-H(44)	0.9500
C(45)-C(46)	1.390(3)
C(45)-C(48)	1.511(3)
C(46)-C(47)	1.391(3)
C(46)-H(46)	0.9500
C(47)-H(47)	0.9500
C(48)-H(48A)	0.9800
C(48)-H(48B)	0.9800
C(48)-H(48C)	0.9800
N(1)-Ru(1)	2.1043(17)
N(1)-Ru(2)	2.1533(16)
N(1)-H(1)	0.9300
N(2)-S(1)	1.5874(17)
N(2)-Ru(1)	2.1478(16)
N(3)-Ru(2)	2.1146(16)
N(3)-Ru(1)	2.1406(16)
N(3)-H(3A)	0.9300
N(4)-S(2)	1.5895(17)
N(4)-Ru(2)	2.1410(16)
O(1)-S(1)	1.4422(16)
O(2)-S(1)	1.4486(16)
O(3)-S(2)	1.4449(15)
O(4)-S(2)	1.4511(16)

C(2)-C(1)-H(1A)	109.5
C(2)-C(1)-H(1B)	109.5
H(1A)-C(1)-H(1B)	109.5
C(2)-C(1)-H(1C)	109.5
H(1A)-C(1)-H(1C)	109.5
H(1B)-C(1)-H(1C)	109.5
C(3)-C(2)-C(7)	116.94(19)

C(3)-C(2)-C(1)	121.71(19)
C(7)-C(2)-C(1)	121.33(19)
C(3)-C(2)-Ru(1)	70.35(12)
C(7)-C(2)-Ru(1)	68.33(11)
C(1)-C(2)-Ru(1)	131.26(15)
C(2)-C(3)-C(4)	122.0(2)
C(2)-C(3)-Ru(1)	72.67(12)
C(4)-C(3)-Ru(1)	72.02(12)
C(2)-C(3)-H(3)	119.0
C(4)-C(3)-H(3)	119.0
Ru(1)-C(3)-H(3)	128.7
C(5)-C(4)-C(3)	120.53(19)
C(5)-C(4)-Ru(1)	72.30(12)
C(3)-C(4)-Ru(1)	70.43(12)
C(5)-C(4)-H(4)	119.7
C(3)-C(4)-H(4)	119.7
Ru(1)-C(4)-H(4)	130.1
C(4)-C(5)-C(6)	118.28(19)
C(4)-C(5)-C(8)	123.61(19)
C(6)-C(5)-C(8)	118.07(19)
C(4)-C(5)-Ru(1)	71.09(12)
C(6)-C(5)-Ru(1)	68.68(11)
C(8)-C(5)-Ru(1)	133.98(15)
C(7)-C(6)-C(5)	120.62(19)
C(7)-C(6)-Ru(1)	70.60(11)
C(5)-C(6)-Ru(1)	73.51(12)
C(7)-C(6)-H(6)	119.7
C(5)-C(6)-H(6)	119.7
Ru(1)-C(6)-H(6)	128.5
C(6)-C(7)-C(2)	121.55(19)
C(6)-C(7)-Ru(1)	71.65(11)
C(2)-C(7)-Ru(1)	73.70(12)
C(6)-C(7)-H(7)	119.2
C(2)-C(7)-H(7)	119.2
Ru(1)-C(7)-H(7)	127.6
C(5)-C(8)-C(10)	114.64(19)

C(5)-C(8)-C(9)	107.41(18)
C(10)-C(8)-C(9)	110.10(19)
C(5)-C(8)-H(8)	108.2
C(10)-C(8)-H(8)	108.2
C(9)-C(8)-H(8)	108.2
C(8)-C(9)-H(9A)	109.5
C(8)-C(9)-H(9B)	109.5
H(9A)-C(9)-H(9B)	109.5
C(8)-C(9)-H(9C)	109.5
H(9A)-C(9)-H(9C)	109.5
H(9B)-C(9)-H(9C)	109.5
C(8)-C(10)-H(10A)	109.5
C(8)-C(10)-H(10B)	109.5
H(10A)-C(10)-H(10B)	109.5
C(8)-C(10)-H(10C)	109.5
H(10A)-C(10)-H(10C)	109.5
H(10B)-C(10)-H(10C)	109.5
C(16)-C(11)-C(12)	119.04(18)
C(16)-C(11)-N(1)	122.79(18)
C(12)-C(11)-N(1)	118.11(17)
C(13)-C(12)-C(11)	121.62(19)
C(13)-C(12)-H(12)	119.2
C(11)-C(12)-H(12)	119.2
C(12)-C(13)-C(14)	119.53(19)
C(12)-C(13)-H(13)	120.2
C(14)-C(13)-H(13)	120.2
C(15)-C(14)-C(13)	119.20(19)
C(15)-C(14)-H(14)	120.4
C(13)-C(14)-H(14)	120.4
C(14)-C(15)-C(16)	122.60(19)
C(14)-C(15)-H(15)	118.7
C(16)-C(15)-H(15)	118.7
C(11)-C(16)-C(15)	117.99(19)
C(11)-C(16)-C(17)	126.44(18)
C(15)-C(16)-C(17)	115.56(18)
N(2)-C(17)-C(16)	116.72(16)

N(2)-C(17)-H(17A)	108.1
C(16)-C(17)-H(17A)	108.1
N(2)-C(17)-H(17B)	108.1
C(16)-C(17)-H(17B)	108.1
H(17A)-C(17)-H(17B)	107.3
C(19)-C(18)-C(23)	119.71(19)
C(19)-C(18)-S(1)	119.94(16)
C(23)-C(18)-S(1)	120.34(16)
C(18)-C(19)-C(20)	119.9(2)
C(18)-C(19)-H(19)	120.0
C(20)-C(19)-H(19)	120.0
C(19)-C(20)-C(21)	121.4(2)
C(19)-C(20)-H(20)	119.3
C(21)-C(20)-H(20)	119.3
C(20)-C(21)-C(22)	117.93(19)
C(20)-C(21)-C(24)	121.3(2)
C(22)-C(21)-C(24)	120.78(19)
C(23)-C(22)-C(21)	121.22(19)
C(23)-C(22)-H(22)	119.4
C(21)-C(22)-H(22)	119.4
C(22)-C(23)-C(18)	119.8(2)
C(22)-C(23)-H(23)	120.1
C(18)-C(23)-H(23)	120.1
C(21)-C(24)-H(24A)	109.5
C(21)-C(24)-H(24B)	109.5
H(24A)-C(24)-H(24B)	109.5
C(21)-C(24)-H(24C)	109.5
H(24A)-C(24)-H(24C)	109.5
H(24B)-C(24)-H(24C)	109.5
C(26)-C(25)-H(25A)	109.5
C(26)-C(25)-H(25B)	109.5
H(25A)-C(25)-H(25B)	109.5
C(26)-C(25)-H(25C)	109.5
H(25A)-C(25)-H(25C)	109.5
H(25B)-C(25)-H(25C)	109.5
C(31)-C(26)-C(27)	118.24(19)

C(31)-C(26)-C(25)	121.2(2)
C(27)-C(26)-C(25)	120.6(2)
C(31)-C(26)-Ru(2)	71.03(12)
C(27)-C(26)-Ru(2)	68.74(11)
C(25)-C(26)-Ru(2)	131.46(15)
C(28)-C(27)-C(26)	120.68(19)
C(28)-C(27)-Ru(2)	71.29(11)
C(26)-C(27)-Ru(2)	73.43(11)
C(28)-C(27)-H(27)	119.7
C(26)-C(27)-H(27)	119.7
Ru(2)-C(27)-H(27)	127.7
C(27)-C(28)-C(29)	121.47(19)
C(27)-C(28)-Ru(2)	71.05(11)
C(29)-C(28)-Ru(2)	72.91(11)
C(27)-C(28)-H(28)	119.3
C(29)-C(28)-H(28)	119.3
Ru(2)-C(28)-H(28)	129.3
C(30)-C(29)-C(28)	117.17(18)
C(30)-C(29)-C(32)	123.38(18)
C(28)-C(29)-C(32)	119.44(18)
C(30)-C(29)-Ru(2)	70.41(11)
C(28)-C(29)-Ru(2)	69.12(11)
C(32)-C(29)-Ru(2)	132.01(14)
C(29)-C(30)-C(31)	121.40(19)
C(29)-C(30)-Ru(2)	72.47(11)
C(31)-C(30)-Ru(2)	71.84(12)
C(29)-C(30)-H(30)	119.3
C(31)-C(30)-H(30)	119.3
Ru(2)-C(30)-H(30)	128.8
C(26)-C(31)-C(30)	120.97(19)
C(26)-C(31)-Ru(2)	72.36(12)
C(30)-C(31)-Ru(2)	70.45(11)
C(26)-C(31)-H(31)	119.5
C(30)-C(31)-H(31)	119.5
Ru(2)-C(31)-H(31)	130.3
C(29)-C(32)-C(34)	114.34(17)

C(29)-C(32)-C(33)	109.18(17)
C(34)-C(32)-C(33)	110.14(17)
C(29)-C(32)-H(32)	107.6
C(34)-C(32)-H(32)	107.6
C(33)-C(32)-H(32)	107.6
C(32)-C(33)-H(33A)	109.5
C(32)-C(33)-H(33B)	109.5
H(33A)-C(33)-H(33B)	109.5
C(32)-C(33)-H(33C)	109.5
H(33A)-C(33)-H(33C)	109.5
H(33B)-C(33)-H(33C)	109.5
C(32)-C(34)-H(34A)	109.5
C(32)-C(34)-H(34B)	109.5
H(34A)-C(34)-H(34B)	109.5
C(32)-C(34)-H(34C)	109.5
H(34A)-C(34)-H(34C)	109.5
H(34B)-C(34)-H(34C)	109.5
C(36)-C(35)-C(40)	119.35(17)
C(36)-C(35)-N(3)	118.73(17)
C(40)-C(35)-N(3)	121.85(17)
C(37)-C(36)-C(35)	121.07(19)
C(37)-C(36)-H(36)	119.5
C(35)-C(36)-H(36)	119.5
C(36)-C(37)-C(38)	119.69(19)
C(36)-C(37)-H(37)	120.2
C(38)-C(37)-H(37)	120.2
C(39)-C(38)-C(37)	119.63(18)
C(39)-C(38)-H(38)	120.2
C(37)-C(38)-H(38)	120.2
C(38)-C(39)-C(40)	121.38(18)
C(38)-C(39)-H(39)	119.3
C(40)-C(39)-H(39)	119.3
C(39)-C(40)-C(35)	118.87(18)
C(39)-C(40)-C(41)	119.05(17)
C(35)-C(40)-C(41)	121.99(17)
N(4)-C(41)-C(40)	113.99(16)

N(4)-C(41)-H(41A)	108.8
C(40)-C(41)-H(41A)	108.8
N(4)-C(41)-H(41B)	108.8
C(40)-C(41)-H(41B)	108.8
H(41A)-C(41)-H(41B)	107.7
C(43)-C(42)-C(47)	120.5(2)
C(43)-C(42)-S(2)	121.54(16)
C(47)-C(42)-S(2)	117.58(16)
C(42)-C(43)-C(44)	119.6(2)
C(42)-C(43)-H(43)	120.2
C(44)-C(43)-H(43)	120.2
C(45)-C(44)-C(43)	121.0(2)
C(45)-C(44)-H(44)	119.5
C(43)-C(44)-H(44)	119.5
C(44)-C(45)-C(46)	118.3(2)
C(44)-C(45)-C(48)	121.2(2)
C(46)-C(45)-C(48)	120.5(2)
C(45)-C(46)-C(47)	121.4(2)
C(45)-C(46)-H(46)	119.3
C(47)-C(46)-H(46)	119.3
C(42)-C(47)-C(46)	119.1(2)
C(42)-C(47)-H(47)	120.4
C(46)-C(47)-H(47)	120.4
C(45)-C(48)-H(48A)	109.5
C(45)-C(48)-H(48B)	109.5
H(48A)-C(48)-H(48B)	109.5
C(45)-C(48)-H(48C)	109.5
H(48A)-C(48)-H(48C)	109.5
H(48B)-C(48)-H(48C)	109.5
C(11)-N(1)-Ru(1)	115.13(12)
C(11)-N(1)-Ru(2)	123.63(12)
Ru(1)-N(1)-Ru(2)	104.29(7)
C(11)-N(1)-H(1)	103.9
Ru(1)-N(1)-H(1)	103.9
Ru(2)-N(1)-H(1)	103.9
C(17)-N(2)-S(1)	113.04(13)

C(17)-N(2)-Ru(1)	120.36(12)
S(1)-N(2)-Ru(1)	124.76(9)
C(35)-N(3)-Ru(2)	115.50(12)
C(35)-N(3)-Ru(1)	124.13(12)
Ru(2)-N(3)-Ru(1)	104.38(7)
C(35)-N(3)-H(3A)	103.4
Ru(2)-N(3)-H(3A)	103.4
Ru(1)-N(3)-H(3A)	103.4
C(41)-N(4)-S(2)	110.35(12)
C(41)-N(4)-Ru(2)	122.92(12)
S(2)-N(4)-Ru(2)	120.75(9)
O(1)-S(1)-O(2)	117.02(10)
O(1)-S(1)-N(2)	108.06(9)
O(2)-S(1)-N(2)	110.94(10)
O(1)-S(1)-C(18)	105.76(10)
O(2)-S(1)-C(18)	104.25(9)
N(2)-S(1)-C(18)	110.58(9)
O(3)-S(2)-O(4)	116.09(10)
O(3)-S(2)-N(4)	110.26(9)
O(4)-S(2)-N(4)	112.19(9)
O(3)-S(2)-C(42)	103.90(10)
O(4)-S(2)-C(42)	105.76(9)
N(4)-S(2)-C(42)	107.88(9)
N(1)-Ru(1)-N(3)	75.59(6)
N(1)-Ru(1)-N(2)	81.14(6)
N(3)-Ru(1)-N(2)	82.57(6)
N(1)-Ru(1)-C(7)	124.18(7)
N(3)-Ru(1)-C(7)	94.25(7)
N(2)-Ru(1)-C(7)	153.01(7)
N(1)-Ru(1)-C(6)	97.07(7)
N(3)-Ru(1)-C(6)	114.75(7)
N(2)-Ru(1)-C(6)	161.74(7)
C(7)-Ru(1)-C(6)	37.76(7)
N(1)-Ru(1)-C(3)	154.13(7)
N(3)-Ru(1)-C(3)	129.25(7)
N(2)-Ru(1)-C(3)	93.99(7)

C(7)-Ru(1)-C(3)	67.31(8)
C(6)-Ru(1)-C(3)	79.66(8)
N(1)-Ru(1)-C(4)	117.53(7)
N(3)-Ru(1)-C(4)	166.79(7)
N(2)-Ru(1)-C(4)	97.43(7)
C(7)-Ru(1)-C(4)	79.72(8)
C(6)-Ru(1)-C(4)	67.12(8)
C(3)-Ru(1)-C(4)	37.54(8)
N(1)-Ru(1)-C(2)	162.02(7)
N(3)-Ru(1)-C(2)	100.53(7)
N(2)-Ru(1)-C(2)	116.09(7)
C(7)-Ru(1)-C(2)	37.96(8)
C(6)-Ru(1)-C(2)	68.26(8)
C(3)-Ru(1)-C(2)	36.98(8)
C(4)-Ru(1)-C(2)	67.51(8)
N(1)-Ru(1)-C(5)	94.53(7)
N(3)-Ru(1)-C(5)	150.47(7)
N(2)-Ru(1)-C(5)	123.98(7)
C(7)-Ru(1)-C(5)	68.04(8)
C(6)-Ru(1)-C(5)	37.81(8)
C(3)-Ru(1)-C(5)	67.07(8)
C(4)-Ru(1)-C(5)	36.61(8)
C(2)-Ru(1)-C(5)	80.24(8)
N(3)-Ru(2)-N(4)	86.27(6)
N(3)-Ru(2)-N(1)	75.11(6)
N(4)-Ru(2)-N(1)	82.74(6)
N(3)-Ru(2)-C(27)	115.39(7)
N(4)-Ru(2)-C(27)	157.91(7)
N(1)-Ru(2)-C(27)	98.09(7)
N(3)-Ru(2)-C(28)	91.96(7)
N(4)-Ru(2)-C(28)	153.87(7)
N(1)-Ru(2)-C(28)	121.98(7)
C(27)-Ru(2)-C(28)	37.67(7)
N(3)-Ru(2)-C(30)	123.21(7)
N(4)-Ru(2)-C(30)	91.96(7)
N(1)-Ru(2)-C(30)	160.72(7)

C(27)-Ru(2)-C(30)	79.98(8)
C(28)-Ru(2)-C(30)	67.33(7)
N(3)-Ru(2)-C(31)	160.92(7)
N(4)-Ru(2)-C(31)	93.97(7)
N(1)-Ru(2)-C(31)	123.88(7)
C(27)-Ru(2)-C(31)	67.12(8)
C(28)-Ru(2)-C(31)	79.46(8)
C(30)-Ru(2)-C(31)	37.71(7)
N(3)-Ru(2)-C(29)	95.11(7)
N(4)-Ru(2)-C(29)	116.18(7)
N(1)-Ru(2)-C(29)	158.52(7)
C(27)-Ru(2)-C(29)	68.46(7)
C(28)-Ru(2)-C(29)	37.97(7)
C(30)-Ru(2)-C(29)	37.13(7)
C(31)-Ru(2)-C(29)	67.66(7)
N(3)-Ru(2)-C(26)	152.54(7)
N(4)-Ru(2)-C(26)	120.13(7)
N(1)-Ru(2)-C(26)	99.29(7)
C(27)-Ru(2)-C(26)	37.82(8)
C(28)-Ru(2)-C(26)	67.85(8)
C(30)-Ru(2)-C(26)	67.37(8)
C(31)-Ru(2)-C(26)	36.61(8)
C(29)-Ru(2)-C(26)	80.48(7)

Table B-4. Anisotropic displacement parameters ($Å^2$ x 10^3) for **11**. The anisotropic displacement factor exponent takes the form: $-2\pi^2[h^2a^{*2}U^{11} + ... + 2 h k a^* b^* U^{12}]$.

	U^{11}	U^{22}	U^{33}	U^{23}	U^{13}	U^{12}
C(1)	16(1)	26(1)	20(1)	-2(1)	1(1)	-2(1)
C(2)	16(1)	19(1)	14(1)	-3(1)	2(1)	1(1)
C(3)	20(1)	15(1)	17(1)	-2(1)	3(1)	-1(1)
C(4)	20(1)	17(1)	16(1)	-2(1)	2(1)	6(1)
C(5)	15(1)	21(1)	14(1)	-4(1)	3(1)	4(1)
C(6)	15(1)	22(1)	11(1)	0(1)	3(1)	1(1)
C(7)	14(1)	19(1)	11(1)	-1(1)	2(1)	2(1)
C(8)	14(1)	31(1)	17(1)	-2(1)	3(1)	5(1)
C(9)	18(1)	50(2)	21(1)	-3(1)	8(1)	11(1)
C(10)	18(1)	37(1)	22(1)	-4(1)	1(1)	11(1)
C(11)	11(1)	15(1)	10(1)	-1(1)	1(1)	2(1)
C(12)	13(1)	19(1)	13(1)	0(1)	4(1)	0(1)
C(13)	10(1)	23(1)	17(1)	-3(1)	2(1)	2(1)
C(14)	13(1)	20(1)	15(1)	-2(1)	-4(1)	6(1)
C(15)	21(1)	15(1)	12(1)	1(1)	0(1)	5(1)
C(16)	13(1)	16(1)	12(1)	-1(1)	2(1)	2(1)
C(17)	16(1)	17(1)	15(1)	5(1)	2(1)	1(1)
C(18)	13(1)	16(1)	19(1)	4(1)	7(1)	0(1)
C(19)	16(1)	24(1)	17(1)	8(1)	2(1)	-1(1)
C(20)	19(1)	22(1)	18(1)	2(1)	2(1)	-5(1)
C(21)	15(1)	16(1)	20(1)	3(1)	8(1)	1(1)
C(22)	18(1)	19(1)	15(1)	6(1)	2(1)	2(1)
C(23)	17(1)	18(1)	15(1)	2(1)	4(1)	0(1)
C(24)	26(1)	17(1)	26(1)	1(1)	8(1)	-2(1)
C(25)	14(1)	42(1)	18(1)	-7(1)	-3(1)	3(1)
C(26)	14(1)	29(1)	10(1)	-4(1)	1(1)	2(1)
C(27)	18(1)	21(1)	8(1)	3(1)	2(1)	7(1)
C(28)	14(1)	17(1)	10(1)	1(1)	5(1)	1(1)
C(29)	13(1)	14(1)	11(1)	-1(1)	3(1)	2(1)
C(30)	16(1)	13(1)	14(1)	-1(1)	4(1)	0(1)
C(31)	15(1)	22(1)	16(1)	-4(1)	4(1)	-5(1)

C(32)	11(1)	18(1)	15(1)	-2(1)	2(1)	1(1)
C(33)	15(1)	32(1)	18(1)	1(1)	7(1)	4(1)
C(34)	17(1)	20(1)	17(1)	0(1)	1(1)	7(1)
C(35)	10(1)	14(1)	9(1)	0(1)	1(1)	2(1)
C(36)	12(1)	14(1)	13(1)	0(1)	3(1)	0(1)
C(37)	11(1)	18(1)	15(1)	-2(1)	1(1)	0(1)
C(38)	12(1)	18(1)	13(1)	0(1)	-2(1)	5(1)
C(39)	18(1)	13(1)	9(1)	1(1)	3(1)	2(1)
C(40)	12(1)	13(1)	9(1)	-1(1)	3(1)	1(1)
C(41)	11(1)	18(1)	10(1)	3(1)	2(1)	0(1)
C(42)	15(1)	14(1)	13(1)	1(1)	2(1)	-2(1)
C(43)	15(1)	23(1)	22(1)	6(1)	5(1)	1(1)
C(44)	22(1)	20(1)	25(1)	4(1)	5(1)	8(1)
C(45)	27(1)	16(1)	18(1)	-1(1)	-1(1)	-5(1)
C(46)	24(1)	19(1)	35(1)	0(1)	12(1)	-6(1)
C(47)	21(1)	19(1)	27(1)	1(1)	12(1)	-1(1)
C(48)	40(2)	17(1)	35(1)	2(1)	2(1)	-3(1)
N(1)	10(1)	14(1)	12(1)	3(1)	3(1)	2(1)
N(2)	10(1)	16(1)	13(1)	5(1)	3(1)	1(1)
N(3)	9(1)	13(1)	10(1)	2(1)	2(1)	2(1)
N(4)	9(1)	20(1)	10(1)	5(1)	1(1)	-2(1)
O(1)	13(1)	21(1)	30(1)	13(1)	7(1)	4(1)
O(2)	30(1)	16(1)	23(1)	3(1)	16(1)	2(1)
O(3)	12(1)	34(1)	20(1)	11(1)	-2(1)	-5(1)
O(4)	14(1)	17(1)	31(1)	-1(1)	10(1)	1(1)
S(1)	14(1)	14(1)	19(1)	6(1)	8(1)	3(1)
S(2)	9(1)	16(1)	16(1)	5(1)	3(1)	0(1)
Ru(1)	9(1)	13(1)	10(1)	2(1)	2(1)	2(1)
Ru(2)	8(1)	13(1)	8(1)	2(1)	1(1)	1(1)

Notes for Appendix B:

1) Bruker, **2007**, APEX2 (Version 2.1-4), SAINT (version 7.34A), SADABS (version 2007/4), BrukerAXS Inc; Madison, Wisconsin, USA.

2) a) Altomare, A.; Burla, C.; Camalli, M.; Cascarano, G. L.; Giacovazzo, C.; Guagliardi, A.; Moliterni, A. G. G.; Polidori, G.; Spagna, R., SIR97: a new tool for crystal structure determination and refinement, *J. Appl. Cryst.*, **1999**, *32*, 115-119. b) Altomare, A.; Cascarano, G. L.; Giacovazzo, C.; Guagliardi, A., SIR 92: completion and refinement of crystal structures, *J. Appl. Cryst*., **1993**, *26*, 343-350.

3) Sheldrick, G. M., **1997**, SHELXL-97, Program for the Refinement of Crystal Structures. University of Göttingen, Germany.

4) Mackay, S.; Edwards, C.; Henderson, A.; Gilmore, C.; Stewart, N.; Shankland, K.; Donald, A., **1997**, MaXus: a computer program for the solution and refinement of crystal structures from diffraction data. University of Glasgow, Scotland.

5) Waasmaier, D. and Kirfel, A., New Analytical Scattering Factor Functions for Free Atoms and Ions. *Acta Cryst. A*, **1995**, *51*, 416-430.

6) a) Spek, A., *J. Appl. Cryst.,* **2003**, *36*, 7-13. b) van der Sluis, P. and Spek, A. L. *Acta Cryst.*, **1990**, *A46*, 194-201.

Appendix C: Crystal Structure Data for Chapter 3

*Crystal structure data for **14**, [(^{tBu}POCOP)Rh(CO)H][B(C_6F_5)$_4$]*:

A clear yellow piece, measuring 0.15 x 0.11 x 0.080 mm^3 was mounted on a loop with oil. Data was collected at -173^{o}C on a Bruker APEX II single crystal X-ray diffractometer, Mo-radiation.

Crystal-to-detector distance was 40.00 mm and exposure time was 120 seconds per frame for all sets. The scan width was 1.0^o. Data collection was 100.0 % complete to 25^o in ϑ. A total of 56,547 reflections were collected covering the indices, h = -13 to 13, k = -20 to 20, l = -34 to 34. 10,430 reflections were symmetry independent and the R_{int} = 0.1243 indicated that the data was below average quality (0.07). Indexing and unit cell refinement indicated a Monoclinic lattice. The space group was found to be P 21/c (No.14).

The data was integrated and scaled using SAINT, SADABS within the APEX2 software package by Bruker.[1]

Solution by direct methods (SHELXS, SIR97[2]) produced a complete heavy atom phasing model consistent with the proposed structure. The structure was completed by difference Fourier synthesis with SHELXL97.[3,4] Scattering factors are from Waasmair and Kirfel[5]. Hydrogen atoms were placed in geometrically idealised positions and constrained to ride on their parent atoms with C-H distances in the range 0.95-1.00 Angstrom. Isotropic thermal parameters U_{eq} were fixed such that they were 1.2U_{eq} of their parent atom Ueq for CH's and 1.5U_{eq} of their parent atom U_{eq} in case of methyl groups. All non-hydrogen atoms were refined anisotropically by full-matrix least-squares.

During refinement of the structure, two large infinite voids around (0.0, 0.0, 0.0) and (0.0, 0.5, 0.5) were discovered and appeared to be filled with disordered pentane. Therefore the application of squeeze[6] was used to resolve the contribution of solvent in these voids. A total of 358 electrons were found, 179 in each void.

Table C-1. Crystal data and structure refinement for **14**.

Empirical formula	$C_{47}\ H_{40}\ B\ F_{20}\ O_3\ P_2\ Rh$	
Formula weight	1208.45	
Temperature	100(2) K	
Wavelength	0.71073 Å	
Crystal system	Monoclinic	
Space group	P 1 21/c 1	
Unit cell dimensions	a = 11.2020(12) Å	a= 90°.
	b = 16.4233(19) Å	b= 95.383(6)°.
	c = 27.815(2) Å	g = 90°.
Volume	5094.7(9) $Å^3$	
Z	4	
Density (calculated)	1.576 Mg/m^3	
Absorption coefficient	0.511 mm^{-1}	
F(000)	2424	
Crystal size	0.45 x 0.15 x 0.11 mm^3	
Theta range for data collection	1.44 to 26.44°.	
Index ranges	-13<=h<=13, -20<=k<=20, -34<=l<=34	
Reflections collected	56547	
Independent reflections	10430 [R(int) = 0.1243]	
Completeness to theta = 25.00°	100.0 %	
Absorption correction	Semi-empirical from equivalents	
Max. and min. transmission	0.9459 and 0.8026	
Refinement method	Full-matrix least-squares on F^2	
Data / restraints / parameters	10430 / 0 / 683	
Goodness-of-fit on F^2	0.976	
Final R indices [I>2sigma(I)]	R1 = 0.0575, wR2 = 0.1031	
R indices (all data)	R1 = 0.1069, wR2 = 0.1211	
Largest diff. peak and hole	0.930 and -0.541 $e.Å^{-3}$	

Table C-2. Atomic coordinates (x 10^4) and equivalent isotropic displacement parameters ($Å^2$x 10^3) for **14**. U(eq) is defined as one third of the trace of the orthogonalized U^{ij} tensor.

	x	y	z	U(eq)
C(1)	7133(4)	7559(3)	6638(2)	16(1)
C(2)	7180(4)	6709(3)	6657(1)	17(1)
C(3)	8274(4)	6315(3)	6698(2)	26(1)
C(4)	9306(5)	6781(3)	6697(2)	31(1)
C(5)	9283(4)	7630(3)	6641(2)	24(1)
C(6)	8187(4)	8013(3)	6607(1)	18(1)
C(7)	7545(4)	9388(3)	5610(1)	21(1)
C(8)	8557(6)	10015(4)	5678(2)	60(2)
C(9)	8040(5)	8578(3)	5441(2)	36(2)
C(10)	6563(5)	9686(4)	5230(2)	39(2)
C(11)	6401(5)	10020(3)	6523(2)	23(1)
C(12)	7395(5)	10639(4)	6660(2)	49(2)
C(13)	5320(5)	10427(3)	6237(2)	42(2)
C(14)	5967(5)	9652(3)	6987(2)	33(1)
C(15)	4841(4)	5992(3)	5775(2)	23(1)
C(16)	3674(5)	6154(4)	5462(2)	44(2)
C(17)	4927(6)	5094(3)	5914(2)	40(2)
C(18)	5905(5)	6205(3)	5482(2)	36(2)
C(19)	3777(4)	6597(3)	6709(1)	19(1)
C(20)	4231(4)	7089(3)	7166(1)	27(1)
C(21)	2636(4)	7006(3)	6484(2)	24(1)
C(22)	3515(5)	5718(3)	6840(2)	31(1)
C(23)	4392(5)	8374(3)	5735(2)	24(1)
C(24)	6571(4)	7398(3)	3675(1)	15(1)
C(25)	5921(4)	6937(3)	3321(2)	19(1)
C(26)	4720(5)	6765(3)	3325(2)	26(1)
C(27)	4082(4)	7058(3)	3684(2)	31(1)
C(28)	4678(5)	7515(3)	4044(2)	27(1)
C(29)	5880(5)	7682(3)	4026(2)	21(1)
C(30)	8777(4)	7124(3)	3329(1)	17(1)

C(31)	9614(4)	7419(3)	3027(2)	19(1)
C(32)	10364(4)	6924(3)	2793(2)	23(1)
C(33)	10281(5)	6097(3)	2831(2)	31(1)
C(34)	9463(5)	5771(3)	3121(2)	28(1)
C(35)	8764(4)	6291(3)	3362(2)	22(1)
C(36)	7911(4)	8645(3)	3547(2)	14(1)
C(37)	8183(4)	9313(3)	3837(2)	20(1)
C(38)	8013(5)	10112(3)	3688(2)	26(1)
C(39)	7513(5)	10281(3)	3232(2)	24(1)
C(40)	7202(4)	9651(3)	2925(2)	22(1)
C(41)	7409(4)	8862(3)	3088(2)	17(1)
C(42)	8774(4)	7491(3)	4220(2)	20(1)
C(43)	9944(4)	7800(3)	4298(2)	24(1)
C(44)	10690(5)	7710(4)	4713(2)	33(1)
C(45)	10267(5)	7304(3)	5091(2)	33(1)
C(46)	9143(5)	6981(3)	5038(2)	30(1)
C(47)	8423(4)	7063(3)	4609(2)	23(1)
O(1)	8098(3)	8844(2)	6531(1)	21(1)
O(2)	6127(3)	6277(2)	6629(1)	19(1)
O(3)	3631(3)	8612(2)	5472(1)	38(1)
B(1)	7992(5)	7671(3)	3689(2)	16(1)
F(1)	6450(2)	6630(2)	2942(1)	27(1)
F(2)	4147(3)	6312(2)	2967(1)	42(1)
F(3)	2905(3)	6891(2)	3691(1)	51(1)
F(4)	4076(3)	7818(2)	4404(1)	42(1)
F(5)	6381(2)	8179(2)	4380(1)	26(1)
F(6)	9743(2)	8224(2)	2957(1)	26(1)
F(7)	11184(3)	7252(2)	2522(1)	36(1)
F(8)	10987(3)	5594(2)	2600(1)	52(1)
F(9)	9392(3)	4953(2)	3173(1)	44(1)
F(10)	8027(2)	5923(2)	3661(1)	26(1)
F(11)	8641(3)	9223(2)	4306(1)	29(1)
F(12)	8330(3)	10736(2)	3995(1)	39(1)
F(13)	7319(3)	11059(2)	3092(1)	40(1)
F(14)	6698(3)	9793(2)	2476(1)	30(1)
F(15)	7092(2)	8262(2)	2763(1)	22(1)

F(20)	7348(3)	6678(2)	4586(1)	32(1)
F(19)	8713(3)	6589(2)	5417(1)	42(1)
F(18)	10953(3)	7236(2)	5517(1)	51(1)
F(17)	11799(3)	8022(2)	4758(1)	48(1)
F(16)	10403(2)	8223(2)	3941(1)	29(1)
P(2)	6885(1)	9137(1)	6178(1)	17(1)
P(4)	4974(1)	6700(1)	6296(1)	17(1)
Rh(1)	5661(1)	8000(1)	6157(1)	16(1)

Table C-3. Bond lengths [Å] and angles [°] for **14**.

C(1)-C(2)	1.397(6)
C(1)-C(6)	1.406(6)
C(1)-Rh(1)	2.148(4)
C(1)-H(1R)	1.08(5)
C(2)-O(2)	1.373(5)
C(2)-C(3)	1.381(6)
C(3)-C(4)	1.387(7)
C(3)-H(3)	0.9500
C(4)-C(5)	1.403(7)
C(4)-H(4)	0.9500
C(5)-C(6)	1.375(6)
C(5)-H(5)	0.9500
C(6)-O(1)	1.383(5)
C(7)-C(8)	1.529(7)
C(7)-C(10)	1.532(6)
C(7)-C(9)	1.533(7)
C(7)-P(2)	1.852(4)
C(8)-H(8A)	0.9800
C(8)-H(8B)	0.9800
C(8)-H(8C)	0.9800
C(9)-H(9A)	0.9800
C(9)-H(9B)	0.9800
C(9)-H(9C)	0.9800
C(10)-H(10A)	0.9800
C(10)-H(10B)	0.9800
C(10)-H(10C)	0.9800
C(11)-C(12)	1.530(7)
C(11)-C(13)	1.538(7)
C(11)-C(14)	1.544(6)
C(11)-P(2)	1.850(5)
C(12)-H(12A)	0.9800
C(12)-H(12B)	0.9800
C(12)-H(12C)	0.9800
C(13)-H(13A)	0.9800

C(13)-H(13B)	0.9800
C(13)-H(13C)	0.9800
C(14)-H(14A)	0.9800
C(14)-H(14B)	0.9800
C(14)-H(14C)	0.9800
C(15)-C(16)	1.525(7)
C(15)-C(17)	1.526(7)
C(15)-C(18)	1.545(6)
C(15)-P(4)	1.852(5)
C(16)-H(16A)	0.9800
C(16)-H(16B)	0.9800
C(16)-H(16C)	0.9800
C(17)-H(17A)	0.9800
C(17)-H(17B)	0.9800
C(17)-H(17C)	0.9800
C(18)-H(18A)	0.9800
C(18)-H(18B)	0.9800
C(18)-H(18C)	0.9800
C(19)-C(22)	1.524(6)
C(19)-C(21)	1.526(6)
C(19)-C(20)	1.550(6)
C(19)-P(4)	1.855(5)
C(20)-H(20A)	0.9800
C(20)-H(20B)	0.9800
C(20)-H(20C)	0.9800
C(21)-H(21A)	0.9800
C(21)-H(21B)	0.9800
C(21)-H(21C)	0.9800
C(22)-H(22A)	0.9800
C(22)-H(22B)	0.9800
C(22)-H(22C)	0.9800
C(23)-O(3)	1.139(6)
C(23)-Rh(1)	1.862(5)
C(24)-C(29)	1.383(6)
C(24)-C(25)	1.392(6)
C(24)-B(1)	1.650(7)

C(25)-F(1)	1.356(5)
C(25)-C(26)	1.376(6)
C(26)-F(2)	1.355(5)
C(26)-C(27)	1.371(7)
C(27)-F(3)	1.348(5)
C(27)-C(28)	1.372(7)
C(28)-F(4)	1.355(5)
C(28)-C(29)	1.380(7)
C(29)-F(5)	1.358(5)
C(30)-C(35)	1.371(6)
C(30)-C(31)	1.404(6)
C(30)-B(1)	1.658(7)
C(31)-F(6)	1.346(5)
C(31)-C(32)	1.375(6)
C(32)-F(7)	1.354(5)
C(32)-C(33)	1.367(7)
C(33)-F(8)	1.347(5)
C(33)-C(34)	1.384(7)
C(34)-F(9)	1.354(5)
C(34)-C(35)	1.376(6)
C(35)-F(10)	1.367(5)
C(36)-C(37)	1.379(6)
C(36)-C(41)	1.392(6)
C(36)-B(1)	1.648(7)
C(37)-F(11)	1.362(5)
C(37)-C(38)	1.384(6)
C(38)-F(12)	1.359(5)
C(38)-C(39)	1.367(6)
C(39)-F(13)	1.348(5)
C(39)-C(40)	1.365(6)
C(40)-F(14)	1.341(5)
C(40)-C(41)	1.384(6)
C(41)-F(15)	1.362(5)
C(42)-C(47)	1.377(6)
C(42)-C(43)	1.403(6)
C(42)-B(1)	1.671(7)

C(43)-F(16)	1.351(5)
C(43)-C(44)	1.370(6)
C(44)-F(17)	1.338(6)
C(44)-C(45)	1.367(7)
C(45)-F(18)	1.356(5)
C(45)-C(46)	1.361(7)
C(46)-F(19)	1.363(5)
C(46)-C(47)	1.383(6)
C(47)-F(20)	1.356(5)
O(1)-P(2)	1.672(3)
O(2)-P(4)	1.669(3)
P(2)-Rh(1)	2.3143(13)
P(4)-Rh(1)	2.3129(13)
Rh(1)-H(1R)	1.84(4)

C(2)-C(1)-C(6)	120.2(5)
C(2)-C(1)-Rh(1)	112.6(3)
C(6)-C(1)-Rh(1)	112.6(3)
C(2)-C(1)-H(1R)	122(3)
C(6)-C(1)-H(1R)	115(3)
Rh(1)-C(1)-H(1R)	59(2)
O(2)-C(2)-C(3)	120.8(4)
O(2)-C(2)-C(1)	119.0(4)
C(3)-C(2)-C(1)	120.1(5)
C(2)-C(3)-C(4)	118.3(5)
C(2)-C(3)-H(3)	120.9
C(4)-C(3)-H(3)	120.9
C(3)-C(4)-C(5)	122.9(5)
C(3)-C(4)-H(4)	118.6
C(5)-C(4)-H(4)	118.6
C(6)-C(5)-C(4)	117.9(5)
C(6)-C(5)-H(5)	121.0
C(4)-C(5)-H(5)	121.0
C(5)-C(6)-O(1)	120.8(4)
C(5)-C(6)-C(1)	120.2(5)
O(1)-C(6)-C(1)	118.9(4)

C(8)-C(7)-C(10)	110.2(5)
C(8)-C(7)-C(9)	109.7(5)
C(10)-C(7)-C(9)	108.7(4)
C(8)-C(7)-P(2)	113.3(3)
C(10)-C(7)-P(2)	110.0(3)
C(9)-C(7)-P(2)	104.7(3)
C(7)-C(8)-H(8A)	109.5
C(7)-C(8)-H(8B)	109.5
H(8A)-C(8)-H(8B)	109.5
C(7)-C(8)-H(8C)	109.5
H(8A)-C(8)-H(8C)	109.5
H(8B)-C(8)-H(8C)	109.5
C(7)-C(9)-H(9A)	109.5
C(7)-C(9)-H(9B)	109.5
H(9A)-C(9)-H(9B)	109.5
C(7)-C(9)-H(9C)	109.5
H(9A)-C(9)-H(9C)	109.5
H(9B)-C(9)-H(9C)	109.5
C(7)-C(10)-H(10A)	109.5
C(7)-C(10)-H(10B)	109.5
H(10A)-C(10)-H(10B)	109.5
C(7)-C(10)-H(10C)	109.5
H(10A)-C(10)-H(10C)	109.5
H(10B)-C(10)-H(10C)	109.5
C(12)-C(11)-C(13)	111.0(5)
C(12)-C(11)-C(14)	109.4(4)
C(13)-C(11)-C(14)	108.0(4)
C(12)-C(11)-P(2)	114.1(4)
C(13)-C(11)-P(2)	109.1(3)
C(14)-C(11)-P(2)	104.9(3)
C(11)-C(12)-H(12A)	109.5
C(11)-C(12)-H(12B)	109.5
H(12A)-C(12)-H(12B)	109.5
C(11)-C(12)-H(12C)	109.5
H(12A)-C(12)-H(12C)	109.5
H(12B)-C(12)-H(12C)	109.5

C(11)-C(13)-H(13A)	109.5
C(11)-C(13)-H(13B)	109.5
H(13A)-C(13)-H(13B)	109.5
C(11)-C(13)-H(13C)	109.5
H(13A)-C(13)-H(13C)	109.5
H(13B)-C(13)-H(13C)	109.5
C(11)-C(14)-H(14A)	109.5
C(11)-C(14)-H(14B)	109.5
H(14A)-C(14)-H(14B)	109.5
C(11)-C(14)-H(14C)	109.5
H(14A)-C(14)-H(14C)	109.5
H(14B)-C(14)-H(14C)	109.5
C(16)-C(15)-C(17)	110.1(4)
C(16)-C(15)-C(18)	108.8(4)
C(17)-C(15)-C(18)	108.6(4)
C(16)-C(15)-P(4)	109.8(3)
C(17)-C(15)-P(4)	114.2(3)
C(18)-C(15)-P(4)	105.1(3)
C(15)-C(16)-H(16A)	109.5
C(15)-C(16)-H(16B)	109.5
H(16A)-C(16)-H(16B)	109.5
C(15)-C(16)-H(16C)	109.5
H(16A)-C(16)-H(16C)	109.5
H(16B)-C(16)-H(16C)	109.5
C(15)-C(17)-H(17A)	109.5
C(15)-C(17)-H(17B)	109.5
H(17A)-C(17)-H(17B)	109.5
C(15)-C(17)-H(17C)	109.5
H(17A)-C(17)-H(17C)	109.5
H(17B)-C(17)-H(17C)	109.5
C(15)-C(18)-H(18A)	109.5
C(15)-C(18)-H(18B)	109.5
H(18A)-C(18)-H(18B)	109.5
C(15)-C(18)-H(18C)	109.5
H(18A)-C(18)-H(18C)	109.5
H(18B)-C(18)-H(18C)	109.5

C(22)-C(19)-C(21)	110.0(4)
C(22)-C(19)-C(20)	110.7(4)
C(21)-C(19)-C(20)	107.8(4)
C(22)-C(19)-P(4)	113.6(3)
C(21)-C(19)-P(4)	109.3(3)
C(20)-C(19)-P(4)	105.2(3)
C(19)-C(20)-H(20A)	109.5
C(19)-C(20)-H(20B)	109.5
H(20A)-C(20)-H(20B)	109.5
C(19)-C(20)-H(20C)	109.5
H(20A)-C(20)-H(20C)	109.5
H(20B)-C(20)-H(20C)	109.5
C(19)-C(21)-H(21A)	109.5
C(19)-C(21)-H(21B)	109.5
H(21A)-C(21)-H(21B)	109.5
C(19)-C(21)-H(21C)	109.5
H(21A)-C(21)-H(21C)	109.5
H(21B)-C(21)-H(21C)	109.5
C(19)-C(22)-H(22A)	109.5
C(19)-C(22)-H(22B)	109.5
H(22A)-C(22)-H(22B)	109.5
C(19)-C(22)-H(22C)	109.5
H(22A)-C(22)-H(22C)	109.5
H(22B)-C(22)-H(22C)	109.5
O(3)-C(23)-Rh(1)	178.6(5)
C(29)-C(24)-C(25)	113.1(4)
C(29)-C(24)-B(1)	119.6(4)
C(25)-C(24)-B(1)	127.1(4)
F(1)-C(25)-C(26)	115.3(4)
F(1)-C(25)-C(24)	121.0(4)
C(26)-C(25)-C(24)	123.7(4)
F(2)-C(26)-C(27)	119.0(5)
F(2)-C(26)-C(25)	120.3(4)
C(27)-C(26)-C(25)	120.7(4)
F(3)-C(27)-C(26)	121.0(5)
F(3)-C(27)-C(28)	120.8(5)

C(26)-C(27)-C(28)	118.2(5)
F(4)-C(28)-C(27)	119.9(5)
F(4)-C(28)-C(29)	120.5(5)
C(27)-C(28)-C(29)	119.6(4)
F(5)-C(29)-C(28)	115.7(4)
F(5)-C(29)-C(24)	119.6(4)
C(28)-C(29)-C(24)	124.8(4)
C(35)-C(30)-C(31)	113.3(4)
C(35)-C(30)-B(1)	119.4(4)
C(31)-C(30)-B(1)	126.7(4)
F(6)-C(31)-C(32)	115.7(4)
F(6)-C(31)-C(30)	120.8(4)
C(32)-C(31)-C(30)	123.5(4)
F(7)-C(32)-C(33)	119.4(4)
F(7)-C(32)-C(31)	120.4(5)
C(33)-C(32)-C(31)	120.2(4)
F(8)-C(33)-C(32)	121.8(5)
F(8)-C(33)-C(34)	119.3(5)
C(32)-C(33)-C(34)	118.8(4)
F(9)-C(34)-C(35)	121.4(5)
F(9)-C(34)-C(33)	119.8(5)
C(35)-C(34)-C(33)	118.9(5)
F(10)-C(35)-C(30)	119.5(4)
F(10)-C(35)-C(34)	115.3(4)
C(30)-C(35)-C(34)	125.2(4)
C(37)-C(36)-C(41)	112.3(4)
C(37)-C(36)-B(1)	128.9(4)
C(41)-C(36)-B(1)	118.5(4)
F(11)-C(37)-C(36)	121.0(4)
F(11)-C(37)-C(38)	114.7(4)
C(36)-C(37)-C(38)	124.2(4)
F(12)-C(38)-C(39)	119.3(5)
F(12)-C(38)-C(37)	120.4(4)
C(39)-C(38)-C(37)	120.2(4)
F(13)-C(39)-C(40)	120.9(4)
F(13)-C(39)-C(38)	120.0(4)

C(40)-C(39)-C(38)	119.0(5)
F(14)-C(40)-C(39)	120.6(4)
F(14)-C(40)-C(41)	120.8(4)
C(39)-C(40)-C(41)	118.6(4)
F(15)-C(41)-C(40)	115.7(4)
F(15)-C(41)-C(36)	118.7(4)
C(40)-C(41)-C(36)	125.6(4)
C(47)-C(42)-C(43)	113.3(4)
C(47)-C(42)-B(1)	128.3(4)
C(43)-C(42)-B(1)	118.5(4)
F(16)-C(43)-C(44)	115.5(4)
F(16)-C(43)-C(42)	119.2(4)
C(44)-C(43)-C(42)	125.3(5)
F(17)-C(44)-C(45)	120.1(4)
F(17)-C(44)-C(43)	121.7(5)
C(45)-C(44)-C(43)	118.2(5)
F(18)-C(45)-C(46)	120.4(5)
F(18)-C(45)-C(44)	120.2(5)
C(46)-C(45)-C(44)	119.4(4)
C(45)-C(46)-F(19)	119.4(4)
C(45)-C(46)-C(47)	120.9(4)
F(19)-C(46)-C(47)	119.7(5)
F(20)-C(47)-C(42)	121.2(4)
F(20)-C(47)-C(46)	116.0(4)
C(42)-C(47)-C(46)	122.8(5)
C(6)-O(1)-P(2)	114.6(3)
C(2)-O(2)-P(4)	115.6(3)
C(36)-B(1)-C(24)	103.1(4)
C(36)-B(1)-C(30)	113.6(4)
C(24)-B(1)-C(30)	113.8(4)
C(36)-B(1)-C(42)	113.3(4)
C(24)-B(1)-C(42)	113.5(3)
C(30)-B(1)-C(42)	100.1(4)
O(1)-P(2)-C(11)	100.5(2)
O(1)-P(2)-C(7)	101.4(2)
C(11)-P(2)-C(7)	115.3(2)

O(1)-P(2)-Rh(1)	103.26(12)
C(11)-P(2)-Rh(1)	116.33(16)
C(7)-P(2)-Rh(1)	116.28(16)
O(2)-P(4)-C(15)	100.0(2)
O(2)-P(4)-C(19)	100.63(18)
C(15)-P(4)-C(19)	114.7(2)
O(2)-P(4)-Rh(1)	102.96(12)
C(15)-P(4)-Rh(1)	116.94(16)
C(19)-P(4)-Rh(1)	117.24(16)
C(23)-Rh(1)-C(1)	179.3(2)
C(23)-Rh(1)-P(4)	99.40(15)
C(1)-Rh(1)-P(4)	80.43(13)
C(23)-Rh(1)-P(2)	99.46(15)
C(1)-Rh(1)-P(2)	80.69(13)
P(4)-Rh(1)-P(2)	161.09(5)
C(23)-Rh(1)-H(1R)	150.6(16)
C(1)-Rh(1)-H(1R)	30.1(15)
P(4)-Rh(1)-H(1R)	83.6(15)
P(2)-Rh(1)-H(1R)	80.6(15)

Table C-4. Anisotropic displacement parameters ($Å^2 x\ 10^3$) for **14**. The anisotropic displacement factor exponent takes the form: $-2p^2[\ h^2 a^{*2} U^{11} + ... + 2\ h\ k\ a^*\ b^*\ U^{12}\ ]$

	U^{11}	U^{22}	U^{33}	U^{23}	U^{13}	U^{12}
C(1)	14(3)	15(3)	19(2)	2(2)	-1(2)	4(2)
C(2)	17(3)	23(3)	12(2)	4(2)	2(2)	-2(2)
C(3)	19(3)	23(3)	36(3)	8(2)	1(2)	6(2)
C(4)	18(3)	32(3)	44(3)	9(3)	1(2)	4(2)
C(5)	12(3)	35(3)	26(3)	5(2)	1(2)	-2(2)
C(6)	19(3)	18(3)	16(2)	-1(2)	-4(2)	1(2)
C(7)	23(3)	28(3)	12(2)	0(2)	2(2)	-10(2)
C(8)	72(5)	83(5)	29(3)	-10(3)	23(3)	-56(4)
C(9)	45(4)	45(4)	20(3)	4(2)	12(3)	15(3)
C(10)	43(4)	54(4)	22(3)	12(3)	4(3)	13(3)
C(11)	29(3)	19(3)	23(3)	-3(2)	6(2)	-6(2)
C(12)	46(4)	42(4)	63(4)	-28(3)	21(3)	-21(3)
C(13)	51(4)	35(4)	44(3)	6(3)	17(3)	16(3)
C(14)	45(4)	31(3)	24(3)	-5(2)	12(3)	3(3)
C(15)	19(3)	26(3)	24(3)	-8(2)	5(2)	-5(2)
C(16)	45(4)	57(4)	27(3)	-19(3)	-8(3)	1(3)
C(17)	58(4)	26(3)	39(3)	-12(3)	13(3)	-8(3)
C(18)	43(4)	37(4)	32(3)	-10(3)	20(3)	-9(3)
C(19)	20(3)	21(3)	15(2)	2(2)	-2(2)	0(2)
C(20)	22(3)	40(3)	20(2)	-3(2)	3(2)	-6(3)
C(21)	16(3)	32(3)	25(3)	1(2)	4(2)	2(2)
C(22)	33(3)	30(3)	32(3)	6(2)	16(2)	-2(3)
C(23)	27(3)	26(3)	19(3)	4(2)	1(2)	-8(2)
C(24)	15(3)	17(3)	13(2)	8(2)	-1(2)	0(2)
C(25)	19(3)	17(3)	21(2)	-2(2)	3(2)	0(2)
C(26)	23(3)	17(3)	35(3)	-1(2)	-8(2)	-7(2)
C(27)	11(3)	34(3)	49(3)	12(3)	7(2)	-5(2)
C(28)	28(3)	29(3)	25(3)	2(2)	13(2)	2(2)
C(29)	26(3)	18(3)	20(2)	3(2)	0(2)	-2(2)
C(30)	15(3)	19(3)	15(2)	-2(2)	-4(2)	1(2)
C(31)	19(3)	21(3)	17(2)	1(2)	0(2)	3(2)

C(32)	18(3)	31(3)	20(2)	2(2)	11(2)	1(2)
C(33)	33(3)	34(3)	26(3)	-9(2)	12(2)	14(3)
C(34)	27(3)	14(3)	42(3)	4(2)	1(3)	4(2)
C(35)	18(3)	23(3)	25(3)	1(2)	9(2)	-4(2)
C(36)	11(3)	11(2)	21(2)	2(2)	6(2)	0(2)
C(37)	24(3)	26(3)	11(2)	1(2)	5(2)	-6(2)
C(38)	26(3)	20(3)	36(3)	-9(2)	15(2)	-6(2)
C(39)	28(3)	15(3)	32(3)	5(2)	14(2)	3(2)
C(40)	20(3)	23(3)	22(3)	7(2)	8(2)	0(2)
C(41)	13(3)	17(3)	22(2)	-4(2)	6(2)	3(2)
C(42)	17(3)	25(3)	19(2)	-9(2)	4(2)	-1(2)
C(43)	20(3)	38(3)	16(2)	-1(2)	3(2)	2(2)
C(44)	12(3)	60(4)	27(3)	-8(3)	2(2)	2(3)
C(45)	31(4)	48(4)	19(3)	2(2)	-4(2)	12(3)
C(46)	33(3)	40(3)	16(2)	13(2)	6(2)	7(3)
C(47)	23(3)	30(3)	18(2)	6(2)	6(2)	4(2)
O(1)	20(2)	18(2)	24(2)	0(1)	-1(1)	-2(2)
O(2)	12(2)	19(2)	25(2)	5(1)	1(1)	-3(1)
O(3)	30(2)	40(3)	41(2)	17(2)	-14(2)	-3(2)
B(1)	15(3)	15(3)	19(3)	2(2)	3(2)	-1(2)
F(1)	30(2)	24(2)	26(1)	-10(1)	1(1)	-2(1)
F(2)	33(2)	37(2)	52(2)	-8(2)	-12(2)	-16(2)
F(3)	16(2)	58(2)	80(2)	-2(2)	6(2)	-14(2)
F(4)	29(2)	50(2)	50(2)	-1(2)	23(2)	-2(2)
F(5)	23(2)	34(2)	20(1)	-6(1)	5(1)	-3(1)
F(6)	30(2)	20(2)	31(2)	8(1)	13(1)	-1(1)
F(7)	31(2)	47(2)	33(2)	8(1)	22(1)	9(2)
F(8)	48(2)	48(2)	65(2)	-12(2)	31(2)	19(2)
F(9)	43(2)	21(2)	71(2)	1(2)	18(2)	9(2)
F(10)	24(2)	18(2)	38(2)	4(1)	8(1)	0(1)
F(11)	35(2)	27(2)	25(2)	-8(1)	4(1)	-7(1)
F(12)	54(2)	21(2)	44(2)	-13(1)	16(2)	-9(2)
F(13)	52(2)	17(2)	52(2)	4(1)	19(2)	6(2)
F(14)	35(2)	26(2)	29(2)	10(1)	1(1)	4(1)
F(15)	23(2)	23(2)	19(1)	1(1)	-1(1)	0(1)
F(20)	22(2)	41(2)	34(2)	17(1)	9(1)	1(1)

F(19)	49(2)	52(2)	26(2)	14(1)	8(2)	16(2)
F(18)	40(2)	83(3)	28(2)	6(2)	-10(1)	19(2)
F(17)	16(2)	87(3)	40(2)	-13(2)	-7(1)	-3(2)
F(16)	18(2)	39(2)	30(2)	-2(1)	3(1)	-7(1)
P(2)	18(1)	16(1)	17(1)	0(1)	2(1)	-1(1)
P(4)	15(1)	16(1)	19(1)	0(1)	1(1)	-1(1)
Rh(1)	14(1)	17(1)	16(1)	1(1)	0(1)	-1(1)

Table C-5. Hydrogen coordinates (x 10^4) and isotropic displacement parameters ($Å^2$x 10^3) for **14**.

	x	y	z	U(eq)
H(3)	8318	5739	6727	31
H(4)	10061	6514	6736	38
H(5)	10003	7931	6626	29
H(8A)	9140	9843	5943	90
H(8B)	8224	10546	5754	90
H(8C)	8955	10056	5379	90
H(9A)	8328	8650	5121	55
H(9B)	7404	8166	5421	55
H(9C)	8705	8399	5671	55
H(10A)	6909	9778	4923	59
H(10B)	6224	10196	5339	59
H(10C)	5930	9274	5184	59
H(12A)	7122	11029	6893	74
H(12B)	7590	10931	6370	74
H(12C)	8110	10355	6805	74
H(13A)	4950	10816	6445	63
H(13B)	4732	10011	6126	63
H(13C)	5590	10714	5958	63
H(14A)	6645	9395	7178	49
H(14B)	5348	9242	6900	49
H(14C)	5634	10083	7177	49
H(16A)	3656	5827	5166	65
H(16B)	3625	6733	5377	65
H(16C)	2993	6007	5640	65
H(17A)	4187	4925	6047	60
H(17B)	5609	5012	6156	60
H(17C)	5041	4767	5627	60
H(18A)	6657	6155	5690	55
H(18B)	5816	6765	5362	55
H(18C)	5916	5830	5208	55

H(20A)	4387	7652	7075	41
H(20B)	4972	6843	7316	41
H(20C)	3620	7081	7396	41
H(21A)	2251	6654	6230	37
H(21B)	2839	7530	6343	37
H(21C)	2086	7095	6732	37
H(22A)	2970	5709	7095	46
H(22B)	4266	5444	6953	46
H(22C)	3140	5435	6554	46
H(1R)	6410(50)	7890(30)	6771(15)	40(15)

Notes for Appendix C:

1) Bruker, **2007**, APEX2 (Version 2.1-4), SAINT (version 7.34A), SADABS (version 2007/4), BrukerAXS Inc; Madison, Wisconsin, USA.
2) a) Altomare, A.; Burla, C.; Camalli, M.; Cascarano, G. L.; Giacovazzo, C.; Guagliardi, A.; Moliterni, A. G. G.; Polidori, G.; Spagna, R., SIR97: a new tool for crystal structure determination and refinement, *J. Appl. Cryst.*, **1999**, *32*, 115-119. b) Altomare, A.; Cascarano, G. L.; Giacovazzo, C.; Guagliardi, A., SIR 92: completion and refinement of crystal structures, *J. Appl. Cryst*., **1993**, *26*, 343-350.
3) Sheldrick, G. M., **1997**, SHELXL-97, Program for the Refinement of Crystal Structures. University of Göttingen, Germany.
4) Mackay, S.; Edwards, C.; Henderson, A.; Gilmore, C.; Stewart, N.; Shankland, K.; Donald, A., **1997**, MaXus: a computer program for the solution and refinement of crystal structures from diffraction data. University of Glasgow, Scotland.
5) Waasmaier, D. and Kirfel, A., New Analytical Scattering Factor Functions for Free Atoms and Ions. *Acta Cryst. A*, **1995**, *51*, 416-430.
6) a) Spek, A., *J. Appl. Cryst.,* **2003**, *36*, 7-13. b) van der Sluis, P. and Spek, A. L. *Acta Cryst.*, **1990**, *A46*, 194-201.

Appendix D: List of Units and Abbreviations

° .....Degree

Å.....Angstrom

atm.....Atmosphere

:B.....Base

C.....Celsius

ca......Circa

cm.....Centimeter

DCM .....Dichloromethane

e.g......For example

$\Delta\nu_{½}$ .....Full width at half height

equiv.....Equivalent

g.....Gram

h^{-1} .....Per hour

η.....Hapticity

Hz.....Hertz

i.e......That is

*i*Pr.....*iso*-propyl

J_{AB} .....Coupling between nucleus A and B

K.....Kelvin

K_x .....Autoionization constant for x

MeCN.....Acetonitrile

MeOH .....Methanol

mer .....Meridonal

MHz .....Megahertz

µL.....Microliter

mg .....Milligram

mmole .....Millimole

NMR .....Nuclear Magnetic Resonance

Ph .....Phenyl

pK_a.....Acid disassociation constant on a logarithmic scale

ppm .....Parts per million

psig.....Pounds per square inch gauge

*t*Bu.....*tert*-butyl

THF .....Tetrahydrofuran

VITA

Sophia D. T. Cherry was born in 1987 to parents Chanh and Linh Tran. She grew up in Mountlake Terrace, Washington. In 2009, she earned her Bachelor of Science in Chemistry from the University of Washington in Seattle. While earning her degree, she worked under the supervision of Professor James M. Mayer investigating small molecule activation with frustrated Lewis pairs. After graduating, she continued her work in the Mayer lab as a research assistant before beginning graduate studies at the University of Washington in 2010. She has worked under the mentorship of Professor and Chair D. Michael Heinekey. In 2015, Sophia married her husband, Michael J. Cherry. She received her Ph. D. in 2016.